CHARACTERIZATION OF A TRANSGENIC PIG MODEL CARRYING GREEN FLUORESCENT PROTEASOMES

A Thesis

presented to

the Faculty of the Graduate School

at the University of Missouri-Columbia

By

EDWARD LUTHER MILES

Dr. Peter Sutovsky, Thesis Supervisor

May 2013

The undersigned, appointed by the dean of the Graduate School,

Have examined the thesis entitled

CHARACTERIZATION OF A TRANSGENIC PIG MODEL CARRYING GREEN FLUORESCENT PROTEASOMES

Presented by EDWARD MILES

A candidate for the degree of Master of Science

And hereby certify that, in their opinion, it is worthy of acceptance.

_____

Professor Peter Sutovsky

_____

Professor Rodney Geisert

_____

Professor Michael Smith

_____

Professor Kathy Timms

Acknowledgments

I would like to thank the members of my committee Dr. Peter Sutovsky, Dr. Rodney Geisert, Dr. Michael Smith, and Dr. Kathy Timms for all of their guidance throughout my MS program. I would especially like to thank my advisor Dr. Sutovsky, for granting me the opportunity to gain valuable experience in his lab as an undergraduate, and also for his patience and guidance throughout my Master's program.

I would also like to thank the members of the Sutovsky lab who have trained me and aided my various projects. I am blessed to have gotten to know all of you and I am proud to consider you my friends. I would like to thank Miriam Sutovsky for teaching me numerous procedures that became essential to the completion of my thesis projects. To Dr. Young-Joo Yi, I would like to thank you for discussing and assisting me with several aspects of my project. I would also like to thank Dr. Shawn Zimmerman (graduated with PhD) and Wonhee Song (PhD candidate) for their moral support and friendship.

Thank you to Melissa Samuel, Keith Giroux, and Dr. Eric Walters for providing me with weekly transgenic pig semen samples and occasionally tissue samples. I would also like to thank Lonnie Dowell for collecting wild type boar semen for me and others in the lab on a weekly basis. Without these samples, this project would not have been possible.

I would like to thank all of the graduate friendships I have developed throughout my time in the Animal Science graduate program. I would like to give a special thank you

to my family who have always supported and encouraged me through the stressful times and who I could always rely on for help.

TABLE OF CONTENTS

ACKOWLEDGEMENTS ii

LIST OF FIGURES viii

LIST OF TABLES ix

LIST OF APPENDIX FIGURES x

LIST OF APPENDIX TABLES xi

NOMENCLATURE xii

ABSTRACT xv

Chapter 1. Sperm Proteasome as a Putative Egg Coat Lysin in Mammals 1

Abstract 1

Zona lysin and the elusive mechanism of sperm-egg coat penetration 2

Ubiquitin-proteasome system 3

Ubiquitination 4

26S Proteasome 6

Sperm proteasome during plant, ascidian and echinoderm fertilization 8

Plant Fertilization 8

Ascidian Fertilization 10

Echinoderm Fertilization 12

Proteasome localization and activity in mammalian spermatozoa 14

Is the mammalian egg coat ubiquitinated prior to fertilization 20

Sperm proteasomes can degrade zona pellucida proteins in solution and in situ 21

Recent advances in sperm UPS 23

Conclusions 25

Acknowledgements 26

Chapter 2. Transgenic Pig Carrying Green Fluorescent Proteasomes 33

Abstract 33

Introduction 34

Materials and Methods 38

Plasmid constructs and DNA preparation 38

Fibroblast cell culture, transfection, and selection 38

Somatic cell nuclear transfer 39

Semen collection and processing 39

Collection and *in vitro* maturation (IVM) of porcine oocyte 40

In vitro fertilization (IVF) and culture (IVC) of porcine oocytes 41

Evaluation of oocyte fertilization and embryo culture 42

Immunofluorescence of boar spermatozoa 43

Western blotting 43

Acrosomal extracts of boar spermatozoa 44

Immunoprecipitation and MALDI-TOF mass spectroscopy 45

Isolation of enzymatically active proteasomes 46

Measurement of proteasomal activity 47

Statistical analysis 47

Results 47

Creation and validation of the *PSMA1-GFP* transgenic pig 47

Fertility testing of the founder boar and its progeny 48

Characterization of transgenic spermatozoa 50

Identification of sperm proteins that copurify with PSMA1-GFP 51

Discussion 53

Acknowledgements 58

Chapter 3. The 26S Proteasome Degrades MFGE8 to Release Spermatozoa from the Oviductal Sperm Reservoir 66

Abstract 66

Introduction 67

Materials and Methods 71

Semen Collection and Processing 71

Acrosomal Extracts of Boar Spermatozoa 72

Detection and Quantification of the Endogenous MFGE8 in Capacitated Spermatozoa 73

Degradation of Exogenous Recombinant MFGE8 in a Cell-Free System Containing Sperm Acrosomal Extracts 73

Western blotting 74

Results 75

Endogenous MFGE8 Degradation during Sperm Capacitation is inhibited by MG132 75

Sperm Acrosomal Proteasomes Degrade Recombinant MFGE8 in a Cell-Free System 75

Discussion 76

OVERALL CONCLUSIONS 81

BIBLIOGRAPHY 83

APPENDIX 95

VITA 111

List of Figures

Figure		Page
1.1	Diagram of protein ubiquitination and degradation by the 26S proteasome	28
1.2	Variations on the subunit composition of the 26S proteasome	29
2.1	pKW14 plasmid construction	59
2.2	Epifluorescence of PSMA1-GFP cells and tissues	60
2.3	PSMA1-GFP fluorescence in spermatozoa and blastocyst	61
2.4	Histological and immunocytochemical analysis of the gonads and testicular germ cells of the founder PSMA1-GFP boar	62
2.5	Proteomic analysis of PSMA1-GFP fusion protein and the coimmunoprecipitated proteins in the transgenic spermatozoa	64
3.1	Endogenous MFGE8 band density	79
3.2	Recombinant Human MFGE8 band density	80

List of Tables

Table		Page
1.1	26S proteasome subunit function and nomenclature by species	30

List of Appendix Figures

Appendix Figures Page

1. Comparisons of proteasomal-proteolytic activities in spermatozoa of PSMA1-GFP offspring (GFP) and wild type boars (WT) 107
2. Western blots of various PSMA1-GFP and wild-type boar tissues 108
3. Immunofluorescence of MFGE8 in wild-type uncapacitated boar spermatozoa 109

List of Appendix Tables

Appendix Table		Page
1.	Embryo Transfer Outcomes	97
2.	Comparison of semen characteristics between GFP offspring and wild type boars	98
3.	Comparison of sperm motility (%) during storage	99
4.	Comparison of fertilization parameters on porcine IVF	100
5.	Proteasomal Subunits and Putative Proteasome-Interacting Proteins Co-immunoprecipitated with Anti-GFP-Antibody	101
6.	Immunoprecipitation & MS/MS Identification of Proteasome Interacting Sperm Proteins	107

Nomenclature

AA	Amino Acid
ACUC	Animal Care and Use Committee
AE	Acrosome Exocytosis
AM	Acrosomal Membrane
ANOVA	Analysis of Variance
AR	Acrosome Reaction
ATP	Adenosine Triphosphate
BSA	Bovine Serum Albumin
CO2	Carbon Dioxide
COC	Cumulus Oocyte Complex
DAPI	4',6-diamidino-2-phenylindole
DMSO	Dimethyl Sulfoxide
DNA	Deoxyribonucleic Acid
DUB	Deubiquitinating Enzyme
EGF	Epidermal Growth Factor
EtOH	Ethanol
FITC	Fluorescein Isothiocyanate
FSH	Follicle Stimulating Hormone
HRP	Horseradish Peroxidase
IAM	Inner Acrosome Membrane
IgG	Immunoglobulin G

IVF	In Vitro Fertilization
IVM	In Vitro Maturation
K	Lysine
kDa	kilo Dalton
LC	Liquid Chromatography
LH	Luteinizing Hormone
MII	Metaphase II
MS	Mass Spec
MW	Molecular Weight
NaCl	Sodium Chloride
NGS	Normal Goat Serum
OAM	Outer Acrosomal Membrane
PBS	Phosphate Buffer Solution
PCR	Polymerase Chain Reaction
PMSF	Phenylmethanesulfonylfluoride
PVA	Polyvinyl Alcohol
PVDF	Polyvinylidene Fluoride
RNA	Ribonucleic Acid
SEM	Standard Error Mean
TBS	Tris Buffer Solution
TOF	Time of Flight
Tris	Tris(hydroxymethyl)aminomethane

TRITC	Tetramethylrhodamine-5-(and6)-isothiocyanate
UBAL	Ubiquitin Aldehyde
UPS	Ubiquitin Proteasome System
ZP	Zona Pellucida
ZPC	Zona Pellucida Glycoprotein C

Characterization of a Transgenic Pig Model Carrying Green Fluorescent Proteasomes

Edward Luther Miles

Dr. Peter Sutovsky, Thesis Supervisor

ABSTRACT

The Ubiquitin Proteasome System (UPS) participates in many biological processes involving substrate-specific proteolysis, and can be linked to various pathologies and genetic diseases such as Alzheimer's disease, cancer, and liver cirrhosis. Unfortunately, little is known about the interactions of proteasomal subunits with other sperm proteins or structures. Through a joint effort between Dr. Prather, Dr. Wells, and Dr. Sutovsky's labs, a novel transgenic pig model with Green Fluorescent Protein (GFP) fused to the 20S proteasomal core subunit α-type 1 (PSMA1) was created, hypothesizing that the PSMA1-GFP fusion protein will be incorporated into functional sperm proteasomes. The first objective of this thesis was to confirm the presence of these PSMA1-GFP fusion proteins in the transgenic boar sperm and tissues. The second objective was to identify proteasome-interacting proteins that may regulate sperm proteasomal activity during fertilization or may be the substrates of proteasomal proteolysis during fertilization. A novel interaction with seminal plasma/sperm membrane glycoprotein, MFGE8, and the 26S proteasome was revealed. Therefore, a possible role for this interaction was investigated: that the 26S proteasome mediates

the degradation of MFGE8, which allows the gradual release of spermatozoa from the sperm oviductal reservoir prior to fertilization. Furthermore, GFP affinity purification was used to isolate enzymatically active proteasomes which could be used to study sperm-oocyte interactions or wherever the UPS is involved. It was concluded that this transgenic pig model can be used to study proteasome localization, proteasome interacting proteins, and tissue specific proteasome isolation in all areas of UPS research. Collectively, this study gives insight into the mechanisms of fertilization, which could lead to the development of novel treatments of infertility and possible contraceptive applications.

CHAPTER ONE

Sperm Proteasome as a Putative Egg Coat Lysin in Mammals

Reference: Miles EL, Sutovsky P (2013) Sperm Proteasome as a Putative Egg Coat Lysin in Mammals. In: *Sexual Reproduction in Animals and Plants*. Hitoshi Sawada, Naokazu Inoue, and Megumi Iwano, Editors. Springer, In press.

Abstract

During animal and human fertilization, the fertilizing spermatozoon creates and passes through a fertilization slit in the oocyte's vitelline coat (VC). It has been hypothesized that the penetration of the mammalian VC, zona pellucida (ZP) is aided by a proteolytic enzyme capable of locally degrading ZP proteins. This putative "zona lysin" is predicted to reside within the sperm head acrosome and be released or exposed by ZP-induced acrosomal exocytosis. Evidence has been accumulating in favor of the 26S proteasome, the ubiquitin-dependent multi-subunit protease acting as the putative vitelline coat/zona lysin in humans and animals. To confirm this hypothesis, three criteria must be met: 1) the sperm receptor on the ZP must be ubiquitinated, 2) proteasomes must be present, exposed and enzymatically active in the sperm acrosome, and 3) sperm proteasomes must be able to degrade the sperm receptor on the egg coat/ZP during fertilization. This review discusses recent data from a number of mammalian and non-mammalian models addressing these predictions. As a result, it sheds light on the mechanisms controlling sperm interactions with VC and on the evolutionary conservation of the proteasome-assisted fertilization mechanisms.

Zona Lysine and the Elusive Mechanism of Sperm-Egg Coat Penetration

The process of mammalian fertilization has long been studied, but many fundamental questions still remain unanswered. One that continues to be debated despite decades of research is about the mechanism utilized by the fertilizing spermatozoa to penetrate an oocyte's vitelline coat (VC), the zona pellucida (ZP). When a capacitated, fertilization competent spermatozoon binds to the sperm receptor on the ZP, it undergoes acrosomal exocytosis (AE) which causes vesiculation of the acrosomal membrane and exocytosis of the acrosomal cap (Yurewicz et al., 1998; Bleil and Wassarman, 1980). This exposes the acrosome-borne proteolytic enzymes and results in the formation of the acrosomal shroud which allows the spermatozoa to create a local microenvironment that supports the opening of fertilization slit and sperm penetration through the ZP (Yurewicz et al., 1998). There are two schools of thought about the mechanism of sperm-ZP penetration: 1) that mechanical force of the sperm tail motility is sufficient to fully penetrate the ZP (Green and Purves, 1984; Bedford, 1998); 2) that an enzyme originating from the acrosome of the fertilizing spermatozoa acts as a putative zona lysin that digests the fertilization slit in the ZP and allows sperm penetration through the ZP (Austin and Bishop, 1958; Goldstein et al., 1975).

Several candidates have been proposed for this hypothetical zona lysin. Originally, the acrosomal protease acrosin was favored as the most likely zona lysin, but was ruled out when acrosin knockout mice remained fertile with only delayed ZP-penetration (Baba et al., 1994). Acrosin has since been considered to be involved in proteolysis and/or processing of proteins in the acrosome and on acrosomal

membranes (Honda et al., 2002). Then the serine protease Tesp5/Prss21 on the mouse sperm surface was identified as a plausible candidate. Double knockout studies have shown reduced fertility in vitro, which was rescued by exposure of the spermatozoa to the uterine microenvironment or by treatment with uterine fluids (Yamashita et al., 2008; Kawano et al., 2010). These candidates have since been proposed to be involved in initial sperm-ZP binding (Yamashita et al., 2008; Kawano et al., 2010). Evidence has been accumulating in favor of the 26S proteasome as the candidate zona lysin in mammals, ascidians, and invertebrates (Sakai et al., 2004; Yi et al., 2007a; Sutovsky et al., 2004). This review highlights the significant studies and current research examining the possible role of the 26S proteasome as the putative mammalian zona lysin.

Ubiquitin-Proteasome System

Through a multistep enzymatic process, the ubiquitin-proteasome system (UPS) tags outlived or damaged intracellular proteins with a small chaperone protein ubiquitin. This process, referred to as ubiquitination typically targets the ubiquitinated substrates for proteolytic degradation by a multi-subunit protease, the 26S proteasome, (Glickman and Ciechanover 2002). Ubiquitin, an 8.5 kDa, 76 amino acid protein, was first isolated and purified by the Goldstein lab in 1975. They found that this polypeptide induced the differentiation of bovine thymus-derived and bone-marrow-derived immunocytes in vitro (Goldstein et al., 1975). Consequently, they named this newly discovered polypeptide ubiquitous immunopoietic polypeptide (UBIP) due to its high degree of evolutionary conservation, exhibiting close structural, functional, and immunological similarity when isolated from species as diverse as protozoans to

mammals and plants. In 1976, Etlinger and Goldberg first described a novel ATP-dependent proteolytic system responsible for the rapid degradation of abnormal proteins separate from the lysosomal degradation pathway (Etlinger and Goldberg 1977). The discovery that metabolic energy is required for intracellular protein degradation, opposed the commonly accepted idea that cellular proteolysis was an entirely exergonic process occurring in the lysosome. In a joint effort, Aaron Ciechanover, Avram Hershko, and Ervin Rose described the ubiquitin-mediated protein degradation, a discovery for which they shared the Nobel Prize in Chemistry in 2004. Ubiquitin is not just a housekeeping protein that helps recycle outlived or damaged protein molecules. It is also involved in a number of cellular mechanisms and pathologies, including but not limited to antigen presentation in the immune system, apoptosis, Alzheimer's disease, cell cycle control, endocytosis of membrane receptors, HIV particle internalization, protein quality control in the endoplasmic reticulum, reticulocyte differentiation, signaling, and transcriptional control (Pines 1994; Hershko and Ciechanover, 1998; Glickman and Ciechanover, 2002).

Ubiquitination

Ubiquitin is typically a cytoplasmic and nuclear protein, but can be found in the extracellular space in some mammalian, lower vertebrate and invertebrate systems, and is highly substrate specific. Polymerization of substrate-bound ubiquitin molecules into multi-ubiquitin chains serves as a degradation signal for numerous target proteins. The degradation of substrate protein is initiated by the covalent attachment of an isopeptide chain of four or more ubiquitin molecules. These ubiquitin molecules are linked to each

other through one of seven Lysine residues (K6, K11, K27, K29, K33, K48, and K63) to form the poly-ubiquitin chains. All seven of these Lys residues are potential ubiquitin-chain initiation sites, but K48 is the most common linkage site for polyubiquitin chains recognized by the 26S proteasome (Walczak et al., 2012; Iwai, 2012). The K63 site is the most common site of di-ubiquitination, targeting membrane receptors for lysosomal degradation, chromatin remodeling and DNA repair (Walczak et al., 2012; Kim et al., 2006).

The formation and ligation of the poly-ubiquitin chain to its target protein occurs through a concerted series of ATP-dependent enzymatic reactions (**Figure 1.1**). Ubiquitination starts with the activation of a single ubiquitin molecule with a phosphorylation-dependent ubiquitin activating enzyme E1 (UBE1 or UBA1 in HUGO nomenclature). The UBA1 is then supplanted by ubiquitin carrier/ubiquitin conjugating enzyme E2. Simultaneously, an E3-type ubiquitin ligase seeks out and engages the target protein to be ubiquitinated and degraded (Hershko, 2005). The E3-type ligases are highly diverse and responsible for the substrate specificity of protein ubiquitination as there are about two E1 proteins, approximately 30 E2 proteins, and more than 500 different E3 proteins in humans (Tanaka, 2009). The E3-ligases catalyze the covalent ligation of the C-terminal glycine/Gly residue (G76) of ubiquitin to an internal Lys residue of the target protein. Next, the ubiquitin chain elongates from the mono-ubiquitinated substrate protein resulting in a poly-ubiquitinated protein. A poly-ubiquitin tail of four or more ubiquitin molecules is needed to signal proteasomal degradation.

26S Proteasome

The 26S proteasome is a 2.5 MDa multi-catalytic canonical protease localized in the cell cytosol and nucleus (**Figure 1.2**). The 26S proteasome is responsible for degrading ubiquitinated proteins in the cell, although non-ubiquitinated proteins could be substrates as well. The typical enzymatically active proteasome consists of two subcomplexes: A hollow catalytic 20S core particle (20S CP) capped by one or two terminal 19S regulatory particle(s) (19S RP). The 19S RP is responsible for poly-ubiquitin chain recognition and binding, deubiquitination, and substrate protein priming/linearization/unfolding. The 19S RP consists of at least 17 different subunits between two subcomplexes: the lid and the base. The lid complex contains 14 regulatory particle non-ATPase subunits (PSMD1-14) (Hanna and Finley, 2007). Subunit PSMD4 (Rpn10) is the main 19S subunit responsible for substrate recognition. It binds the poly-ubiquitin chains on the target protein during poly-ubiquitin chain recognition by the 26S proteasome (Yi, 2010b). Subunit PSMD14 (Rpn11) then deubiquitinates the captured substrate by cleaving the polyubiquitin chain at a proximal site, which is then further cleaved into single ubiquitin molecules by deubiquitinases (DUBs) that can associate with the 19S RP (Verma, 2002). The cleaved ubiquitin molecules can be reused for ubiquitination of other protein molecules. New functions are still being discovered for subunits composing the 19S lid. **Table 1.1** lists the known 26S proteasomal subunits and their proposed functions by species.

The 19S RP base subcomplex is responsible for 1) capturing target proteins via poly-ubiquitin chain recognition, 2) unfolding the substrate protein, and 3) opening the

channel into the 20S CP. The base subcomplex contains six homologous AAA-ATPase subunits, (PSMC1-6) and three non-ATPase subunits (PSMD1, 2 and 4). These subunits create a narrow gated channel, which only allows unfolded proteins to enter the 20S core. PSMD1 and 2 have been proposed to work together as a functional unit and are required for substrate translocation and opening of the 20S channel. This compartmentalized design of the 26S proteasome separates proteolysis from the cellular milieu and restricts degradation to unfolded and imported proteins. Subunit PSMD2 attaches to the 20S CP, while subunit PSMD1 is located on top of PSMD2 and serves as a docking site for substrate recruitment factors (Rosenzweig et al., 2008). Subunit PSMD4 functions as an integral ubiquitin receptor to trap polyubiquitinated proteins; PSMD4 does this by its C-terminal ubiquitin-interacting motif (Deveraux et al., 1995). Six ATPase subunits (PSMC1-6) surrounding the base are organized into a hexameric ring that controls the opening of the channel and allows the protein to reach the catalytic sites of the 20S CP. The base ATPases are not only required to open the channel into the 20S CP, but to also unfold the substrate protein. This allows the protein to be threaded through the narrow channel of the 20S CP where the catalytic protease subunits are located. The details of the ATP-dependent mechanisms behind these processes are still unknown, but it is certain that these subunits work through a process that requires ATP hydrolysis (Liu et al., 2006).

The 20S CP is a 750 kDa cylindrical protein complex responsible for the proteolysis of the substrate protein. The 20S CP contains 28 subunit molecules of 14 types formed from the stacking of two outer α-rings and two inner β-rings. Each ring is

composed of seven structurally similar α and β subunits, respectively. The rings are heptamerically stacked in an α1-7β1-7β1-7α1-7 pattern. The subunits of the α-ring (PSMA1-7) connect the 20S CP to the 19S base and act as a gate that opens in the presence of an ubiquitinated protein. The two inner rings are composed of seven β-type subunits (PSMB1-7) each and confer the threonine protease activities of the 26S proteasome. There are three catalytic β-type subunits: PSMB6 (β1), PSMB7 (β2), and PSMB5 (β5). The β1 subunit is associated with caspase-like/PGPH (peptidylglutamyl-peptide hydrolyzing) activity, β2 with trypsin-like activity, and β5 with chymotrypsin-like activities, which confer the ability to cleave peptide bonds at the C-terminal side of acidic, basic and hydrophobic amino-acid residues, respectively (Tanaka, 2009). The 20S proteasome then degrades the target protein into 3 to 15 amino-acid oligopeptides which are released into the cytosol and are further hydrolyzed into single amino acids by cytosolic oligopeptidases and/or amino-carboxyl peptidases (Tanaka, 2009).

Sperm Proteasome during Plant, Ascidian and Echinoderm Fertilization

Plant Fertilization

The sexual reproduction cycle in higher plants occurs in the reproductive organs of the flower. Similar to animal spermatozoon, pollen, the male gametophyte, is a highly specialized structure; it consists of two or three cells. Pollen is released from the anthers and adheres to the surface of the female stigma equipped with a cytoplasmic extension known as the pollen tube (Boavida et al., 2005). The pollen tube rapidly grows through the style to the ovules (Boavida et al., 2005). Pollen tube adhesion and growth guides the pollen toward the ovary where it fertilizes the embryo sac, the female gametophyte

(Boavida et al., 2005). For a more in-depth account of fertilization in higher plants, please refer to the review by Boavida et al., 2005.

Evolutionary conservation of the components and roles of the UPS appear to reach beyond the animal kingdom to plants, where pollen adhesion and guidance seem to depend on ubiquitin. For example, during maize pollen development, the levels of ubiquitin and ubiquitin-protein conjugates in young pollen precursors, the microspores without vacuoles were 10 to 50 times lower than compared to mature pollen grains (Callis and Bedinger, 1994). Treatment with 26S proteasomal inhibitors, MG132 and epoxomicin, significantly reduced pollen tube growth in kiwifruit (*Actinidia deliciosa*) (Speranza et al., 2001). Kim et al. (2006) showed that pollen adhesion to lily (*Lilium longiflorum Thunb*.) styles can be enhanced in vitro with the addition of exogenous ubiquitin. Furthermore, in Arabidopsis thaliana the proper conformation of SCF E3 ubiquitin-ligases which direct ubiquitination is required for male fertility (Devoto et al., 2002). Mutations in genes encoding 26S proteasomal subunits, ubiquitin-specific proteases, deubiquitinating enzymes and 19S regulatory particle non-ATPases, result in infertility due to defects in pollen maturation and/or transmission (Doelling et al., 2007; Book et al., 2009). Several E3s have been shown to play key roles in self-nonself pollen recognition in snapdragons (*Antirrhinum*) (Qiao et al., 2004). In snapdragons, the SCFAhSLF2 complex acts as an E3 that targets non-self S-RNases for ubiquitination and destruction by the 26S proteasome; however, it leaves self S-RNases active during the self-incompatibility response, thus functioning as a cytotoxin that degrades RNA and terminates pollen tube growth (Qiao et al., 2004).The current data strongly suggests a

role for the UPS in plant germination and gametophyte development, but more research must be done to elucidate how the UPS is utilized in these processes.

Ascidian Fertilization

Ascidians are hermaphrodites that reproduce by releasing sperm and eggs simultaneously into the surrounding seawater during the spawning season; thus, large quantities of readily fertilizable gametes can be easily obtained for research. The exposure to alkaline seawater activates the spermatozoa, much like capacitation in mammals, suggesting that the proteasome is then secreted to the sperm surface. The spermatozoa then undergo species-specific binding to the proteinaceous vitelline coat, which they must penetrate via sperm surface proteases that act as a VC-lysin in order to complete the fertilization process. It has been shown that the proteasomes are exposed on the ascidian sperm surface; proteasomal proteolytic activity was specifically detected in the sperm head region and was clearly increased upon sperm activation (Sawada and Takahashi, 2002). Anti-proteasome antibodies, and proteasomal inhibitors MG115 and MG132, inhibit ascidian fertilization (Sawada and Takahashi, 2002).

Studies in two ascidian species, *Ciona intestinalis* and *Halocynthia roretzi*, have shown a strict self-sterility in fertilization (Sawada and Sakai, 2002). After self-nonself recognition via interactions between the sperm and VC, the sperm-borne egg coat lysin system is activated (Sawada and Sakai, 2002). Data from Sawada's laboratory have provided evidence that ascidian sperm-VC penetration involves the sequential ubiquitination and proteasomal degradation of the sperm receptor protein HrVC70, a major protein component of the ascidian VC. Ubiquitination of HrVC70 is accomplished

by a 700 kDa ubiquitin-conjugating enzyme complex released during sperm activation (Sawada and Sakai, 2002; Sakai et al., 2003). A 930 kDa proteasome (26S-like proteasome) seems to function as the egg coat lysin that directly degrades the VC. This data suggests that an extracellular, sperm borne, ubiquitin-conjugating enzyme system is essential for the formation of these polyubiquitin chains on HrVC70 and for ascidian fertilization.

The HrVC70 is a 70 kDa component of the VC that has been shown to be a novel sperm receptor which bears a significant similarity to components of the mammalian zona pellucida, particularly the proposed mammalian/murine sperm receptor ZPC (Sawada and Sakai, 2002). Three N-terminal Cys residues in the ZP domain of the 120-kDa HrVC70 precursor (HrVC120) share conserved positions within mammalian and frog ZPC (Sawada and Sakai, 2002). The HrVC70 contains 12 EGF (epidermal growth factor)-like repeats that confer its role in sperm binding to VC (Sawada and Takahashi, 2002). This protein has been shown to be degraded by purified ascidian sperm 26S-like proteasomes only in the presence of ubiquitin, ATP, and the ubiquitin-conjugating enzymes purified from a rabbit reticulocyte lysate (Sawada and Takahashi 2002, Sakai and Sawada, 2004). These results reveal that an extracellular UPS is essential for ascidian fertilization, particularly in the degradation of the proteinaceous vitelline coat.

Recently, Yokota and Sawada investigated an extracellular transport signal and have discovered a novel post-translational modification of the ascidian sperm proteasome. They found that the 20S core PSMA1/α6 subunit of purified sperm proteasomes is distinct from purified egg and muscle proteasomes (Yokota et al., 2011).

Tissue specific α- subunits are not commonplace, but several are expressed in the testis of Drosophila (α3T, α4T2, and α6T) (Belote and Zhong, 2009). Among these testis-specific α-subunits, α6T is reported to be crucial for spermatogenesis and fertility (Belote and Zhong, 2009). The α6 subunit of H. roretzi contains a cluster of acidic amino acid residues and the removal of this cluster may mimic the state of dephosphorylation of the α6 subunit which may affect function and localization of the sperm proteasome (Yokota et al., 2011). Alternatively, it is also possible that the conserved sequence of the α6 subunit in *H. roretzi* and *C. intestinalis* may function as a transport signal to the acrosome during ascidian spermiogenesis. It is not known at present if similar modifications exist in the mammalian sperm proteasome.

Echinoderm Fertilization

Most echinoderms can reproduce sexually by spawning eggs and spermatozoa into the seawater, much like ascidians, and asexually by regenerating body parts. For the purpose of this review, only sexual reproduction will be examined. It has been confirmed that the proteasomes are present in sea urchin spermatozoa and that the sperm proteasome may be involved in the acrosome reaction; but unlike ascidians, the proteasome is not essential for sperm binding to the echinoderm VC (Yokota and Sawada, 2007; Matsumura and Aketa, 1991). The role of sperm proteasomes in echinoderm fertilization has been investigated in the sea urchin Pseudocentrotus depressus by Yokota and Sawada (2007). They examined the effects of proteasomal inhibitors and synthetic peptide substrates for the proteasome on different steps of the fertilization process. The inhibition of fertilization by proteasomal inhibitors suggests

that the echinoderm sperm proteasomes play an important role in the acrosome reaction and in sperm penetration through the VC, most likely as an egg coat lysin (Yokota and Sawada, 2007). Among the examined proteasomal substrates and inhibitors, a caspase substrate (Z-Leu-Leu-Glu-MCA) competitively inhibited the caspase-like catalytic center (β1 subunit) of the proteasome which decreased fertilization in a concentration dependent manner (Yokota and Sawada, 2007). This suggests that the caspase-like activity of the proteasomes' β1 subunit must play a key role in sea urchin fertilization.

Echinoderm spermatozoa undergo acrosome reaction/acrosomal exocytosis when they enter the jelly coat surrounding the VC. Protein kinase A (PKA) has been implicated in the acrosome reaction in sea urchins (Su et al., 2005), and shown to stimulate the function of mammalian 26S proteasome (Zhang et al., 2007). Therefore, the sperm proteasome may act to degrade certain unknown PKA modulators which would result in the irreversible activation of PKA during the acrosome reaction. During the acrosome reaction, the acrosomal contents containing an egg coat lysin is exposed and released, allowing spermatozoa to penetrate the VC (Yokota and Sawada, 2007). For the sperm proteasome to act as egg coat/VC lysin, the VC must be ubiquitinated prior to fertilization and extracellular ATP must be present (Yokota and Sawada, 2007). Yokota and Sawada used Western blotting with a monoclonal anti-ubiquitin antibody FK2, which recognizes both mono- and multi-ubiquitinated proteins, to reveal a band pattern indicative of VC ubiquitination. The identity of the ubiquitinated VC protein(s) remains to be determined, but the current data supports the hypothesis that the echinoderm

sperm 26S proteasome is released during the acrosome reaction and degrades the ubiquitinated VC proteins in an ATP-dependent fashion.

Proteasome Localization and Activity in Mammalian Spermatozoa

Mammalian fertilization is a unique cellular-recognition event that comprises sequential interactions between the sperm and the oocyte's vitelline coat, (Yanagimachi, 1994). First, a capacitated spermatozoon penetrates the cumulus oophorus, facilitated by a sperm membrane bound hyaluronidase, and then binds to the zona pellucida, a protective glycoprotein matrix that surrounds the ovulated oocyte. The ZP plays a pivotal role in the species-specificity of sperm-oocyte recognition, binding, as well as in the induction of acrosomal exocytosis (AE), anti-polyspermy defense and protection of the embryo until before implantation. In most of the mammals studied, only spermatozoa with an intact acrosome bind to the ZP, in a species-specific manner. The fertilizing spermatozoa's interaction with zona glycoprotein that serves as sperm receptor, (ZP3/ZPC in mouse/human and ZPB/ZPC complex in pig) triggers the AE via signal transduction events in the sperm acrosome, such as the opening of T-type, low voltage activated Ca2+ channels, causing an influx of Ca2+ and the activation of heterotrimeric G proteins (Pasten and Morales, 2005; Ikawa et al., 2010). This causes an increase in intracellular pH, resulting in sustained Ca2+ influx which drives AE. This results in the release or exposure of acrosomal enzymes and, when combined with vigorous sperm motility, allows the spermatozoon to penetrate the ZP and fuse with the oocyte plasma membrane, the oolemma (Pasten and Morales, 2005; Ikawa et al., 2010).

The role of the UPS has been well documented in the reproductive processes of several mammalian species. For example, multi-enzymatic sperm protease complexes with similar sedimentation coefficients as purified proteasomes from other tissues have been isolated from mouse (Pasten and Morales, 2005), pig (Zimmerman and Sutovsky, 2009), and human (Morales et al., 2003, 2004; Baker et al., 2007) spermatozoa. Accordingly, the substrate-specific enzymatic activities (trypsin-like, chymotrypsin-like, and peptidylglutamyl peptide-hydrolyzing activities) of these sperm proteasomes have been recorded in mice (Pasten and Morales, 2005; Bedard et al., 2011; Rivkin et al., 2009), pigs (Sutovsky et al., 2004; Yi et al., 2007a, 2009), and humans (Morales et al., 2003; Chakravarty et al., 2008; Kong et al., 2009).

The sperm associated proteasomes are tethered to the acrosomal surface in mice (Pasten et al., 2005), pigs (Sutovsky et al., 2004; Yi et al., 2009), and humans (Morales et al., 2004). The proteasomes probably become associated with the spermatozoa's inner and outer acrosomal membranes during acrosomal biogenesis at the spermatid stage (Rivkin et al., 2009). It appears that the extracellular proteasomes exposed on the acrosomal surface of mammalian spermatozoa are involved in the ZP-induced AE and are able to directly interact with the ZP during fertilization (Sutovsky et al., 2004; Yi et al., 2007a, 2009, 2012). The proteasomes located on the cell surface could participate in sperm-ZP binding in some mammalian species, such as humans (Chakravarty et al., 2008; Naz and Dhandapani, 2009) and mice (Pasten et al., 2005). Then the intracellular and extracellular proteasomes would blend into the acrosomal shroud and participate during the AE. Sperm proteasomes have been shown to be

essential for acrosomal function and sperm-zona penetration during fertilization in several mammalian species such as mouse, pig, and human (Pasten and Morales, 2005; Kong et al., 2009; Zimmerman et al., 2011). It is possible that the proteasomes modulating these cellular events could participate in other steps of fertilization as well.

In addition to proteasomes, other UPS components have been implicated in spermatogenesis, epididymal sperm maturation and fertilization. For instance, ubiquitinated substrates have been detected in the epididymal fluid, seminal plasma, on the surface of defective epididymal spermatozoa, and on the outer surface of the ZP (Sutovsky et al., 2001, 2004; Zimmerman et al., 2011). Anti-proteasome antibodies have been reported to be present in the seminal plasma of infertile men (Bohring et al., 2001, 2003). Addition of the deubiquitinating enzyme inhibitor, ubiquitin-aldehyde, to boar in vitro fertilization assays promotes polyspermy, which might be related to an increase in ubiquitination and degradation of the ZP since this C-terminally modified ubiquitin species accelerates proteasomal proteolysis (Yi et al., 2007b). More recently, sperm deubiquitinating enzymes have been explored by the Wing laboratory in Canada. They reported that the spermatozoa of deubiquitinating enzyme Usp2 knockout mice are severely sub fertile. This appeared to be caused by a defect in ZP binding and/or penetration, even though the USP2 protein in wild type mice does not seem to be specifically localized in the acrosome. In elongating spermatids, USP2 was localized perinuclearly in a thin layer between the outer acrosomal membrane and the plasma membrane, but absent from the nucleus (Lin et al., 2000). The Usp2 null spermatozoa are motile and undergo the AE, but fail to penetrate the ZP (Bedard et al., 2011). This

data suggests that the deubiquitination of sperm or spermatid proteins by USP2 is an important regulatory mechanism required for the acquisition of fertilizing ability by mammalian spermatozoa. It is not clear if the observed severe subfertility is a result of impaired deubiquitinating activity of the acrosomal USP2 enzyme during fertilization, or if it is rather a result of abnormal assembly of the sperm acrosome during spermiogenesis. Either way, the failure of motile Usp2 null spermatozoa to penetrate the zona supports the view that sperm motility alone is not sufficient to propel sperm head through zona matrix.

The role of UPS in sperm penetration through the ZP has been well documented. Proteasomal inhibitors and anti-proteasome antibodies effectively block mouse, pig, and human sperm's ability to penetrate the ZP of their respective species (Morales et al., 2003; Sutovsky et al., 2004; Pasten et al., 2005). The co-incubation of pig spermatozoa with proteasomal inhibitors prevents sperm-ZP penetration without affecting sperm motility and binding (Sutovsky et al., 2003, 2004; Yi et al., 2007a; Zimmerman and Sutovsky, 2009). However, if the zona is removed prior to fertilization, fertilization proceeds even with the addition of proteasomal inhibitors (Sutovsky et al., 2004), which suggests a role for the proteasome in sperm-ZP penetration. Chakravarty et al. (2008) reported that the human sperm-associated proteasomal activity is not stimulated by binding of recombinant ZP proteins, but that it remains steady after AE, most likely due to the association of the proteasomes with the inner acrosomal membrane, which is not removed by AE (Chakravarty et al., 2008).

The ZP3/ZPC in mice/humans has been identified as the primary sperm binding receptor on the ZP and perhaps the inducer of AE (Naz and Dhandapani, 2009). The human sperm ubiquitin-associated protein UBAP2L was identified as a ZP-interacting protein by the Naz Lab (Naz and Dhandapani, 2009) using a yeast two-hybrid screen (Y2H) and was further tested when UBAP2L antibodies were shown to inhibit sperm-ZP binding when tested in vitro. The Y2H procedure is used to identify proteins that interact with a target protein expressed in yeast as a hybrid with a DNA-binding domain and has been widely used to examine protein-protein interactions (Naz and Dhandapani, 2009). Human sperm-oocyte recognition, binding, and AE have been proposed to be mediated by sugar residues (O- and N-linked) and peptide moieties of ZP3 (Chakravarty et al., 2005; Gupta et al., 2009). Results from the Naz lab may suggest that ubiquitination, in addition to glycosylation of the ZP proteins, may regulate the sperm-ZP interactions (Naz and Dhandapani, 2009).

In agreement with the above study, Aitken and colleagues found that the proteasome is a component of a multimeric ZP-binding complex found in human spermatozoa (Redgrove et al., 2011). They propose that sperm-ZP binding requires the concerted action of several sperm proteins that form multimeric recognition complexes on the sperm surface, which is an alternate and novel view different from the traditional simple lock and key mechanism of one receptor, one ligand. The formation of these complexes on the sperm surface is purported to depend upon post-testicular maturation driven by the environmental changes the spermatozoa are exposed to in the epididymis and within the female reproductive system. They report that human

spermatozoa express a number of high molecular weight protein complexes on their surface and that subsets of these complexes display affinity for homologous ZP (Redgrove et al., 2011). Two of these complexes were revealed to be a chaperonin-containing TCP-1 (CCT) which harbors a putative ZP binding protein, ZPBP2, and several components of the 20S proteasome which were found previously in an analysis of the human sperm proteome (Redgrove et al., 2011; Johnston et al., 2005). The role of these protein complexes in sperm-ZP interactions was further confirmed when antibodies against the individual components of the complex, including proteasomal subunits inhibited sperm binding to zona-intact oocytes (Redgrove et al., 2011). Since many sperm proteins exhibit ZP binding affinity, it is possible that complexes containing these ZP-binding proteins may participate in sequential or hierarchical molecular interactions or act synergistically to ensure successful sperm-ZP binding. It is important to note that the proteasome complex was shown as three large bands when examined by blue native polyacrylamide gel electrophoresis. Aitken and Redgrove (2011) theorize that this is due to post-translational modifications of certain subunits of the complex (α1-7, β1, and β4) that displayed charge shift signatures characteristic of tyrosine phosphorylation (Redgrove et al., 2011). This is consistent with the proteasomal subunit phosphorylation reported in the acrosome that modulates the fertilizing capacity of human spermatozoa by inducing AE (Diaz et al., 2007). This suggests that proteasome complexes may be differentially activated during the individual steps of fertilization.

Is the Mammalian Egg Coat Ubiquitinated Prior to Fertilization?

To confer with the hypothesis that the 26S proteasome acts as the putative egg coat lysin in mammalian fertilization, there must be an ubiquitinated sperm receptor on porcine ZP that is degraded by the sperm acrosome-borne proteasomes during porcine fertilization. This requires these three prerequisites: 1) the sperm receptor on the mammalian egg coat is ubiquitinated, 2) proteasomes are present, exposed and enzymatically active in the sperm acrosomal cap, and 3) sperm proteasomes degrade the sperm receptor on the egg coat during fertilization.

There is evidence that the sperm receptor complex ZPB-ZPC on the porcine ZP is ubiquitinated. In porcine oocytes, the ZPB-ZPC complex has been shown to be responsible for sperm-ZP binding (Yurewicz et al., 1998). Furthermore, the porcine ZPC homologs in mouse (ZP3) and human (ZP3) have been implicated in sperm binding and induction of acrosomal exocytosis (Shur et al., 2006; Gupta et al., 2009). Sutovsky et al. (2004) have shown the presence of ubiquitinated proteins in the unfertilized porcine egg coat. They reported that ubiquitin-immunoreactive proteins can be detected on the outer surface of porcine ZP, visualized ZP digestion with immunofluorescence microscopy with anti-ubiquitin antibodies, and recorded the presence of ubiquitinated proteins in ZP preparations from high quality metaphase II ova. More recently, they have observed Gly-Gly modifications, a fingerprint of ubiquitinated internal Lys-residues, on all three components of porcine ZP (ZPA, ZPB, and ZPC) using Nanospray LC-MS/MS spectroscopy (Peng et al., 2003; Zimmerman et al., 2011). These findings corroborate the pattern of sequential ubiquitination and proteasomal degradation of the ascidian sperm receptor protein HrVC70, an analogue of mammalian ZP. Similarly, Yokota and

Sawada (2007) reported that the vitelline envelopes of sea urchin eggs are already ubiquitinated prior to fertilization.

Enzymatically active proteasomes have been found in the boar sperm acrosome. There is evidence that sperm proteasomes are exposed onto the sperm surface and remain associated with acrosomal membranes during sperm-ZP penetration. Boar sperm proteasomes are associated with acrosomal membranes and matrix prior to AE and remain associated with the inner acrosomal membrane after AE (Morales et al., 2004; Zimmerman and Sutovsky, 2009; Yi et al., 2009, 2010a, 2010b). Proteasomal activity is present in motile boar spermatozoa (Yi et al., 2009). Adenosine triphosphate (ATP) is essential for the integrity of the 26S proteasome, which is maintained by the six 19S ATPase subunits. Depletion of sperm surface ATP by S. tuberosum apyrase inhibits sea urchin fertilization (Yokota and Sawada, 2007) and porcine IVF (Yi et al., 2009). Enzymatic activity of boar sperm proteasomes was confirmed in whole, motile spermatozoa, sperm acrosomal fractions and affinity purified proteasomes (Yi et al., 2009, Miles et al., 2013). These purified proteasomes were also tested for functionality via casein degradation (G. Manandhar and P. Sutovsky, unpublished data).

Sperm Proteasomes Can Degrade Zona Pellucida Proteins in Solution and In Situ

Studies in porcine and avian models suggest that sperm proteasomes can degrade the sperm receptor on porcine ZP (ZPC) and on the vitelline coat of Japanese quail egg (ZP3), respectively (Zimmerman et al., 2011; Sasanami et al., 2012). It is difficult to capture the action of sperm acrosomal enzymes during fertilization, but the Sutovsky lab developed an in vitro assay using live, freshly collected and capacitated

boar spermatozoa co-incubated with the ZP-proteins solubilized from 100 meiotically mature, fertilization competent porcine oocytes (Zimmerman et al., 2011). This enables the soluble ZP proteins to bind to sperm acrosomal surface as the zona matrix would during fertilization and induce acrosomal exocytosis, resulting in the formation of acrosomal shrouds similar to those seen on the surface of ZP during IVF. Since there is no solid zona matrix in this assay, the acrosomal shroud are easily separated from spermatozoa and interrogated for the degradation of the bound ZP-proteins. A distinct degradation pattern of the porcine sperm receptor component ZPC was observed, similar to the degradation pattern of ZPC with purified sperm proteasomes (Zimmerman et al., 2011). The observed, rapid degradation of ZPC by spermatozoa and purified sperm proteasomes was inhibited by ATP depletion with S. tuberosum apyrase and with proteasomal inhibitors (MG132, CLBL, and Epoxomicin); it was accelerated by ubiquitin-aldehyde, a C-terminally modified ubiquitin protein that stimulates proteasomal proteolysis (Zimmerman et al., 2011). Furthermore, they were able to record that purified boar sperm proteasomes can digest intact pig ZP of in vitro maturing ova and reduce the rate of polyspermic fertilization after IVF (Zimmerman et al., 2011). These results were corroborated by a study in Japanese quail model that used a similar in vitro system to demonstrate that the sperm proteasome is important for avian fertilization and helps sperm penetration through the perivitelline membrane which is homologous to ZP in mammals. Japanese quail spermatozoa contain proteasomes localized in the acrosomal region and can degrade the ZP1 protein in a fashion similar to the degradation of ZP3/ZPC in porcine model; this degradation is also inhibited by

proteasomal inhibitor MG132 and by extracellular ATP depletion by apyrase (Sasanami et al., 2012).

Recent Advances in the Study of Sperm Ubiquitin Proteasome System

There is a growing acceptance of the involvement of ubiquitin proteasome system in the reproductive process in plants, ascidians, echinoderms, and mammals, but many questions remain unanswered. How is sperm proteasomal activity regulated during sperm storage, capacitation, AE, and ZP-penetration? How are proteasomes inserted in the acrosome during spermiogenesis? What is the role of deubiquitinating enzymes in fertilization? Can we target sperm proteasomes for a contraceptive effect? Novel animal models and assays will pave the way to elucidate these mechanisms.

A novel transgenic boar model with green fluorescent protein (GFP) fused to the C-terminus of 20S proteasomal core subunit alpha-type 1 (PSMA1) has been developed through a joint effort between the Sutovsky, Prather, and Wells laboratories at the University of Missouri – Columbia (Miles et al., 2013). Functional GFP tagged proteasomes have been shown to be incorporated in not only fertilization competent spermatozoa, but in other tissues and cell types (Miles et al., 2013). Using cross-immunoprecipitation experiments, the authors identified various proteins interacting with the GFP-PSMA1 subunit such as lactadherin/MFGE8, spermadhesins and disintegrins/ADAM metalloproteinases; these proteins may regulate sperm proteasomal activity or may be the substrates of proteasomal proteolysis during fertilization (Miles et al., 2013). They have also proposed a method of isolating enzymatically active GFP-proteasomes through GFP affinity purification (Miles et al., 2013). This novel model will

be useful for studies of fertilization and wherever UPS plays a role in cellular function or pathology.

A protection assay utilizing proteasomal inhibitors was used as an alternative method of identifying sperm-proteasome interacting proteins. The treatment of porcine spermatozoa with proteasomal inhibitors during coincubation with solubilized ZP proteins led to the accumulation of sperm acrosomal surface-associated proteins which would otherwise be degraded during AE (Zimmerman et al., 2011). The identified proteins that were protected from degradation by proteasomal inhibitors included Sperm Adhesion Molecule 1 (SPAM1), lactadherin/MFGE8, Zona Pellucida Binding Protein 2 (ZPBP2), and fragments of Acrosin-Binding Protein ACRBP (SP32) (Zimmerman et al., 2011). Proteasomal degradation of these acrosomal zona-binding proteins could facilitate the ZP-induced acrosomal exocytosis and/or serve to terminate primary sperm-ZP binding as the fertilizing spermatozoon starts to move forward and penetrate deeper into the ZP. Furthermore, proteasomal inhibitors suppressed the induction of AE when human spermatozoa were incubated with recombinant human ZP3 and ZP4 (Chakravarty et al., 2008). Current research also implicates the ubiquitin proteasome system in sperm capacitation and AE, and that these sperm transformations may be regulated and reversed by deubiquitinating enzymes that also regulate oocyte anti-polyspermy defense and oocyte maturation. Inhibition of the Ubiquitin Activating Enzyme UBA1 (E1) during boar sperm capacitation alters proteasomal subunit properties and sperm fertilizing ability in vitro in a dose-dependent manner (Yi et al., 2012). Ubiquitin conjugating enzyme, the ubiquitin-ligase UBR7, has been detected in

the boar sperm acrosome, and de novo ubiquitination of UBB+1 has been achieved using sperm acrosomal extract (S.W. Zimmerman and P. Sutovsky, unpublished data). Deubiquitinating enzymes from the ubiquitin C-terminal hydrolase (UCHL) family have been shown to regulate anti-polyspermy defense and oocyte cortex and meiotic spindle formation. Block of sperm UCHL3 increases porcine polyspermy in vitro while supplementation of recombinant UCHs to IVF media reduced polyspermy and increased the rate of monospermic fertilization (Yi et al., 2007b). Interference with bovine oocyte UCHL1 alters cortical granule maturation and causes polyspermy (Susor et al., 2010). Block of murine oocyte UCHL1 and UCHL3 prevents sperm incorporation in the ooplasm and causes meiotic spindle anomalies and polar body extrusion defects (Mtango et al., 2012a and b). Subfertility, in vitro polyspermy and failed morula compaction have been reported in the gad mutant mouse expressing an inactive form of UCHL1 (Kwon et al., 2003; Mtango et al., 2012a). This data suggests that ubiquitination plays a key role in sperm function and that the deubiquitinating enzymes (UCHL1 and UCHL3) are important during fertilization and preimplantation embryo development.

Conclusions

Accumulating evidence suggests that the putative mammalian egg coat lysin is the 26S proteasome. There is data supporting all of the prerequisites in the porcine fertilization model: 1) all three pig zona components (ZPA, ZPB, ZPC) are ubiquitinated, 2) enzymatically active proteasomes are present in the boar sperm acrosome and exposed onto the acrosomal surface, and 3) motile boar spermatozoa and isolated boar

sperm proteasomes are capable of degrading the sperm receptor components of the zona pellucida in vitro.

Recent advancements have elucidated more ways in which the UPS affects mammalian reproduction that could possibly be manipulated to develop novel forms of non-hormonal contraceptives. Sperm proteasomes have been shown to co-purify with various acrosomal sperm-membrane binding proteins. Sperm capacitation and acrosome reaction have been reported to be altered by interference with UPS enzymes responsible for ubiquitin-substrate conjugation, deubiquitination, and proteasomal proteolysis. Acrosomal extracts can ubiquitinate exogenous substrates. Therefore, the properties of sperm borne proteasomes are consistent with their proposed role of mammalian zona lysin. Evidence from several laboratories, animal models and human gamete studies supports the participation of sperm proteasomes in multiple aspects of the fertilization process, including sperm capacitation, sperm zona binding, acrosomal exocytosis, and sperm-zona/vitelline coat penetration.

Acknowledgements

We thank Ms. Kathryn Craighead for editorial and clerical assistance. Our gratitude belongs to our colleagues/associates Dr. Young-Joo Yi, Ms. Miriam Sutovsky, Ms. Wonhee Song, Dr. Peter Vargovic, Dr. Gaurishankar Manandhar and Dr. Shawn Zimmerman, as well as to our collaborators Drs. Randal Prather, Kevin Wells, Richard Oko, Satish Gupta and David Miller. Some of the work reviewed in this manuscript was supported by Agriculture and Food Research Initiative Competitive Grant no. 2011-

67015-20025 from the USDA National Institute of Food and Agriculture, and by the seed funding from the Food for the 21st Century Program of the University of Missouri.

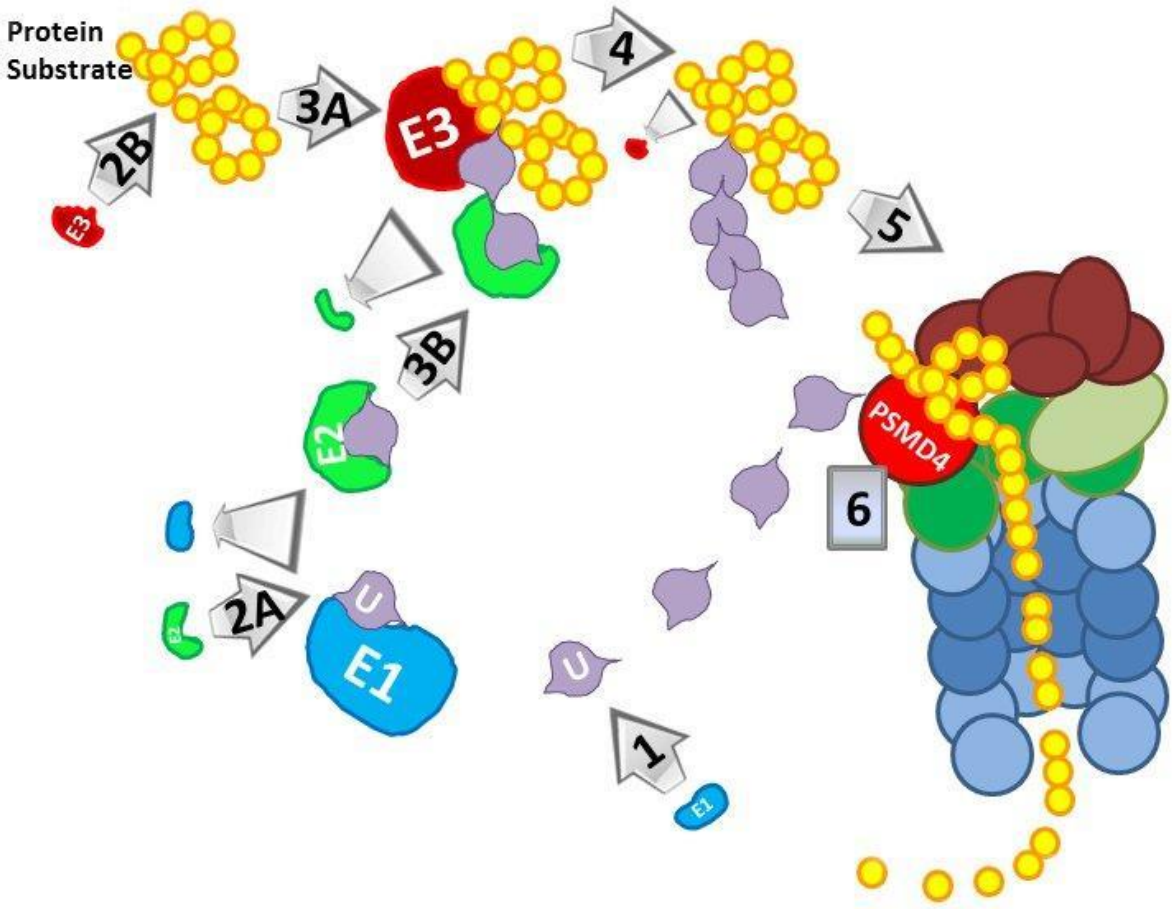

Figure 1.1 Diagram of protein ubiquitination and degradation by the 26S proteasome. (Step 1) Monoubiquitin is activated by a phosphorylated ubiquitin activating enzyme E1 (UBA1). (Step 2A) UBE1 is supplanted by ubiquitin carrier enzyme/ubiquitin conjugating enzyme E2 (UBE2). (Step 2B) Concurrently, the substrate protein is engaged by an E3-type ubiquitin ligase. (Step 3A) Ubiquitin ligase E3 covalently links an activated monoubiquitin to an internal Lys-residue of the substrate protein. (Step 3B) A second activated ubiquitin molecule is linked to the substrate bound ubiquitin. (Step 4) The ensuing tandem ligation of additional activated ubiquitin molecules results in the formation of a multi-ubiquitin chain. (Step 5) Multi-ubiquitin chain of four or more ubiquitin molecules is recognized and engaged by subunit PSMD4 of the 19S proteasomal regulatory complex. (Step 6) The substrate protein is deubiquitinated (liberated ubiquitin molecules re-enter the cycle), unfolded, threaded through the 20S core, and cleaved into small peptides, released from the 20S core lumen. [Sutovsky, P. (2011). "Sperm Proteasome and Fertilization." Society for Reproduction and Fertility Volume 142, pgs 1-14.]

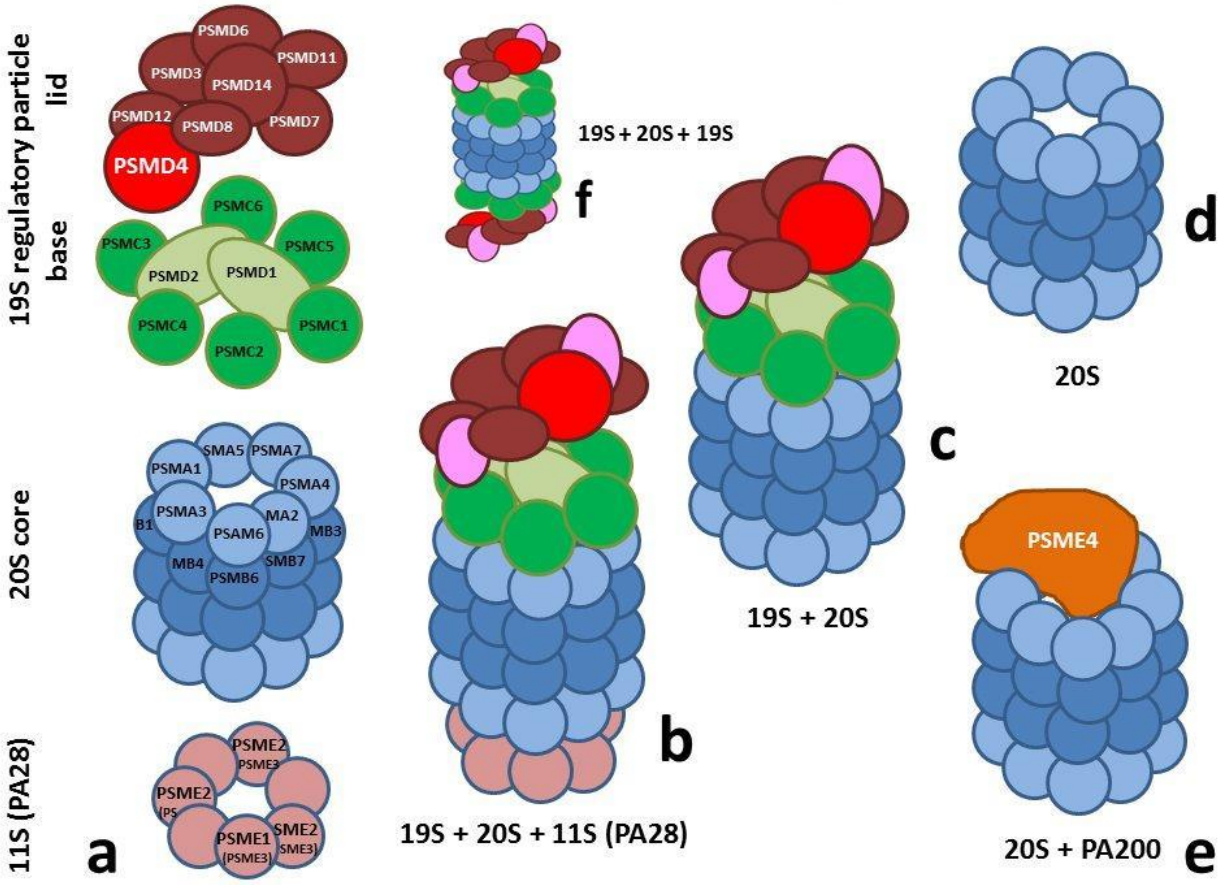

Figure 1.2. Variations on the subunit composition of the 26S proteasome. (a) Subunit makeup of the (top to bottom) 19S regulatory particle (lid+base), 20S core, and 11S particle (PA28). (b) 20S core capped with 19S particle on one side and an 11S complex/PA28 on the other. (c) 20S core capped with one 19S particle. (d) Uncapped 20S proteasome. (e) 20S core capped with proteasome activator PA200. (f) Canonical 26S proteasome, with one 19S particle/cap on each side of 20S core. [Sutovsky, P. (2011). "Sperm Proteasome and Fertilization." Society for Reproduction and Fertility Volume 142, pgs 1-14. © Society for Reproduction and Fertility (2013). Reproduced by permission.]

Table 1.1 26S Proteasome subunit function and nomenclature by species

	Hugo/GDB symbol	*H. sapiens*	*B. Taurus*	*S. Scrofa*	*R. norvegicus*	*M. musculus*	*C. elegans*	*S. cerevisiae*	Function
20S *α*-type subunits									
*α*1	PSMA6	Pros27/ Iota/ p27k	PSMA6	PSMA6	Psma6	Psma6/ Pros-27	PAS-1	Scl1/YC7	Gate to 20S core
*α*2	PSMA2	HC3	PSMA2	PSMA2	Psma2	Psma2	PAS-2	Pre8/Y7	Gate to 20S core
*α*3	PSMA4	HC9	PSMA4	PSMA4	Psma4	Psma4	PAS-3	Pre9/Y13	Gate to 20S core
*α*4	PSMA7	XAPC7-S	PSMA7	PSMA7	Psma7	Psma7	PAS-4	Pre6	Gate to 20S core
α5	PSMA5	Zeta	PSMA5	PSMA5	Psma5	Psma5	PAS-5	Pup2/Doa5	Gate to 20S core
α6	PSMA1	HC2/ Pros30	PSMA1	PSMA1	Psma1	Psma1/ Pros-30	PAS-6	Pre5	Gate to 20S core
α7	PSMA3	HC8	PSMA3	PSMA3	Psma3	Psma3	PAS-7	Pre10/YC1	Gate to 20S core
20S *β*-type subunits									
*β*1	PSMB6	Y/Delta	PSMB6	PSMB6	Psmb6	Psmb6/ Lmp19/ Mpnd	PBS-1	Pre3	Caspase-like peptidase activity
*β*2	PSMB7	Z	PSMB7	PSMB7	Psmb7	Psmb7/ MC14	PBS-2	Pup1	Trypsin-like protease activity
*β*3	PSMB3	HC10	PSMB3	PSMB3	Psmb3	Psmb3	PBS-3	Pup3	
*β*4	PSMB2	HC7	PSMB2	PSMB2	Psmb2	Psmb2	PBS-4	Pre1	
*β*5	PSMB5	X/MB1	PSMB5	PSMB5	Psmb5	Psmb5	PBS-5	Pre2/Doa3	Chymotrypsin-like protease activity
*β*6	PSMB1	HC5	PSMB1	PSMB1	Psmb1	Psmb1	PBS-6	Pre7	
*β*7	PSMB4	HN3	PSMB4	PSMB4	Psmb4	Psmb4	PBS-7	Pre4	
*β*1i	PSMB9	LMP2/ RING12	PSMB9	PSMB9	Psmb9/Lmp2	Psmb9/ Lmp2			Caspase-like activity/immunoproteasome
*β*2i	PSMB10	MECL1	PSMB10	PSMB10	Psmb10	Psmb10/ Mecl-1/ Lmp7			Trypsin-like activity/immunoproteasome
*β*5i	PSMB8	LMP7/ RING10	PSMB8/ LMP7	PSMB8	Psmb8/ Ring10	Psmb8			Chymotrypsin-like activity/immunoproteasome
19S ATPase subunits									
Rpt1/ S7	PSMC2	MSS1/S7	PSMC2/ MSS1	PSMC2	Psmc2/Mss1	Psmc2/ Mss1	RPT-1	Yta3/Cim5	ATPase, Substrate unfolding

Table 1.1 26S Proteasome subunit function and nomenclature by species continued									
Rpt2/ S4	PSMC1	p56/S4	PSMC1/ p56	PSMC1	Psmc1/S4	Psmc1/ P26S4	RPT-2	Yta5/mts2	ATPase, Substrate unfolding, Gate-opening
Rpt3/ S6b	PSMC4	TBP7/S6/ p48	PSMC4/ p48	PSMC4	Psmc4/Tbp7	Psmc4	RPT-3	Yta2	ATPase, Substrate unfolding, Gate-opening
Rpt4/ S10b	PSMC6	p42/ CADP44/ SUG2	PSMC6/ p42	PSMC6	Psmc6	Psmc6	RPT-4	Sug2/Pcs1/ Crl13	ATPase, Substrate unfolding
Rpt5/ S6a	PSMC3	TBP1/S6a	PSMC3/ p50	PSMC3	Psmc3/Tbp1	Psmc3	RPT-5	Yta1	ATPase, Substrate unfolding, Gate-opening
Rpt6/ S8	PSMC5	p45/S8/ TRIP1/ SUG1	PSMC5/ p45	PSMC5	Psmc5/Sug1	Psmc5/ FZA-B/ Sug1/M56	RPT-6	Sug1/Cim3 /let1/Crl3	ATPase, Substrate unfolding
19S non-ATPase subunits									
Rpn1/ S2	PSMD2	p97/ TRAP-2/ 55.11/S2	PSMD2/ p97	PSMD2	Psmd2	Psmd2/ Tex190	RPN-1	Nas1/mts4/ Hrd2	PIPs scaffolding, PIPs translocation, Gate-opening
Rpn2/ S1	PSMD1	p112/S1	PSMD1/ p112	PSMD1	Psmd1	Psmd1/ P112	RPN-2	Sen3	PIPs scaffolding, PIPs translocation, Gate-opening
Rpn3/ S3	PSMD3	p58/S3/ TSTA2	PSMD3/ p58	PSMD3	Psmd3	Psmd3/ P91A	RPN-3	Sun2	
Rpn4								Son1/Ufd5	Proteasome gene, transcription
Rpn5/ p55	PSMD12	p55	PSMD12 /p55	PSMD12	Psmd12	Psmd12/ P55	RPN-5	Nas5	
Rpn6/ S9	PSMD11	p44.5/S9	PSMD11 /p44.5	PSMD11	Psmd11	Psmd11/ P44.5	RPN-6	Nas4	
Rpn7/ S10a	PSMD6	p44/S10a	PSMD6/ p44	PSMD6	Psmd6	Psmd6	RPN-7		
Rpn8/ S12	PSMD7	p40/S12/ MOV34	PSMD7/ p40	PSMD7	Psmd7	Psmd7/ Mov-34	RPN-8	Nas3	
Rpn9/ S11	PSMD13	p40.5/S11	PSMD13 /p40.5	PSMD13	Psmd13	Psmd13	RPN-9	Nas7/mts1	
Rpn10/ S5a	PSMD4	S5a/AF	PSMD4	PSMD4	Psmd4	Psmd4/ S5a/Mcb1	RPN-10	Mcb1/pus1 /Sun1	Ub receptor

Table 1.1 26S Proteasome subunit function and nomenclature by species									
S5b	PSMD5	p50.5/S5b	PSMD5/ p50.5	PSMD5	Psmd5	Psmd5			
Rpn11/ S13	PSMD14	S13/ POH1/ PAD1	PSMD14	PSMD14	Psmd14	Psmd14/ Pad1/Poh1	RPN-11	Mpr1/pad1/ mts5	DUB
Rpn12/ S14	PSMD8	p31/S14/ HIP6/ Nin1p	PSMD8/ p31	PSMD8	Psmd8	Psmd8	RPN-12	Nin1/mts3	
Rpn13	ADRM1	ADRM1						DAQ1	Ub receptor, UCH37 recruitment
p28	PSMD10	p28/S15	PSMD10 /p28	PSMD10	Psmd10/ p28Gank	Psmd10/ P28/ gankyrin		Nas6	
p27/ S15	PSMD9	p27/S15	PSMD9/ p27	PSMD9	Psmd9/ Bridge	Psmd9/P27		Nas2	PSM modulator

Table 1.1. Proteasome subunit function and nomenclature by species. HUGO: Human Genome Organization, GDB: Human Genome Database, DUB: Deubiquitinating enzyme, Ub: ubiquitin, PSM: Proteasome, PIPs: Proteasome-interacting proteins/proteasome substrates. (Voges et al., 1999; Chen et al., 2008; Tanaka, 2009).

CHAPTER TWO

Transgenic Pig Carrying Green Fluorescent Proteasomes

Reference: Miles, E.L., O'Gorman, C., Zhao, J., Samuel M., Walters, E., Yi, Y-J., Sutovsky, M., Prather, R.S., Wells, K., Sutovsky, P. (2013). Transgenic Pig Carrying Green Fluorescent Proteasomes. *Proceedings of the National Academy of Sciences of the United States of America*.

Abstract

Among its many functions, the ubiquitin–proteasome system regulates substrate-specific proteolysis during the cell cycle, apoptosis, and fertilization and in pathologies such as Alzheimer's disease, cancer, and liver cirrhosis. Proteasomes are present in human and boar spermatozoa, but little is known about the interactions of proteasomal subunits with other sperm proteins or structures. We have created a transgenic boar with green fluorescent protein (GFP) tagged 20S proteasomal core subunit α-type 1 (PSMA1-GFP), hypothesizing that the PSMA1-GFP fusion protein will be incorporated into functional sperm proteasomes. Using direct epifluorescence imaging and indirect immunofluorescence detection, we have confirmed the presence of PSMA1-GFP in the sperm acrosome. Western blotting revealed a protein band corresponding to the predicted mass of PSMA1-GFP fusion protein (57 kDa) in transgenic spermatozoa. Transgenic boar fertility was confirmed by in vitro fertilization, resulting in transgenic blastocysts, and by mating, resulting in healthy transgenic offspring. Immunoprecipitation and proteomic analysis revealed that PSMA1-GFP

copurifies with several acrosomal membrane-associated proteins (e.g., lactadherin/MFGE8 and spermadhesin alanine-tryptophan-asparagine). The interaction of MFGE8 with PSMA1-GFP was confirmed through cross-immunoprecipitation. The identified proteasome-interacting proteins may regulate sperm proteasomal activity during fertilization or may be the substrates of proteasomal proteolysis during fertilization. Proteomic analysis also confirmed the interaction/coimmunoprecipitation of PSMA1-GFP with 13/14 proteasomal core subunits. These results demonstrate that the PSMA1-GFP was incorporated in the assembled sperm proteasomes. This mammal carrying green fluorescent proteasomes will be useful for studies of fertilization and wherever the ubiquitin–proteasome system plays a role in cellular function or pathology.

Introduction

There has been growing acceptance of the essential role of the ubiquitin–proteasome system (UPS) in many aspects of the fertilization process in mammals, lower vertebrates, and invertebrates (Sakai et al., 2004; Sutovsky, 2011; Signoreli et al., 2012). Sperm capacitation, acrosomal exocytosis, sperm binding to and penetration through the zona pellucida, and degradation of the sperm-borne mitochondria and mtDNA inside the zygote all involve proteasomal proteolysis in mammals (Sutovsky et al., 2004; Zimmerman et al., 2011; Redgrove et al., 2011). Multiple laboratories have reported the presence and involvement of sperm-borne proteasomes in human, mouse, porcine, bovine, avian, ascidian, and echinoderm (Sawada et al., 2002; Morales et al., 2004; Pasten et al., 2005; Kong et al., 2009; Zimmerman et al., 2011; Sasanami et al.,

2012). Spermborne proteasomes and associated enzymes have been detected in the cytosol/matrix of the acrosome and bound to the inner and outer acrosomal membranes of the sperm head (Morales et al., 2004; Sutovsky et al., 2004; Yi et al., 2010a, 2010b; Zimmerman et al., 2011). Proteasome-specific proteolytic and deubiquitinating activities have been measured in live, intact spermatozoa by using specific fluorometric substrates (Yi et al., 2007b; Zimmerman et al., 2011). Fertilization has been shown to rely on proteasomal proteolysis by the application of a variety of proteasome specific inhibitors and antibodies (Morales et al., 2003, 2004; Sutovsky et al., 2004; Diaz et al., 2007; Chakravarty et al., 2008). Phosphoproteome studies detected many UPS proteins undergoing phosphorylation during sperm capacitation and acrosome reaction in the mouse, boar, and rat (Ficarro et al., 2003; Baker et al., 2010; Signorelli et al., 2012).

The UPS tags outlived or damaged intracellular proteins through a multistep process with a small chaperone protein ubiquitin (8.5 kDa) that targets them for degradation by the 26S proteasome, a multisubunit protease (Glickman and Ciechanover, 2002). A substrate protein first is marked for degradation by the covalent attachment of a single 76-amino acid ubiquitin molecule. Subsequent ubiquitin molecules are covalently attached, typically to the K48 or K63 residue of the previous ubiquitin molecule through a series of enzymatic reactions. This process is initiated by the activation of an unconjugated monoubiquitin with phosphorylation-dependent ubiquitin-activating enzyme E1 (UBE1).UBE1 then is replaced with ubiquitin-conjugating enzyme E2. Simultaneously, the targeted substrate protein is located and secured by

ubiquitin ligase E3, which is the enzyme responsible for substrate specificity of protein ubiquitination. The E3 ligase catalyzes the covalent binding of the C-terminal Gly residue (G76) of ubiquitin to an internal Lys residue of the substrate protein. Subsequently, tandem ligation of additional ubiquitin molecules results in the formation of a multiubiquitin chain (four or more ubiquitin molecules) that makes the substrate protein recognizable to the PSMD4 subunit of the 19S regulatory complex of the 26S proteasome.

The canonical 26S proteasome is a large cylindrical multisubunit protease containing a 20S core catalytic particle capped at one or both ends by a 19S regulatory particle. The 20S core is composed of 28 subunit molecules of 14 different kinds, arranged in four heptamerically stacked rings in an α7β7β7α7 pattern. The inner two β rings each contain seven β-type/PSMB subunits, three of which have active protease sites responsible for proteolysis. Subunit β1/PSMB6 has a caspase-like peptidase activity, subunit β2/PSMB7 has a trypsin-like peptidase activity, and subunit β5/PSMB5 displays a chymotrypsin-like peptidase activity (Pasten et al., 2005; Tanaka, 2009). The α-type subunits connect the 20S core to the 19S regulatory particle and have no known protease activity; however, some are reported to have RNase/endonuclease activities (reviewed by Brooks, 2010). The 19S regulatory particle contains 19 subunits divided between the lid and base subcomplexes. The lid contains up to 14 non-ATPase subunits (PSMD1–14) that recognize the polyubiquitin chain linked to the target protein, which then is removed by the Rpn11/PSMD14 subunit's deubiquitinating activity. The base

contains six ATPase subunits (Rpt1–6/PSMC1–6) that unfold and translocate the substrate protein and regulate proteasome activity (Tanaka, 2009).

Little is known about the interactions of specific proteasomal subunits with proteasome-interacting proteins (PIPs) and the mechanisms behind these proteasome-dependent events. To give insight into the identity of these PIPs and their mechanisms during fertilization, a transgenic boar was created carrying the fluorescently tagged 20S core particles with the enhanced green fluorescent protein (GFP) fused to the proteasomal subunit α-6/PSMA1 (PSMA1-GFP transgene). The purpose of this study is to report the localization and subunit composition of the sperm-borne proteasomes, and to promote the use of this unique transgenic pig model in the investigation of the cellular mechanism and pathologies associated with the function or dysfunction of UPS, respectively. By using the transgenic boar spermatozoa for epifluorescence, immunofluorescence, Western blotting, immunoprecipitation, and tandem mass spectrometry (MS/MS), we provide evidence that the subunits of the sperm acrosome-borne proteasomes interact with acrosomal membrane proteins that may anchor proteasomes to the acrosomal structures and/or depend on proteasomes for their function during fertilization. These results might provide insight into the proteasome-dependent mechanisms behind the UPS's role in fertilization and encourage the use of this unique transgenic boar model for the study of the UPS in all areas of research (fertilization, neurodegenerative disorders, and genetic diseases).

Materials and Methods

Plasmid Constructs and DNA Preparation

The full-length sequence for porcine PSMA1 subunit of 20S proteasomal core was first constructed in silico from public data (Figure 2.1). This sequence was used to identify a GenBank EST sequence that appeared to be full length (accession no. CO946059), which was then retrieved from cryopreserved archive. The PSMA1 coding region was modified for cloning and recovered from the plasmid by PCR (primers: TTTTGGCAAAGAATTCGGAACCATGTTTCGCAACCAGT,CATGGTGGCGACCGGTGCATGTTCCA TTGGTTCAT). The amplimer was cloned into pCAG-CreGFP (Addgene plasmid 13776) at the *AgeI* sites. Both vector and insert were gel purified, incubated in In-Fusion (Clontech) according to the manufacturer's instructions, and transformed into NEB 5-alpha chemically competent cells (New England BioLabs). Positive colonies were sequenced to confirm correct ligation and the absence of PCR induced point mutations. The PSMA1-GFP transgene, a selectable marker (pKW4, *AphII*) (Lorson et al., 2011), and the chicken egg-white lysozyme matrix attachment region (cMAR) (Wells et al., 1999) were purified from vector sequence for cotransfection. The resulting linearized DNA fragments were transfected using 10 µg of total DNA at a ratio of 5:2:2 (PSMA1-GFP:*AphII*:cMAR).

Fibroblast Cell Culture, Transfection, and Selection

Male porcine fetal fibroblast (104821, NSRRC) cells were cultured for 72 h before electroporation in DMEM with pyruvate and 12% FBS at 38.5°C in 5% CO2, 5% O2, 90% air, and 100% humidity. Culture, transfection, and selection were performed as described previously (Ross et al., 2010). Following selection, fluorescent colonies were

harvested. Approximately two-thirds of each colony was placed back into culture and one-third was used for cell lysis and PCR analysis of positive clones.

Somatic Cell Nuclear Transfer

Mature oocytes were purchased from ART, Inc. and used for somatic cell nuclear transfer essentially as described (Zhao et al., 2009, 2010). The oocytes were shipped overnight in maturation medium no. 1 (Li et al., 2009). After 24 h of culture, they were transferred to medium no. 2. After 40 h of maturation, they were enucleated and fused with a single intact donor cell by using two direct pulses of 1.2 kV/cm for 30 μs (BTX Electro Cell Manipulator 200) in 0.3 M mannitol, 1.0 mM $CaCl_2$, 0.1 mM $MgCl_2$, and 0.5 mM Hepes (pH adjusted to 7.0 to 7.4). Fused oocytes were placed in 500 μL porcine zygote medium-3 (PZM3) containing 500 nM Scriptaid, a histone deacetylase inhibitor (Zhao et al., 2009), and cultured for 14 to 16 h at 38.5°C in humidified 5% CO_2, 5% O_2, and 90% N_2. Cloned zygotes were transferred surgically to the oviducts of gilts in standing estrus. Six embryo transfers were performed, transferring 881 embryos. Eight piglets were recovered at caesarian section (six breathed). Five of the eight did not express, and one healthy expressing founder was identified (Appendix Table 1). Animal care followed a protocol approved by Animal Care and Use Committee of the University of Missouri.

Semen Collection and Processing

Ejaculates from wild type boar and the *PSMA1-GFP* transgenic Minnesota Mini boars were collected under the guidance of approved Animal Care and Use (ACUC) protocols of the University of Missouri, Columbia (UM). The wild-type boar was placed

on a routine weekly collection while the transgenic boars were collected less frequently, as needed. Sperm-rich fractions of the ejaculates with greater than 85% sperm motility and normal sperm acrosomes were used. Sperm concentrations were estimated using a hemacytometer (Fisher Scientific, Houston, TX, USA). The percentage of motile sperm was estimated at 38.5°C by light microscope at 250 x magnification. Semen was slowly cooled to room temperature (20°C) within 2 hrs after collection. Semen was then transferred into 15 ml tubes, centrifuged at room temperature for 10 min at 800 x *g*, and the supernatant was removed. The spermatozoa were processed according to each experiment's requirements and stored at -80°C. In order to use the semen for *in vitro* fertilization (IVF), the semen was diluted with X-Cell Extender (Cat. #USA851X, IMV Technologies, Maple Grove, MN; final concentration of 1×10^8 spermatozoa/ml). The diluted semen was stored in a styrofoam box at room temperature for 5 days. Unless otherwise noted, all chemicals used in this study were purchased from Sigma Chemical Co. (St. Louis, MO).

Collection and In Vitro Maturation (IVM) of Porcine Oocyte

Ovaries were collected from prepubertal gilts at a local slaughterhouse and transported to the laboratory in a warm box (25 to 30°C). Cumulus-oocyte complexes (COCs) were aspirated from antral follicles (3 to 6 mm in diameter), washed three times in HEPES-buffered Tyrode lactate (TL-HEPES-PVA) medium containing 0.01% (w/v) polyvinyl alcohol (PVA), then washed three times with the maturation medium (Abeydeera et al., 1998). Each time, a total of 50 COCs were transferred to 500 µl of the maturation medium that had been covered with mineral oil in a 4-well multidish (Nunc,

Roskilde, Denmark) and equilibrated at 38.5°C, with 5% CO2 in air. The medium used for oocyte maturation was tissue culture medium (TCM) 199 (Gibco, Grand Island, NY) supplemented with 0.1% PVA, 3.05 mM D-glucose, 0.91 mM sodium pyruvate, 0.57 mM cysteine, 0.5 μg/ml LH (L5269, Sigma), 0.5 μg/ml FSH (F2293, Sigma), 10 ng/ml epidermal growth factor (E4127, Sigma), 10% porcine follicular fluid, 75 μg/ml penicillin G, and 50 μg/ml streptomycin. After 22 h of culture, the oocytes were washed twice and cultured in TCM199 without LH and FSH for 22 h at 38.5°C, 5% CO2 in air.

In Vitro Fertilization (IVF) and Culture (IVC) of Porcine Oocytes

After IVM, cumulus cells were removed with 0.1% hyaluronidase in TL-HEPES-PVA medium and ova were washed three times with TL-HEPES-PVA medium and three times with Tris-buffered (mTBM) medium [1] containing 0.2% BSA (A7888, Sigma). Thereafter, 20 oocytes were placed into each of four 100 μl drops of the mTBM medium, which had been covered with mineral oil in a 35 mm polystyrene culture dish. The dishes were allowed to equilibrate in the incubator for 30 min until spermatozoa were added for fertilization. One ml liquid semen preserved in X-Cell Extender was washed twice in PBS containing 0.1% PVA (PBS-PVA) at 800 × *g* for 5 min, respectively. At the end of the washing procedure, the spermatozoa were resuspended in mTBM medium. After appropriate dilution, 1 μl of this sperm suspension was added to the medium that contained oocytes to give a final sperm concentration of 5×10^5 sperm/ml. Oocytes were co-incubated with spermatozoa for 6 hrs at 38.5°C, 5% CO2 in air. At 6 hrs after IVF, oocytes were transferred into 500 μl PZM-3 medium (Yoshioka et al., 2002) containing 0.4% BSA (A6003, Sigma) for further culture during 16 to 19 hrs or 144 hrs.

Evaluation of Oocyte Fertilization and Embryo Culture

Semen collection, in vitro oocyte maturation and in vitro fertilization were performed using standard methods described above. For evaluation of fertilization, oocytes/zygotes or embryos were fixed with 2% formaldehyde for 40 min at room temperature, washed with PBS three times, permeabilized with PBS-TX for 40 min at room temperature, and stained with 2.5 µg/ml DAPI (Molecular Probes, Eugene, OR) for 40 min. Sperm penetration and fertilization status of the zygotes (unfertilized, fertilized-monospermic or fertilized-polyspermic) or the number of nuclei in embryos/blastocyst were assessed under epifluorescence microscope. Image acquisition was performed on a Nikon Eclipse 800 microscope (Nikon Instruments Inc., Melville, NY) with Cool Snap camera (Roper Scientific, Tucson, AZ) and MetaMorph software (Universal Imaging Corp., Downington, PA). The same imaging system was used for the analysis of tissue fragments collected from stillborn transgenic siblings of the founder boar (Figure 2.2); microscopic tissue fragments were whole-mounted on ceroscopy slides in TL-HEPES medium with 10% PVP and directly imaged under epifluorescence illumination at the excitation wave length corresponding to peak excitation wavelength of GFP. To assure that the resultant signals were not due to autofluorescence, control acquisitions were also made in the UV and red excitation and emission bands. None of the GFP-patterns described in this study were observed in tissues of non-transgenic offspring.

Immunofluorescence of Boar Spermatozoa

Spermatozoa were affixed to poly-lysine treated microscopy coverslips and fixed in 2% formaldehyde, washed, permeablized in PBS with 0.1% Triton-X-100 (PBS-TX) and

blocked in PBS-TX containing 5% normal goat serum. Spermatozoa were incubated with mouse monoclonal antibody raised against the green fluorescent protein (GFP) from the jellyfish *Aequorea victoria* (1:100 dilution, cat #33-2600; Zymed Laboratories Inc., South San Francisco, CA, USA) overnight. Then they were incubated in PBS-TX containing 1% normal goat serum with goat-anti-mouse (GAM)-IgG-FITC (1:100 dilution; Zymed – Invitrogen) and DAPI (1:100; Molecular Probes - Invitrogen) for 40 min. Image acquisition was performed as described for oocytes.

Western Blotting

Sperm were washed in protein-free PBS and sperm concentration was determined using a hemocytometer so that approximately 1 x 10^9 spermatozoa/ml were loaded per lane after extraction. Spermatozoa were washed again in PBS and boiled for 5 min with loading buffer (50 mM Tris (pH 6.8), 150 mM NaCl, 2% SDS, 20% glycerol, 5% β-mercaptoethanol, 0.02% bromophenol blue). Gel electrophoresis of 10 µl total protein/lane was performed on 4 -20% gradient gels (PAGEr Gels, Lonza, Rockland, ME), followed by protein transfer to PVDF membranes (Immobilon P, Millipore Corp., Billerica, MA) using an Owl wet transfer system (Fisher Scientific, Houston, TX) at a constant 50 V for 4 hrs. The membranes were sequentially incubated with 10% non-fat milk for 1 hr and with one of the following antibodies: mouse monoclonal anti-GFP antibody (1:2000 dilution, cat. # 33-2600; Zymed - Invitrogen), mouse monoclonal anti-GFP antibody (1:2000 dilution, cat. #A11120; Invitrogen), mouse monoclonal anti-PSMA1/α-6 proteasome subunit (1:2000 dilution, cat. #PW9390; Enzo), mouse monoclonal anti-proteasome 20S core subunits alpha-type 1,2,3,5,6, and 7 (1:2,000

dilution, cat. #PW8195; Enzo), mouse monoclonal anti-proteasome 20S core antibodies (1:2,000 dilution, cat. #PW8155; Enzo), or mouse monoclonal anti-MFGE8 antibody (1:1,000 dilution, cat. #D199-3; MBL) overnight. The membranes were washed and incubated with an appropriate species-specific secondary antibody such as the HRP-conjugated goat-anti-mouse (GAM-IgG-HRP), HRP-goat-anti-rabbit IgG or goat-anti-Armenian hamster IgG-HRP antibodies (1:10,000 dilution; used to detect anti-MFGE8 antibody) for 1 hr at room temperature in 1% nonfat dry milk in TBS/Tween. The membranes were washed and reacted with 1.5 mL of chemiluminescent substrate (Illuminata Crescendo, Millipore Corp., Billerica, MA) for 5 min prior to being exposed to Kodak BioMax Light film (Kodak, Rochester, NY, USA).

Acrosomal Extracts of Boar Spermatozoa

Fresh boar spermatozoa were transferred to 15-mL Falcon tubes and centrifuged at 350 × g in a Fisher Scientific centrifuge for 5 min to remove the seminal plasma. The supernatant was removed, and the pellet was resuspended and washed in 9 mL of TL-Hepes containing 0.1% polyvinyl alcohol and 0.5% hyaluronidase, each time collected by centrifugation at 350 × g for 5 min. After washing, sperm pellets were resuspended in RIPA buffer (50 mM Tris·HCl, pH 8; 150 mM NaCl; 1% Triton; 0.5% sodium deoxycholate; 0.1% SDS; and PMSF, 1:200) or modified RIPA buffer (50 mM Tris·HCl, pH 8; 150 mM NaCl; 1% Nonidet P-40; 0.5% sodium deoxycholate; 1 mg/mL leupeptin; and 1 mg/mL pepstatin); resuspended samples were sonicated by using Digital Sonifier (Branson) for 1 min at 30% intensity. A modified RIPA buffer (Nonidet P-40) was included because the regular RIPA buffer (Triton X-100) may disrupt some protein–protein interactions. To

prepare the acrosome extract, the disrupted spermatozoa were centrifuged at 5,000 × *g* for 10 min at 4 °C, and supernatants were collected free of sperm head/tail fragments, as determined by light microscopy. The final supernatant fraction was stored at −80 °C.

Immunoprecipitation and MALDI-TOF Mass Spectroscopy

Boar sperm extracts were immunoprecipitated with the anti-GFP antibody (catalog no. A11120; Invitrogen) by using the Seize X Protein G Immunoprecipitation Kit (Pierce), separated on 4–20% gradient gels (PAGE resolving Gels; Lonza) and stained with Coomassie blue. The immunoprecipitated bands were excised carefully from the Coomassie blue-stained gel, destained, reduced with DTT, alkylated with iodoacetamide, and then trypsinized overnight. The digest solutions were recovered from the gel pieces and transferred to Axygen MAXYMum Recovery microtubes. The gel pieces were extracted further, pooled, and lyophilized dry. The dried digests were reconstituted and analyzed by Nano-LC Nanospray quadrupole time-of-flight MS plus MS/MS on an Agilent 6520A mass spectrometer. The “MS plus MS/MS” data were analyzed with the “Find Compounds by Auto MS/MS” program in the Agilent Mass Hunter software (version B.04.00) suite. The MALDI-TOF MS spectra peak lists were obtained for the spectra after internal recalibration using trypsin autolysis fragment masses, computer baseline correction, noise removal, and peak de-isotoping. The threshold for generating peak lists was set to 2% of the maximum observed peak area. Data were exported in the Mascot Generic Format (.mgf) required for submission to an in-house copy of Matrix Science’s Mascot program (www.matrixscience.com). Database searches were performed against the NCBInr Mammalian protein databases (last updated September

19, 2011) and were adjusted for trypsin digestion with no missed cleavage, fixed modification by carbamidomethylation, and variable modification by methionine oxidation. Mowse and Mascott ion scores were used to identify highly probable matches with known amino acid sequences.

Isolation of Enzymatically Active Proteasomes

The GFP-binding agarose beads from the Fusion-Aid GFP Kit (MB-0732; Vector Laboratories) were washed with PBS (10 mM phosphate, 150 mM NaCL, pH 7.5) according to the manufacturer's protocol. Then, 0.5 mL of boar sperm acrosomal extract prepared by sonication, as described above, was added to the gel in the spin column, supplemented with 1 mM ATP and incubated for 2 h at room temperature. The spin column was centrifuged for 1 min at 350 × g, and the anti-GFP beads were washed in 0.4 mL of PBS once. The anti-GFP beads were transferred to a new microcentrifuge tube with 0.1 mL of elution buffer (PBS with 0.5% SDS) and incubated for 10 min at 37°C. The spin column was centrifuged for 1 min at 350 × *g*, and the flow-through was collected. This elution procedure was repeated to maximize recovery. The purified GFP flowthrough fraction was analyzed by fluorometry with specific proteasomal substrates. In some replicates, the eluted fractions were heated to 55°C for 20 min to activate proteasomes before measurement.

Measurement of Proteasomal Activity

Eluted proteasomal fractions were loaded onto a 96-well black plate (final concentration 1×10^6 spermatozoa per milliliter or equivalent eluted GFP fraction) and incubated at 37.5°C with Z-Leu-Leu-Glu-AMC (Z-LLE-AMC) [a specific substrate for 20S

chymotrypsin-like peptidyl-glutamyl peptide hydrolase (PGPH), final conc. 100 µM; Enzo Life Sciences] or ubiquitin-AMC (specific substrate for ubiquitin-C-terminal hydrolase activity, final conc. 1 µM; Enzo). Each well was supplemented with 2.5 mM ATP. The emitted fluorescence (no units) was measured every 2 min for a period of 20 min in a Thermo Fluoroskan fluorometer (Thermo/Fisher Scientific; excitation: 355 nm, emission: 460), yielding a curve of relative fluorescence.

Statistical Analysis

Analyses of variance were carried out using the Statistical Analysis Software package in a completely randomized design. Duncan's multiple range test was used to compare values of individual treatment when the F-value was significant ($P < 0.05$).

Results

Creation and Validation of the PSMA1-GFP Transgenic Pig

To create a transgene-carrying proteasomal subunit PSMA1 fused to the GFP, a porcine PSMA1 sequence was assembled in silico from public data and used to identify an EST that appeared to be full length (GenBank accession no. CO946059). Primers were designed to remove the stop codon and create homology for cloning with In-Fusion (Clontech). The CO946059 amplimer was inserted into pCAG-CreGFP (Addgene, 13776) replacing the Cre coding region (Figure 2.1A). The resulting plasmid (pKW14) was functionally validated in porcine fetal fibroblasts. After insert purification, GFP-PSMA1, a selectable marker, and the chicken egg-white matrix attachment region (Figure 2.1 B and C) were coelectroporated into male fetal fibroblasts (10 µg total DNA; 5:2:2 ratio, respectively). Transfected cells were cultured in DMEM (10% FBS) for 12 d in 400 mg/L

G418, during which time they developed a diffuse cytoplasmic and concentrated nuclear fluorescence of GFP (Figure 2.2A). Embryos were reconstructed from pooled integration events via somatic cell nuclear transfer (Figure 2.2B) and transferred to three surrogates (120 to 125 clones per surrogate). Two females delivered two piglets each on day 114 by caesarean section. One live piglet was produced from each litter. One male piglet survived beyond day 3 and reached adulthood; this piglet became the founder piglet of our PSMA1-GFP line. A third surrogate delivered a litter of five piglets, but the four surviving piglets did not harbor the transgene. Expression of PSMA1-GFP initially was confirmed by black light exposure of the founder piglet (Figure 2.2C) and by epifluorescence imaging of the reproductive and other tissues collected from stillborn transgenic siblings (Figure 2.2D).

Fertility Testing of the Founder Boar and Its Progeny

Upon reaching puberty, the transgenic founder boar was trained for semen collection and mated with fertile gilts to develop the PSMA1-GFP line available through the National Swine Resource and Research Center (NSRRC; www.nsrrc.missouri.edu). Epifluorescence imaging revealed GFP fluorescence in the sperm head acrosomal region of live spermatozoa (Figure 2.3A), which was confirmed further by amplification with a monoclonal anti-GFP antibody in the fixed and permeabilized spermatozoa (Figure 2.3A). Histology of the adult transgenic boar gonads revealed normal testicular and epididymal tissue architecture, normal spermatogenesis in the testis, and abundant spermatozoa within the epididymal tubule lumen (Figure 2.4 A and B). Analysis of adult spermatids and spermatocytes revealed the accumulation of GFP-PSMA1 in the

hotspots of proteasomal degradation, such as the nucleus, caudal manchette, acrosomal cap, and cytoplasmic droplet (Figure 2.4 C and D). Localization of a proteasomal subunit to the chromatoid body was observed. In vitro fertilization (IVF) was performed successfully by using semen from the founder as well as from one of his transgenic sons: a wild-type boar used as a control. The semen characteristics of transgenic offspring were examined after semen collection (Appendix, Table 2). The sperm concentration and motility of PSMA1-GFP offspring were significantly lower than those of the wild-type boar ($P < 0.05$) (Appendix, Table 3), but there was no significant difference in monospermic fertilization (polyspermy was significantly lower; $P < 0.05$; Appendix, Table 4). Proteasomal–proteolytic activities of transgenic spermatozoa were comparable with those of wild-type spermatozoa, whereas the deubiquitinating activity associated with transgenic spermatozoa was slightly lower than that of the wild type (Appendix, Figure 2). The percentage of cleaving oocytes was higher in the wild-type boar ($P < 0.05$). Although there was no significant difference in blastocyst rate, the mean cell number per blastocyst was significantly higher in the transgenic offspring ($P < 0.05$; Appendix, Table 4). Consistent with the onset of maternal–embryonic transition of the control of gene expression, the expression of PSMA1-GFP first was observed at late two-cell and four-cell embryos, and increased to the blastocyst stage (Figure 2.3B). Consequently, we could confirm that the male of GFP offspring is fertile by IVF trials. This founder male subsequently transmitted the transgene to offspring via artificial insemination.

Characterization of Transgenic Spermatozoa

Western blotting was used to establish the successful fusion of the GFP to the PSMA1 protein in the transgenic boar spermatozoa. Semen samples from a fertile wild-type boar and the transgenic, PSMA1-GFP boar were processed for Western blotting experiments (Figure 2.5). Mouse monoclonal anti-GFP antibodies from two different purveyors, anti-PSMA1 antibody, and an antibody recognizing the conserved domain shared by 20S core α-type subunits 1 to 7 (anti-PSMA1-7) were used to confirm the presence of the PSMA1-GFP fusion protein in the transgenic boar spermatozoa (Figure 2.5 A, i and ii). The anti-GFP antibody revealed a single band of ∼57 kDa specific to transgenic boar spermatozoa, with no corresponding band in wild type boar spermatozoa. The migration pattern of this band corresponds to the calculated mass of the PSMA1-GFP fusion protein (263-aa residues PSMA1 + 238-aa residues GFP). This band also corresponds to PAGE protein band identified as PSMA1-GFP fusion protein by MS/MS (Appendix Table 5,6 and Figure 2.5B). The anti-PSMA1 (Figure 2.5 A, i) and anti-PSMA1–7 antibodies (Figure 2.5 A, ii) also revealed a 57-kDa band unique to transgenic boar spermatozoa, in addition to the anticipated wild-type PSMA1 band at 25 to 27 kDa. A larger group of proteins also was detected in the 27 to 30 kDa range for both wild-type and transgenic boar sperm, corresponding to the calculated masses of α-type subunits PSMA1 to 7. Based on the comparison of band densities, it is concluded that transgenic boar spermatozoa carried the PSMA1-GFP fusion protein as well as the more abundant wild-type PSMA1 protein.

Identification of Sperm Proteins that Copurify with PSMA1-GFP

Immunoprecipitation (IP) was used to identify the sperm-associated proteins interacting with the PSMA1-GFP protein, including proteins of spermatogenic origin and proteins adhering to the sperm surface that originate from epididymal fluid or seminal plasma. Semen from a fertile wild-type boar and the transgenic, PSMA1-GFP boar were processed for immunoprecipitation experiments. Anti-GFP antibodies were used to immunoprecipitate the PSMA1-GFP protein and to coimmunoprecipitate possible interacting proteins. The transgenic boar sperm extracts were prepared with two different variants of extortion buffer; wildtype semen not carrying GFP was used as a negative control. The putative PSMA1-interacting protein bands then were resolved on PAGE (Figure 2.5B), excised, and submitted for proteomic analysis by MS/MS. As anticipated, proteomics confirmed the presence of the PSMA1-GFP fusion protein and identified most of the coimmunoprecipitated 20S proteasomal core subunit α-type 1, 3, 4, 5, 6, and 7 and β-type 2, 5, 6, and 7, and isoforms of α-type 3, 4, and 7 and β-type 2 (Appendix Table 5; peptide coverage also shown in Appendix Table 6). This shows that the PSMA1-GFP fusion protein was incorporated into fully assembled 20S proteasomes. Additional proteins identified as possible interacting proteins of 20S core, or substrates of proteasomal proteolysis, included predominantly the known acrosomal membrane proteins (e.g., lactadherin/milk fat globule E8 (MFGE8) and spermadhesin alanine-tryptophan-asparagine (AWN); complete list in Appendix Table 6). This list of proteins supports the acrosomal origin of immunoprecipitated 20S proteasomes and corroborates the live GFP imaging and immunolocalization data. Importantly, only two weak protein bands were found in immunoprecipitates of wild-type spermatozoa

lacking the PSMA1-GFP fusion protein even though the same IP method, protein load, and antibodies were used (Figure 2.5B). The band patterns of immunoprecipitated wild-type and transgenic sperm proteins were identical in multiple repeats of IP procedure.

The most prevalent protein identified among known acrosomal proteins was lactadherin MFGE8 because of its high score of 1,264 and high sequence coverage of 74% (Appendix Table 6). Western blotting was used to confirm MFGE8's presence in transgenic boar spermatozoa. Two different anti-MFGE8 antibodies (D161-3 and D199-3) were used, and both revealed a 51-kDa band corresponding to the calculated mass of MFGE8 (Figure 2.5 A, iii). Acrosin inhibitor serine protease inhibitor kazal-type 2 (SPINK2) was another prominent acrosomal protein with a significant score and percent coverage that coimmunoprecipitated with PSMA1-GFP. To confirm the interaction of MFGE8 with the PSMA1-GFP protein, cross-immunoprecipitation trials were performed. Wild-type and transgenic boar sperm extracts were immunoprecipitated with anti-MFGE8 antibodies, resolved by PAGE at identical protein loads, transferred, and probed with anti-GFP antibody (Figure 2.5 A, iv). This cross-precipitation assay revealed the anticipated PSMA1-GFP band of ∼57 kDa. Based on extraction buffer variant, one additional GFP-immunoreactive band was observed in the transgenic immunoprecipitates at ∼15 kDa [regular radioimmunoprecipitation assay buffer (RIPA) extraction] or ∼100 kDa (modified RIPA). A less harsh RIPA buffer (modified) was used because the regular RIPA buffer could disrupt some of the protein-protein interactions we are trying to identify. No GFP bands were observed in the control wild-type immunoprecipitates at a protein load identical to the transgene (Figure 2.5 A, iv).

Altogether, proteomic analysis confirmed the incorporation of PSMA1-GFP subunit in the assembled 20S proteasomes and identified several potential proteasome-interacting proteins/proteasomal substrates in the sperm acrosome.

The affinity purification method described above was modified further to allow for the isolation of the enzymatically active, green fluorescent proteasomes (Figure 2.5C). The GFP purification matrix beads showed high fluorescence intensity after incubation with PSMA1-GFP sperm acrosomal extracts (Figure 2.5 C, ii), but not after incubation wild-type sperm extract (Figure 2.5 C, ii). Eluted fraction revealed the presence of PSMA1-GFP fusion protein by Western blotting (WB), and the proteasomal proteolytic activity in the eluted fraction was detected by proteasomal substrate fluorometry (Figure 2.5 C, iii).

Discussion

This study shows that the PSMA1-GFP fusion protein is incorporated in the assembled 20S proteasomes of the PSMA1-GFP transgenic pig created as a tool to study the UPS in the reproductive system, brain, and any other organs or tissues. The PSMA1-GFP founder boar and his male and female offspring are fertile in vivo and in vitro. Robust GFP fluorescence from the expression of PSMA1-GFP construct at the four-cell stage of preimplantation development agrees with the time of major maternal-to-zygotic transition (MZT) of transcriptional control in porcine in vitro and in vivo embryos, determined by autoradiographic studies and transcriptional analysis (Jarrell et al., 1991; Hyttel et al., 2000; Anderson et al., 2001). Occasionally, we detected weak GFP fluorescence already at the two-cell stage, which might indicate minor transcriptional

reactivation at this early stage of development. Similarly, minor transcription from the male pronucleus already is observed at the one-cell, zygote stage in the mouse (Adenot et al., 1997), a species in which minor transcription is initiated at the one-cell stage and the MZT occurs at the two-cell stage (Zeng and Schultz, 2005). Transcriptional and translational activity already is detectable in one- and two-cell–stage bovine embryos, a species in which the major MZT occurs at the four- to eight-cell stage (Memili and First, 2000).

Although acrosomal fluorescence was difficult to detect in the live PSMA1-GFP spermatozoa, the presence of the GFP-proteasomes in the transgenic sperm acrosome was documented by immunofluorescence with anti-GFP antibodies, and by WB of whole spermatozoa and acrosomal extract fractions. Natural GFP expression in live spermatozoa from the transgenic boar was weaker than we had intended, but this was overcome through GFP amplification methods and the GFP-proteasome location was confirmed to reside in the sperm acrosome. Lower expression in the mature spermatozoa most likely is the result of a reduced expression of the transgene during meiotic and postmeiotic phases of spermatogenesis. Also, it should be noted that the wild-type PSMA1 subunit was expressed from both maternal and paternal copies of the wild-type gene, whereas the transgene expression was only from the paternally contributed chromosome. In the future, the fluorescence intensity of PSMA1-GFP fusion protein in fully differentiated spermatozoa might be improved by using a promoter specific to the late part of spermatogenesis, such as protamine 1 or protamine 2. In WB, the PSMA1-GFP proteasomal subunit comigrated with the acrosomal membrane

fraction. Conversely, the PSMA1-GFP subunit was not detected in the whole wild-type boar spermatozoa and acrosomal extract fractions or the soluble acrosomal matrix fraction obtained after the removal of wild-type acrosomal membranes. The appearance of a high-density band at the 25 to 30 kDa range corresponds to the molecular mass of the wild-type PSMA1 and, when antibodies against a shared domain of α-subunits are used, of the six other 20S proteasomal core α-subunits. The pattern of proteasome compartmentalization in the sperm head supports the proposed role of proteasomes in acrosomal function during fertilization (Sakai et al., 2004; Sutovsky, 2011).

The GFP-tagged proteasomes copurify with known acrosomal/acrosome-binding proteins, including lactadherin MFGE8, spermadhesinAWN, and glycoprotein porcine seminal plasma-I (PSPI). These findings are consistent with the deposition of MFGE8 and spermadhesins on the sperm acrosomal surface during passage or after ejaculation (Petrunkina et al., 2003; Manaskova et al., 2007, 2010), and with the presence of proteasomes in the sperm acrosome and on the acrosomal surface (Morales et al., 2004; Pasten et al., 2005; Zimmerman et al., 2011). Both lactadherin MFGE8 and the aforementioned spermadhesins/seminal plasma proteins have been implicated in the formation of the oviductal sperm reservoir, in sperm capacitation, and in sperm–zona pellucida binding (Liberda et al., 2006; Raymond et al., 2009). These structural proteins also might be the substrates of resident acrosomal proteasomes. Some of the proteins identified in Appendix Table 6 also might serve to anchor the proteasome to acrosomal membranes, or participate in proteasome-assisted acrosomal remodeling during sperm capacitation and acrosomal exocytosis.

The 20S proteasome is composed of four concentric rings. The outer rings on each side of the "barrel" are composed of seven α-type subunits (PSMA1–7), whereas the inner rings, in which the proteolytic activity resides, are composed of seven β-type subunits (PSMB1–7) (Tanaka, 2009; Sutovsky, 2011). Unsurprisingly, the GFP-tagged proteasomes copurified with most of the 20S proteasomal core subunits, including all seven α-type subunits and six of seven β-type subunits as well as several isoforms thereof. The anti-GFP antibody was used for immunopurification, indicating that the PSMA1-GFP fusion protein is incorporated in the structurally sound 20S proteasomes during spermatogenesis. This also indicates that the copurification of GFP-proteasomes with other 20S proteasomal core subunits reveals the successful isolation of the 20S core.No 19S regulatory complex subunits were copurified, probably because of the detachment of the 19S subunit during sperm extract processing. This is consistent with results from protocols that use repeated freeze-thawing and sonication of source cells before immunopurification of proteasomes (Bousquet-Dubouch et al., 2008; Ducoux-Petit et al., 2008). Whether any of the identified subunit isoforms are testis specific remains to be determined. An estimated one-third of sperm proteasomal subunits in Drosophila are testis specific (Zhong and Belote, 2007), and there is at least one testis-specific α-type subunit isoform, designated PSMA8, in human testis (Tanaka, 2009).

As anticipated based on the coimmunopurification of PSMA1-GFP with other proteasomal subunits, we were able to isolate enzymatically active GFP-proteasomes. With further optimization of the purification and elution protocols, these fractions will be useful for studies in cell-free systems, including but not limited to research on

sperm–oocyte interactions. Upcoming experiments will study the interactions of the sperm proteasome with MFGE8, spermadhesins, and other acrosomal proteins that copurify with sperm proteasomes. In addition to the study of fertilization, the PSMA1-GFP pig model might be used to study a variety of reproductive technologies and disorders, such as germ cell transplantation (Luo et al., 2006), ovarian/oocyte function (Nagyova et al., 2012), and endometriosis (Celik et al., 2008). The transgenic animal model described in the present study is available through the National Institutes of Health-sponsored NSRRC and may be used to study the functioning of the UPS in a variety of cellular pathways and pathologies, such as Alzheimer's disease, Huntington disease, Parkinson disease, cancer, immune and inflammatory disorders, and liver cirrhosis. The deregulation of the UPS also has been implicated in the pathogenesis of genetic diseases such as cystic fibrosis, Angelman syndrome, and Liddle syndrome (Schwartz and Ciechanover, 1999). In the case of cystic fibrosis, the PSMA1-GFP pigs might be crossed with the cystic fribrosis transmembrane conductance receptor null (CFTR−/−) pig (Rogers et al., 2008) (www.exemplargenetics.com/cftr/). The fusion of GFP to the proteasome does not appear to interfere with proteasome function in male gametes or in other systems. Consequently, the PSMA1-GFP transgenic pigs are healthy, reach sexual maturity in a timely manner, and produce healthy, fertile offspring. The use of this transgenic pig model to advance the understanding of the role of the UPS has the potential to identify and validate therapeutic targets for the treatment and prevention of several diseases.

Acknowledgments

We thank Dr. Connie Cepko for development of pCAG-CreGFP for Addgene deposit. This work was supported by National Research Initiative Competitive Grant 2011-67015-20025 from the US Department of Agriculture National Institute of Food and Agriculture (to P.S.), National Institutes of Health (NIH) Grant U42 RR018877/OD011140 (to R.S.P. and K.D.W.), and seed funding from the Food for the 21st Century Program of the University of Missouri–Columbia (to P.S., K.D.W. and R.S.P.). P.S. is also supported by NIH–National Institute of Child Health and Human Development Grant 1R21HD066333-01A1.

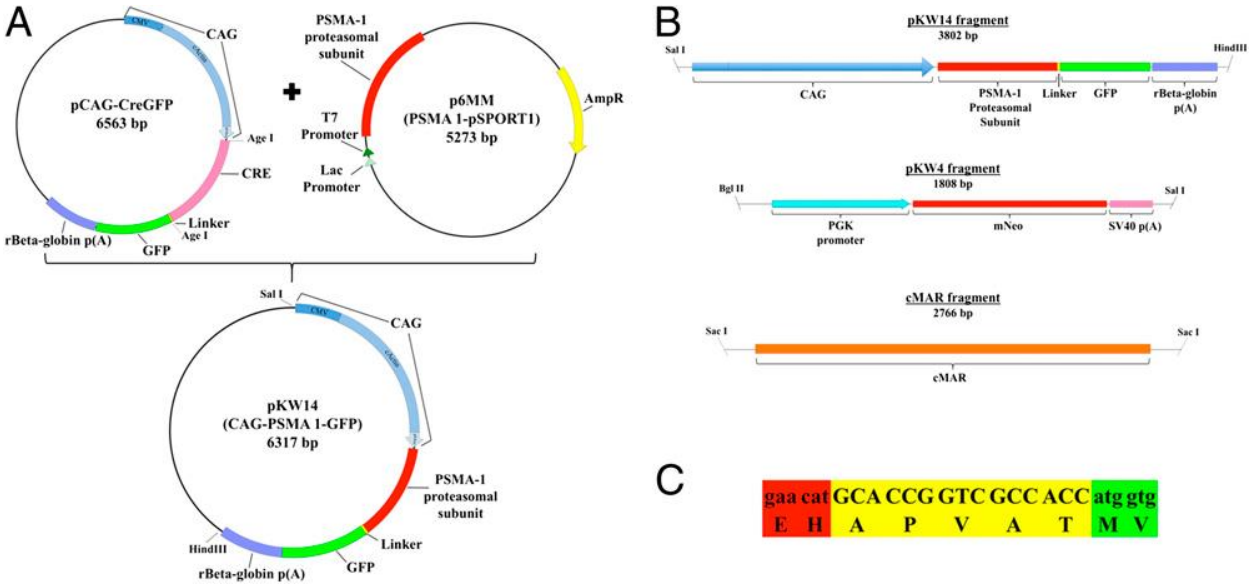

Figure 2.1. (A) pKW14 plasmid construction. Cre was removed from pCAG-CreGFP using AgeI restriction sites, and used as a vector backbone. Generation of the insert was done via PCR. Primers were designed to amplify the *PSMA1* coding region from p6MM, to remove the stop codon, and to create a homology for cloning with In-Fusion (Clontech). (B) Linearized DNA fragments used for cotransfection of porcine fetal fibroblasts. pKW14 (*PSMA1-GFP*), pKW4 (mNeo, selectable marker), and cMAR (insulator). (C) Sequence of the linker used between the *PSMA1* proteasomal subunit and GFP. The linker sequence (yellow) is flanked upstream by *PSMA1* (red) and downstream by *GFP* (green), corresponding to B.

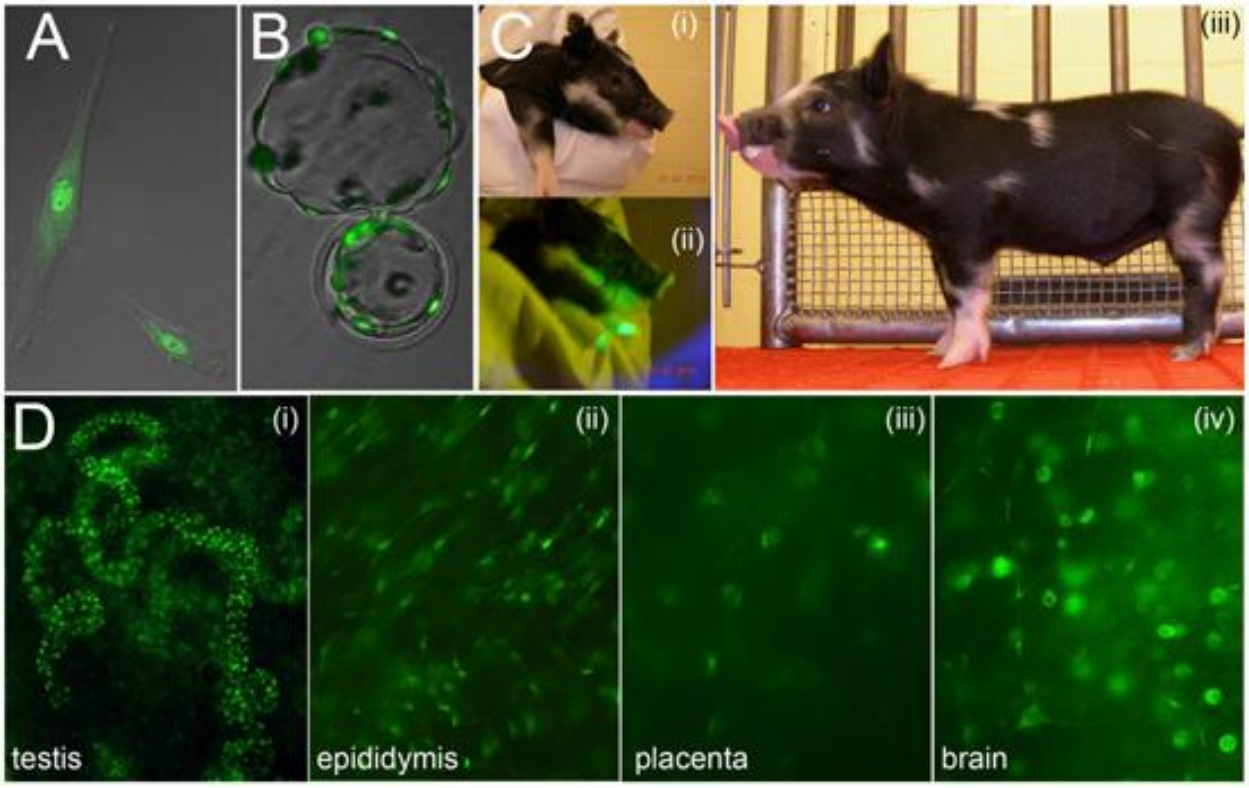

Figure 2.2. (A) Donor cell fibroblast expressing the PSMA1-GFP fusion protein; note the accumulation of GFP fluorescence in the nucleus. (B) Hatching in vitro blastocyst on day 6, obtained by nuclear transfer from the donor cell fibroblast line shown in A. (C) Minnesota miniature pig cloned from fetal fibroblasts expressing GFP-labeled proteasomes, the founder of the *PSMA1-GFP* line. (C, *i* and *ii*) Sequential photographs of the head taken with conventional (i) and black light (*ii*) illumination. (C, *iii*) The whole body photographed at 2 wk of age. (D) PSMA1-GFP fluorescence in various tissues collected from newborn positive clones. Prominent green fluorescence is seen in the spermatogonia within the newborn seminiferous tubules (D, *i*), in the principal cells of the epididymis (D, *ii*), in the placental cell nuclei (D, *iii*), and in the nuclei and axons of some of the neurons in the brain (D, *iv*).

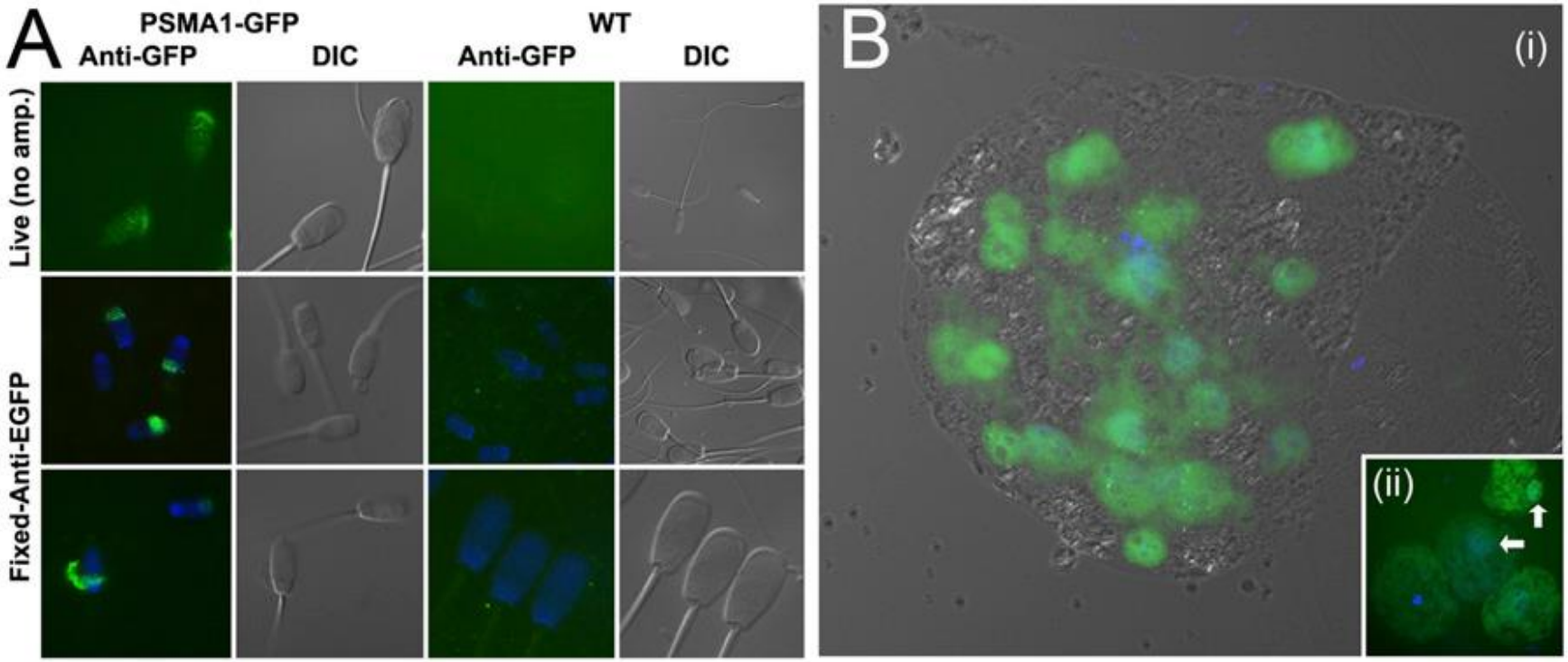

Figure 2.3. (A) GFP fluorescence in live spermatozoa imaged directly under epifluorescence illumination (Top) and in the fixed spermatozoa processed with anti-GFP antibody (Middle and Bottom); spermatozoa from a wild-type boar (WT) served as a negative control. (B) GFP fluorescence is strongest in the nuclei of a live day 6 blastocyst created by in vitro fertilization of wild-type oocytes with spermatozoa from a GFP boar (homozygous son of the *PSMA1-GFP* line founder). (Inset) Onset of *PSMA1-GFP* gene expression at the four-cell stage, coinciding with the major MZT of transcription control.

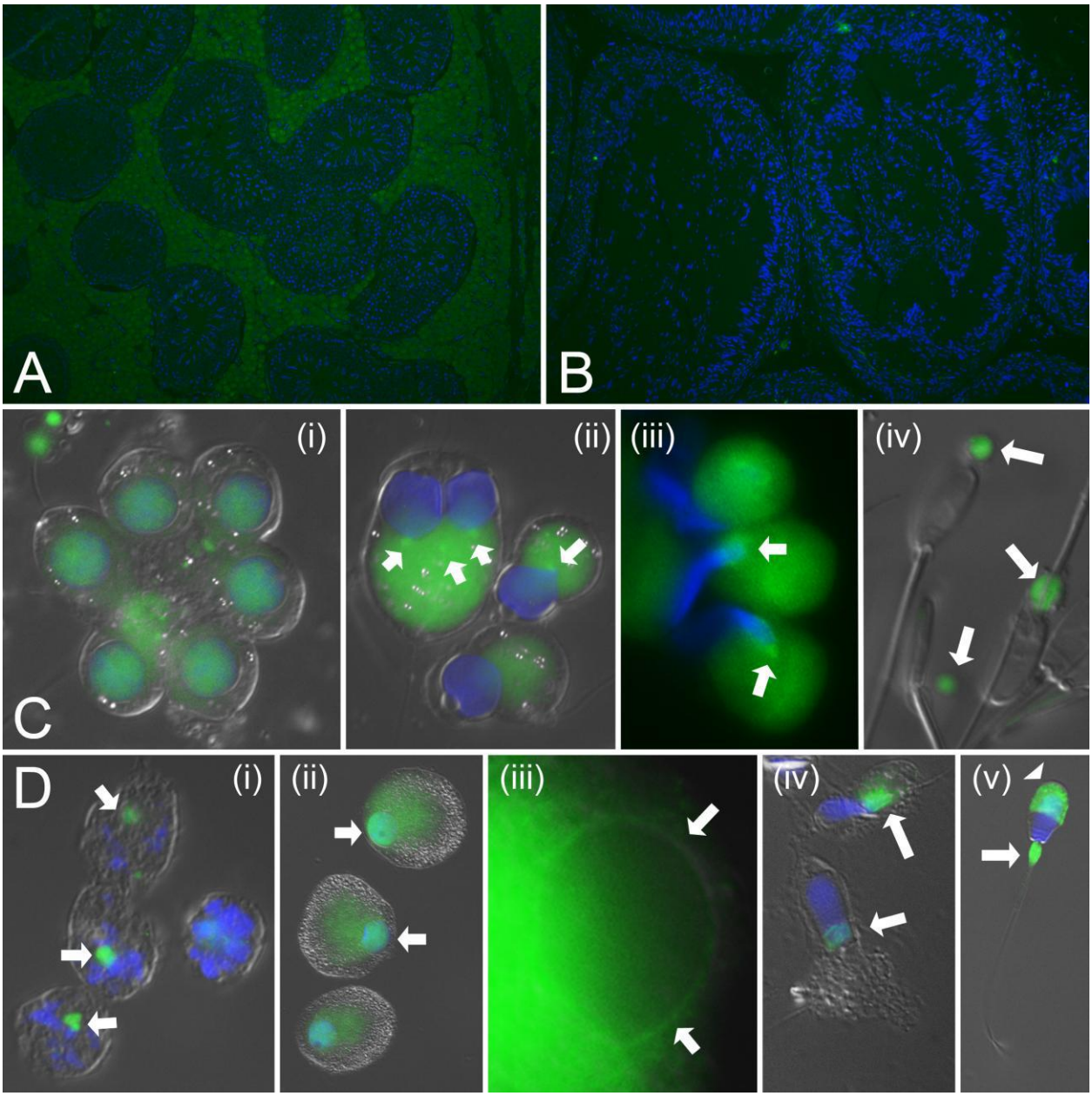

Figure 2.4. Histological and immunocytochemical analysis of the gonads and testicular germ cells of the founder PSMA1-GFP boar. (**A, B**) Histology of adult transgenic male gonads reveals normal testicular (A) and epididymal (B) tissue architecture, normal spermatogenesis in the testis (A) and abundant spermatozoa within the epididymal tubule lumen (B). (**C**) Live cell imaging of PSMA1-GFP fluorescence in the germ cells of founder boar. Green fluorescence is visible in the nuclei of round spermatids (i), at the base of the nucleus, probably the chromatoid body or the site of flagellum biogenesis (arrows point to areas of dense PSMA1-GFP fluorescence) in the early step elongating spermatids (ii), in the caudal manchette (arrows) of elongated spermatids (iii), and in the cytoplasmic droplets (arrows) of fully differentiated spermatozoa (iv). Green color

channel was contrast-enhanced due to its low intensity. (**D**) Amplification of PSMA1-GFP1 fluorescence by anti-GFP antibody in the fixed, permeabilized testicular cells of the founder boar. Fluorescence is concentrated in the chromatoid bodies (arrows) of secondary spermatocytes (i), in the nuclei (arrows) of round spermatids, in the subacrosomal/inner acrosomal membrane layer (arrows) of an early step elongating spermatid (iii), in the caudal manchette (iii) of the elongated spermatids (iv), and in the acrosomal cap (arrowhead) and cytoplasmic droplet (arrow) of a fully differentiated testicular spermatozoon (v). The localization of PSMA1-GFP in panels C and D corroborates previous reports of proteasomal subunit localization in the hotspots of spermatid protein recycling such as the nucleus, redundant nuclear envelopes, caudal manchette, acrosomal cap and cytoplasmic droplet (Haraguchi et al., 2007; Kierszenbaum et al., 2011; Rivkin et al., 2009; Mochida et al., 2000). Localization of a proteasomal subunit to the chromatoid body is reported for the first time.

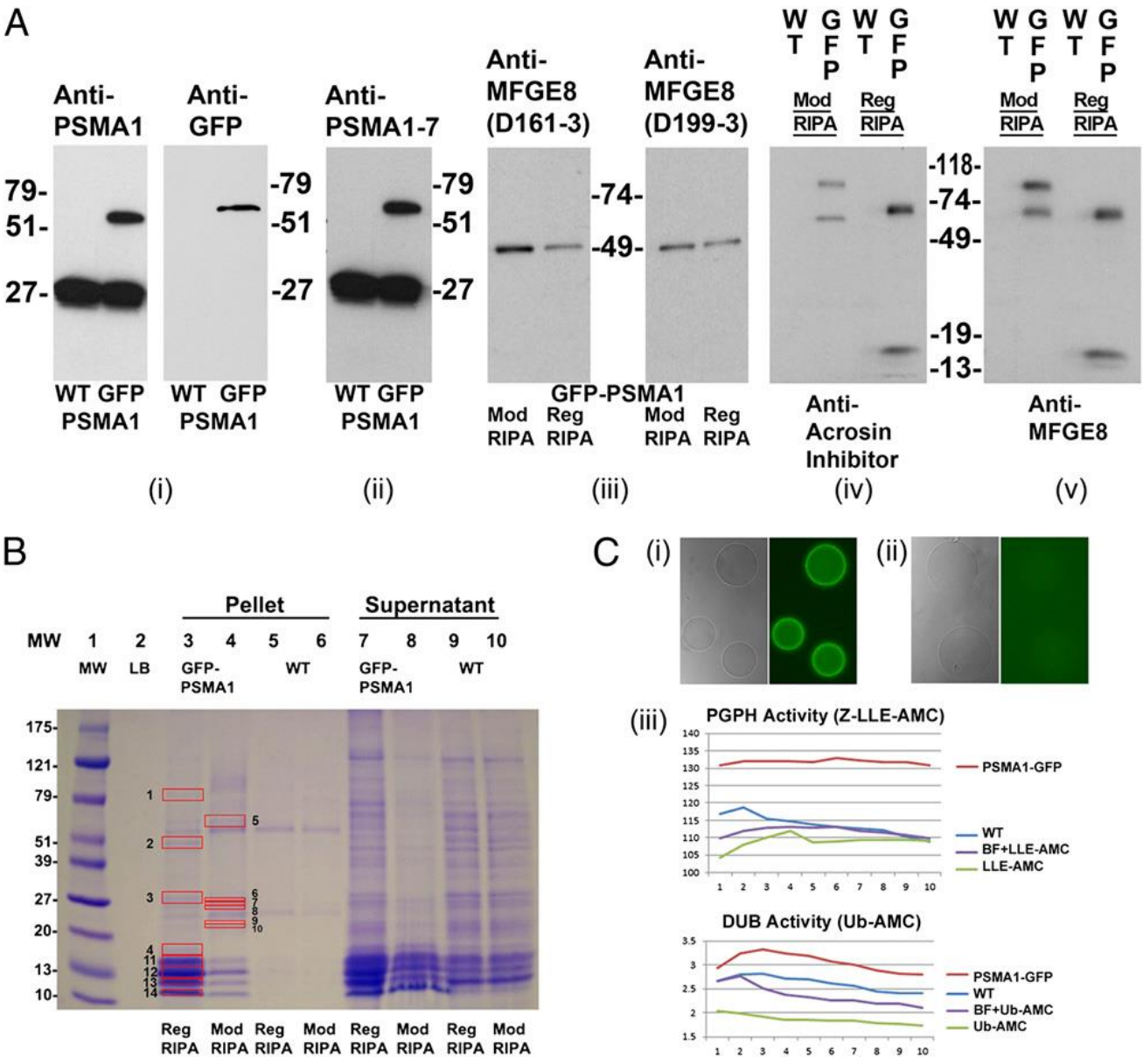

Figure 2.5. Proteomic analysis of PSMA1-GFP fusion protein and the coimmunoprecipitated proteins in the transgenic spermatozoa. (A) A unique band of ~57 kDa, corresponding to the calculated mass of PSMA1-GFP, is detected in the sperm extracts of the transgenic boar (GFP lane), but not in those from a wild-type boar (WT lane) (A, i). Anti-PSMA1 antibody detected both the wild-type PSMA1 band of ~27 kDa and the PSMA1-GFP fusion protein of ~57 kDa (A, i, Left), whereas the anti-GFP antibody detected the PSMA1-GFP band in the transgenic boar only (A, i, Right). A polyclonal antibody recognizing six of seven 20S proteasomal core α-type/PSMA subunits confirms the presence of PSMA1-GFP in the transgenic boar and of the six wild-type PSMA subunits, all of which comigrate in the 25-30 kDa range in both WT and

transgenic spermatozoa (A, ii). Western blotting was used to confirm the coimmunoprecipitation

of lactadherin MFGE8 with sperm proteasomes from transgenic sperm extracts, using two different anti-MFGE8 antibodies, D161-3 and D199-3 (A, iii). Spermatozoa were lysed with regular RIPA buffer (Reg RIPA) or modified RIPA buffer (Mod RIPA), immunoprecipitated with anti-GFP antibodies, and probed with anti-MFGE8 antibodies. A single 51-kDa band was revealed in each lane and corresponds to the calculated mass of MFGE8. A modified RIPA buffer (Nonidet P-40) was included because the regular RIPA buffer (Triton X-100) may disrupt some protein–protein interactions. A cross-precipitation experiment was performed to confirm the interaction of MFGE8 (one of the identified interacting proteins from the proteomics results shown in B) with GFP-tagged proteasomes. Wild-type and transgenic boar spermatozoa were lysed with regular or modified RIPA buffer and immunoprecipitated with anti-MFGE8 antibodies (A, iv). The precipitations then were probed with anti-GFP antibodies. Bands were revealed in all transgenic boar lanes, with no bands detected in the wild-type lanes. (B) Band patterns of the putative proteasome-interacting proteins coimmunoprecipitated from the transgenic boar spermatozoa by using an anti-GFP antibody. Wild-type boar and transgenic boar spermatozoa were solubilized with RIPA or modified RIPA buffer and then immunoprecipitated with anti-GFP antibodies. Red boxes mark proteins unique to transgenic boar sperm that were analyzed by MS. Protein numbers correspond to the protein numbers in SI Appendix, Table 5B. (C) Affinity purification of the enzymatically active green fluorescent proteasomes. The GFP purification matrix beads show high fluorescence intensity after incubation with the PSMA1-GFP sperm extracts (C, i); there is no fluorescence in the beads incubated with the wildtype sperm extract (C, ii). Both types of beads were photographed at an identical magnification and acquisition time. (C, iii) Proteasomal PGPH activity (Upper; measured using the fluorometric proteasomal substrate Z-LLE-AMC) and deubiquitinating activity [Lower; measured by fluorometric substrate ubiquitin (Ub)-AMC] in the eluted fraction from beads incubated with PSMA1-GFP sperm extracts (PSMA1-GFP), in the eluted fraction from beads incubated with wild-type sperm extract (WT), in the assay solution including elution buffer and fluorometric substrate (BF+LLE-AMC or BF+Ub-AMC), or in the assay solution containing only the fluorometric substrate (Z-LLE-AMC or Ub-AMC). Proteasomal activities were measured every 2 min for 20 min.

Chapter Three

The 26S Proteasome Degrades MFGE8 to Release Spermatozoa from the Oviductal Sperm Reservoir

Abstract

The formation of the oviductal sperm reservoir is an important process in the reproduction of many species including cows, pigs, mice, rats, hamsters, sheep, rabbits, horses and possibly humans. However, the mechanisms and proteins involved in spermatozoa binding to the oviductal epithelium have not been fully elucidated. Most of the research on this process focuses on bovine seminal plasma proteins (BSPs) and porcine spermadhesins. Our and others' research suggests that lactadherin MFGE8, a milk fat globule protein also found in spermatozoa, could function similarly to strengthen this binding and/or play a compensatory role. Similar to BSPs and spermadhesins, MFGE8 is a secreted seminal plasma protein deposited onto the sperm surface and has been shown to affect the ability of spermatozoa to bind to their receptors on the oviductal epithelium. In course of characterizing the transgenic pig model carrying GFP-tagged sperm proteasomes, we discovered novel interaction between the 26S proteasome and MFGE8 in porcine spermatozoa. This study examines a possible role for this interaction: that the 26S proteasome mediates the degradation of MFGE8 during sperm capacitation, thus gradually releasing spermatozoa from the sperm oviductal reservoir prior to fertilization. This research gives insight into the mechanisms of oviductal sperm transport and fertilization, which could lead to the development of novel treatments of infertility and possible contraceptive applications.

Introduction

During the process of mammalian fertilization, spermatozoa must traverse the harsh environment of the female reproductive tract. At first, millions of spermatozoa are deposited into the vagina or uterus, but only a few thousand enter the oviduct. Then, even fewer reach the ampulla at ovulation and only one fertilizes the oocyte. This population of spermatozoa that bind to the caudal region of the isthmus and form the oviductal sperm reservoir is highly selected. This selection process seems to be based on intact acrosomes in bovines, uncapacitated sperm status in horse, cow, and pig, and low internal free calcium content and low membrane protein phosphorylation in pigs (Petrunkina et al., 2001.). The oviduct bound sperm population forms the oviductal sperm reservoir which has various functions: 1) Control of sperm transport to the oviductal ampulla, helping prevent polyspermic fertilization; 2) Maintenance of sperm viability to span the time between estrus and fertilization; 3) Modulation of sperm capacitation which synchronizes sperm fertilizing ability with the time of ovulation (Suarez et al., 1998). Sperm release from the oviductal sperm reservoir seems to rely on conditions within the oviduct generated around ovulation that initiate changes of the sperm surface that cause capacitation and hyperactivation.

The ability of spermatozoa to bind to oviductal epithelium and form the oviductal sperm reservoir was examined by Petrunkina *et al*. (2003a) by using a boar oviductal explant assay. They observed that sperm heads were bound to ciliated epithelial cells and were attached over the whole surface of the explants. They found no difference between explants taken from the oviductal isthmus and ampulla, or explants from sows

in different stages of estrous and reproductive status, but this could be due to the culture system lacking appropriate endocrine modulation by the ovaries. They also found that epididymal spermatozoa had significantly lower binding capabilities than ejaculated spermatozoa. This decrease in binding ability of epididymal spermatozoa was also found to be true in other species such as hamsters, cows, and horses (DeMott et al., 1995; Lefebvre and Suarez, 1996; Lefebvre et al., 1995, 1997). These results suggest a role of seminal plasma proteins that are secreted onto the sperm surface during ejaculation maturation and ejaculation to play a role in this binding.

A 53 kDa, 409 amino acid residue seminal plasma glycoprotein, MFGE8, was isolated from solubilized pig sperm plasma membrane proteins bound to immobilized zona pellucida glycoproteins (Ensslin *et al.,* 1998) by affinity chromatography; it is also abundant in the Milk Fat Globule, which is a collection of proteins and triglycerides that rise from the apical surface of mammary epithelia during lactation. This protein has now been investigated in many species and is known by many names such as lactadherin, p47, SED1, rAGS, PAS6/7, and BA-46. It has been implicated in a variety of cellular interactions: adhesion between sperm acrosome and the oocyte zona pellucida, phagocytosis of apoptotic lymphocytes and other apoptotic cells, mammary gland branching/morphogenesis, repair of intestinal mucosa, among others (Raymond and Ensslin, 2009). The MFGE8 protein has two distinct functional domains: 1) An N-terminal domain with two EGF-repeats (Epidermal Growth Factor), the second of which has an integrin-binding RGD (arginine-glycine-aspartic acid) domain; 2) and a C-terminal domain with two Discoidin/F5/8C domains that bind to anionic phospholipids and/or

extracellular matrices (Raymond et al., 2009). MFGE8 knockout male mice have greatly decrease fertility *in vivo,* with some mice showing complete sterility and others producing approximately a third of the litter size compared to control mice (Ensslin and Shur, 2003). When these MFGE8 null mice were examined *in vitro*, a significant decrease in sperm-zona binding was observed, but unfortunately no experiments were performed to compare oviductal sperm reservoir formation between MFGE8 null and wild-type mice.

Mammalian spermatozoa undergo many ultra-structural and biochemical changes when traveling through the male and female reproductive tracts. Epididymal sperm maturation occurs during sperm passage through the epididymis and causes extensive remodeling and addition of proteins on the sperm surface. One of those secreted proteins is MFGE8, and has been localized to the apical ridge or the entire acrosomal region in testicular and ejaculated spermatozoa as shown by Petrunkina *et al*. (2003). They used a polyclonal antibody directed against purified bovine MFGE8 as the sequence identity is about 80% between bovine and porcine MFGE8. Sperm MFGE8 protein can originate from testis, epididymis and accessory sex glands secreting components of the seminal plasma. In the epididymis, the MFGE8 protein is secreted from the initial segment of the epididymis, from apical blebs that come into contact with the sperm plasma membrane overlying the acrosome during epididymal transit (Ensslin and Shur, 2003). This MFGE8 protein was detected in mouse, boar, and human testis in haploid germ cells (spermatids), and in the epididymal compartment including epithelial cells, their apical stereocilia, and spermatozoa in the epididymal lumen

(Petrunkina et al., 2003; Copland et al., 2009).

The localization and intensity of MFGE8 labeling changes during post testicular maturation and capacitation of porcine spermatozoa. Petrunkina *et al*. (2003) observed an increase of MFGE8 at the apical region of the sperm head from the caput epididymis to the cauda epididymis. They saw that only spermatozoa with intact plasma membranes attracted MFGE8, while spermatozoa with damaged plasma membranes did not. This suggests that MFGE8 associates with the intact sperm plasma membrane. Additionally, they performed kinetics studies of MFGE8 expression on the sperm surface during capacitation. They observed that spermatozoa that did not come into contact with accessory gland fluids underwent capacitation related loss of MFGE8 on the apical ridge of the acrosome at a higher rate than ejaculated spermatozoa. This suggests a more rapid functional destabilization of the plasma membrane of epididymal spermatozoa compared to ejaculated spermatozoa (Petrunkina et al., 2003).

The MFGE8 protein has a cleavable signal peptide followed by two N-terminal EGF-like repeats and two C-terminal Discoidin/F5/8C domains (Ensslin et al., 1998). The second EGF domain contains an RGD integrin-binding motif that binds to $\alpha_v\beta_{3/5}$ integrins expressed on oviductal epithelium. This binding facilitates cell adhesion as well as integrin-mediated signal transduction (Ensslin and Shur, 2007). These EGF repeats may pair with one another to form MFGE8 multimers, which is similar to the multimerization of other cell adhesion proteins with EGF repeats (Balzar et al., 2001).

The C-terminal F5/8C domains of MFGE8 are composed of an eight-strand anti-parallel *β*-barrel, from which two or three hypervariable loops extend from the base

(Shur et al., 2004). The exposed amino acids that compose these hairpin loops decide the protein's binding specificity. These loops mediate binding to carbohydrate moieties on the surface of cells and in the extracellular matrix, while coagulation Factor V domain, Factor VIII domain, and the second C-terminal domain bind to anionic phospholipids of cellular membranes (Anderson et al., 2000; Shi et al., 2008).

We have previously shown that the 26S proteasome interacts with MFGE8 through cross-immunoprecipitation experiments and mass spectrometry (Miles et al., 2013). The purpose of this study is to explore the biological purpose of this interaction. This could reveal a potentially novel role for the Ubiquitin Proteasome System (UPS) in the release of spermatozoa from the oviductal sperm reservoir by mediating the degradation of MFGE8. It is also possible that this interaction with MFGE8 allows the proteasome to bind to the acrosomal membranes of spermatozoa to degrade membrane bound proteins.

Materials and Methods

Semen Collection and Processing

Ejaculates from adult wild type Duroc boars were collected under the guidance of approved Animal Care and Use (ACUC) protocols of the University of Missouri, Columbia (UM). The wild-type boar was placed on a routine weekly collection. Sperm-rich fractions of the ejaculates with greater than 85% sperm motility and normal sperm acrosomes were used. Sperm concentrations were estimated using a hemacytometer (Fisher Scientific, Houston, TX, USA). The percentage of motile sperm was estimated at 38.5°C by light microscope at 250 x magnification. Semen was slowly cooled to room

temperature (20°C) within 2 hrs after collection. Semen was then transferred into 15 ml tubes, centrifuged at room temperature for 10 min at 800 x *g*, and the supernatant was removed. The spermatozoa were processed for Western blotting and stored at -80°C. In order to use the semen for *in vitro* fertilization (IVF), the semen was diluted with X-Cell Extender (Cat. #USA851X, IMV Technologies, Maple Grove, MN; final concentration of 1 × 10^8 spermatozoa/ml). The diluted semen was stored in a styrofoam box at room temperature for 5 days. Unless otherwise noted, all chemicals used in this study were purchased from Sigma Chemical Co. (St. Louis, MO).

Acrosomal Extracts of Boar Spermatozoa

Fresh boar spermatozoa were transferred to 15 mL Falcon tubes and centrifuged at 350 × *g* in a Fisher Scientific centrifuge for 5 min to remove the seminal plasma. The supernatant was removed, and the pellet was resuspended and washed in 9 mL of TL-Hepes containing 0.1% polyvinyl alcohol and 0.5% hyaluronidase, each time collected by centrifugation at 350 × *g* for 5 min. After washing, sperm pellets were resuspended in RIPA buffer (50 mM Tris HCl, pH 8; 150 mM NaCl; 1% Triton; 0.5% sodium deoxycholate; 0.1% SDS; and PMSF, 1:200) or modified RIPA buffer (50 mM Tris·HCl, pH 8; 150 mM NaCl; 1% Nonidet P-40; 0.5% sodium deoxycholate; 1 mg/mL leupeptin; and 1 mg/mL pepstatin); resuspended samples were sonicated by using Digital Sonifier (Branson) for 1 min at 30% intensity. A modified RIPA buffer (Nonidet P-40) was included because the regular RIPA buffer (Triton X-100) may disrupt some protein–protein interactions. To prepare the acrosome extract, the disrupted spermatozoa were centrifuged at 5,000 × *g* for 10 min at 4°C, and supernatants were collected free of sperm head/tail fragments, as

determined by light microscopy. The final supernatant fraction was stored at −80 °C.

Detection and Quantification of the Endogenous MFGE8 in Capacitated Spermatozoa

Fresh boar spermatozoa were transferred to 15 mL Falcon tubes and centrifuged at 350 × *g* in a Fisher Scientific centrifuge for 5 min to remove the seminal plasma. The supernatant was removed, and the pellet was resuspended and washed in 9 mL of TL-Hepes containing 0.1% polyvinyl alcohol and 0.5% hyaluronidase, each time collected by centrifugation at 350 × *g* for 5 min. After washing, sperm pellets were resuspended in capacitation medium (5 mM pyruvic acid, 11 mM glucose, and 2% BSA in 50 ml of TL-Hepes containing 0.1% polyvinyl alcohol and 0.5% hyaluronidase) and incubated for 4 hrs in a CO_2 incubator at 38.5°C with either 0, 10, 50, or 100 um of proteasomal inhibitor MG132 or ethanol vehicle. The samples were then examined through Western blotting and probed mouse monoclonal anti-MFGE8 antibody (1:1,000 dilution; Code #D199-3; Medical and Biological Laboratories Co., Woburn, MA, USA) overnight. Protein load was normalized by re-probing the PVDF membrane with anti-Alpha tubulin E7 antibody (Appendix Figure 3).

Degradation of Exogenous Recombinant MFGE8 in a Cell-Free System Containing Sperm Acrosomal Extracts

Recombinant human MFGE8 with a C-terminal 6-Histidine tag (1 µg; Cat# 2767-MF-050; R&D Systems, Inc., Minneapolis, MN, USA) was incubated with fresh boar acrosomal extracts (1 x 10^9 sperm/ml) for two hrs in 37°C with the presence of 0, 10, 50, or 100 µm of proteasomal inhibitor MG132, or a commensurate volume of 100% ethanol (vehicle control). The samples were then analyzed by Western blotting as

described below and probed with anti-polyHistidine horseradish peroxidase-conjugated antibody (1:2500; Cat# MAB050H; R&D Systems, Inc., Minneapolis, MN, USA).

Western blotting

Spermatozoa were washed in protein-free PBS and sperm concentration was determined using a hemocytometer so that approximately 1 x 10^9 spermatozoa/ml were loaded per lane after extraction. Spermatozoa were washed again in PBS and boiled for 5 min with loading buffer (50 mM Tris (pH 6.8), 150 mM NaCl, 2% SDS, 20% glycerol, 5% *β*-mercaptoethanol, 0.02% bromophenol blue). Gel electrophoresis of 10 µl total protein/lane was performed on 4-20% gradient gels (PAGEr Gels, Lonza, Rockland, ME), followed by protein transfer to PVDF membranes (Immobilon P, Millipore Corp., Billerica, MA) using an Owl wet transfer system (Fisher Scientific, Houston, TX) at a constant 50 V for 4 hrs. The membranes were sequentially incubated with 10% non-fat milk for 1 hr with the appropriate primary antibody overnight. The membranes were washed and incubated with an appropriate species-specific secondary antibody such as goat anti-Armenian hamster IgG-HRP antibody (1:10,000 dilution; Cat# sc-2443; Santa Cruz Biotechnology, Inc.) for 1 hr at room temperature in 1% nonfat dry milk in TBS/Tween. The membranes were washed and reacted with 1.5 mL of chemiluminescent substrate (Illuminata Crescendo, Millipore Corp., Billerica, MA) for 5 min prior to being exposed to Kodak BioMax Light film (Kodak, Rochester, NY, USA). The bands on the film representing MFGE8 were then scanned and analyzed with Adobe Photoshop CS5 (Adobe systems, San Jose, CA) and the densitometry graphs were made with Microsoft Excel 2010.

Statistical Analysis

Analysis of variance (ANOVA) was carried out using the SAS package in a completely randomized design. Duncan's multiple range test was used to compare values of individual treatment when the F-value was significant ($P < 0.05$).

Results

Endogenous MFGE8 Degradation during Sperm Capacitation is Inhibited by MG132

Western blotting was used to assess the effect of proteasomal inhibitor MG132 the degradation of sperm MFGE8 during boar sperm capacitation. Capacitating spermatozoa treated with increasing concentrations of proteasomal inhibitor MG132 (0, 10, 50, and 100 µM) were analyzed with Western blotting with anti-MFGE8 antibodies. A protein band at ~53 kDa representing MFGE8 was revealed and densitometry results were recorded (Figure 3.1). A significant difference was observed between the MFGE8 band densities of uncapacitated (0.93 ± 0.03) and capacitated (0.33 ± 0.22) boar spermatozoa showing that MFGE8 is strongly expressed in uncapacitated spermatozoa, but its band density is greatly decreased upon capacitation (Figure 3.1). Furthermore, a trending increase in the MFGE8 band density was observed in spermatozoa treated with increasing concentrations of proteasomal inhibitor MG132 (Figure 3.1). This suggests that the sperm proteasomes are affecting the degradation of endogenous boar sperm MFGE8 during the capacitation process and led us to explore this interaction in a cell-free system.

Sperm Acrosomal Proteasomes Degrade Recombinant MFGE8 in a Cell-Free System

To further examine the MFGE8 degradation by boar sperm proteasomes, 10 µg of recombinant Human MFGE8 were incubated with boar sperm acrosomal extracts (1 x

10^9 sperm/ml) for two hrs at 37°C with increasing concentrations of proteasomal inhibitor MG132 (0, 10, 50, 100 µM) or ethanol (vehicle control). The samples were then analyzed by Western blotting. A protein band at ~53 kDa representing recombinant MFGE8 was revealed by anti-His tag antibody (Figure 3.2), similar in size to intrinsic sperm MFGE8 detected by anti-MFGE8 antibody in whole sperm extracts. The densitometry results show that recombinant human MFGE8 was partially degraded by boar acrosomal extracts during incubation as the band density was greatly decreased from human recombinant MFGE8 incubated in PBS (137 ± 12) to human recombinant MFGE8 incubated with acrosomal extracts (60 ± 4.3) (Figure 3.2). A significant dose dependent increase in the recombinant human MFGE8 band density was observed in samples treated with increasing concentrations of proteasomal inhibitor MG132 (Figure 3.2). This observation supports the proteasome's proposed role of MFGE8 degradation upon capacitation.

Discussion

This study suggests that the seminal plasma sperm membrane binding protein, MFGE8, which plays a part in the formation of the oviductal sperm reservoir, is degraded by the 26S proteasome (Figure 3.1 and 3.2). This finding agrees with previous experiments where these proteins were shown to affect the binding of spermatozoa to the oviductal epithelium. The increased binding abilities and stabilization of the plasma membrane of ejaculated spermatozoa compared to epididymal spermatozoa suggest an essential role of seminal plasma proteins and an intact plasma membrane in the formation of the oviductal sperm reservoir. The MFGE8 protein is deposited onto the

sperm surface during transport through the male reproductive tract and ejaculation. These MFGE8 proteins have been shown to be associated with mature, uncapacitated sperm and are lost, translocated, or degraded from the apical ridge of the acrosome upon capacitation (Petrunkina et al., 2003). Furthermore, the presence of MFGE8 binding sites, $\alpha_V\beta_{3/5}$ integrins, has been found on the stereocilia of the oviductal epithelium and on the sperm surface; oviductal binding has been inhibited with their respective antibodies (Ekhlasi-Hundrieser et al., 2005; Ensslin and Shur, 2007).

Binder of sperm proteins (BSPs) are the most widely characterized sperm surface binding proteins involved in the formation of the oviductal sperm reservoir, in bovines, along with Spermadhesins which are also present in boar oviductal sperm reservoir formation. But like most biological processes, there seems to be multiple pathways or proteins working in a similar fashion in unison or to compensate for protein malfunctions or species differences. These MFGE8 proteins could function alongside BSPs to aid in initial binding of spermatozoa to the oviduct. The 26S proteasome could mediate the release of spermatozoa from the oviductal sperm reservoir by gradually degrading the MFGE8 protein that binds the sperm acrosomes to the oviductal epithelium as suggested in these experiments (Figure 3.1 and 3.2). This corresponds with the traditional view that sperm release from the oviductal sperm reservoir relies on conditions within the oviduct generated around ovulation that initiate changes of the sperm surface that could be related to capacitation and hyperactivation.

This research gives us insight into the mechanisms of fertilization, which could lead to the development of novel treatments of infertility and possible contraceptive

applications. For example, because MFGE8 and other sperm binding proteins are secreted onto the surface of mature spermatozoa, they could be deposited into the vagina before intercourse to increase the fertilization potential of infertile males. There are also possible contraceptive applications by developing vaginal suppositories containing sperm binding protein antibodies or site-specific inhibitors that could coat the spermatozoa and decrease their ability to bind to the oviductal epithelium and/or egg zona pellucida thus preventing fertilization. Further research in humans is required to assess the feasibility of these approaches to controlling reproduction.

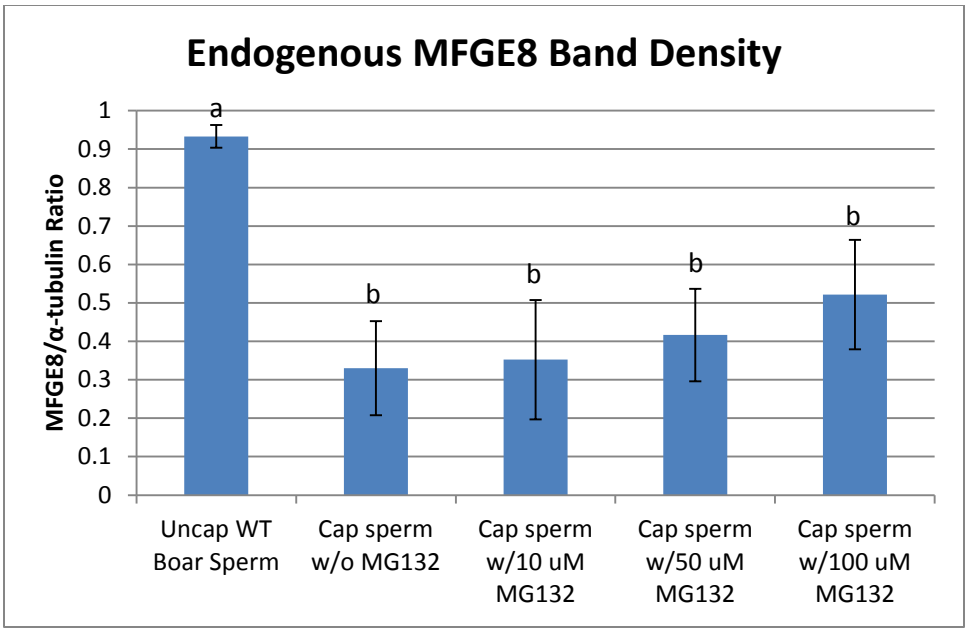

Figure 3.1. Endogenous MFGE8 Band Density. Uncapacitated (Uncap) and Capacitated (Cap) wild-type boar sperm extracts were assessed for the percentage of MFGE8 band density compared to α-Tubulin E7 band density to normalize protein load. Data represents the mean ± SEM, n = 3. Statistical analysis was performed as described in Materials and Methods; $P < 0.05$.

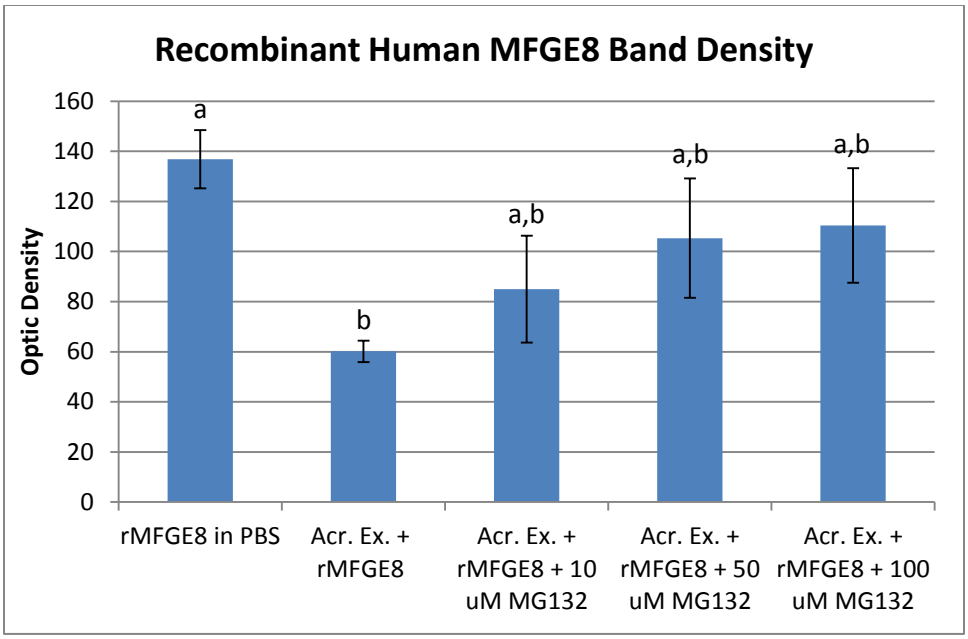

Figure 3.2. Recombinant Human MFGE8 Band Density. Recombinant Human MFGE8 (rMFGE8, 10 µg) was incubated with wild-type boar sperm acrosomal extracts (Acr. Ex.) and increasing concentrations of proteasomal inhibitor MG132. Data represents the mean ± SEM, n = 3. Statistical analysis was performed as described in Materials and Methods; $P < 0.05$.

Overall Conclusions

The work conducted for this thesis has demonstrated the advantages of utilizing the novel transgenic PSMA1-GFP boar model to study the roles of the Ubiquitin Proteasome System in fertilization. Green fluorescent proteasomes are present in the sperm acrosomes of the transgenic PSMA1-GFP boar. This supports the proposed role of proteasomes in acrosomal function during fertilization. Purification procedures targeting the GFP tag of subunit PSMA1-GFP have proven to be successful in facilitating the purification of 20S proteasomal cores and helped to identify a number of candidate proteasome-interacting proteins. Potentially sperm specific enzymatically active 26S proteasomes and/or the 20S core particles can be isolated by using GFP affinity purification on transgenic boar spermatozoa. Immunoprecipitation experiments confirmed the identity of some such proteasome interacting proteins, specifically lactadherin/MFGE8, along with many of the 20S core particle subunits and possible subunit isoforms(PSMA 3, 4, 7 and PSMB2).

Lactadherin MFGE8 showed strong interactions with the PSMA1-GFP protein. This MFGE8 protein is essential to many biological processes such as plasma membrane binding. During fertilization, MFGE8 has been implicated in the initial sperm-zona pellucida binding and the formation of the oviductal sperm reservoir. The sperm 26S proteasomes could gradually degrade MFGE8 during capacitation and release of the bound spermatozoa from the oviductal sperm reservoir. This is suggested from the proteasomal inhibitor MG132 dose dependent increase of endogenous and recombinant human MFGE8 in capacitated spermatozoa and acrosomal extracts,

respectively. This MFGE8 and the other co-purified structural proteins could be the substrates of resident acrosomal proteasomes during acrosomal remodeling that occurs in preparation for fertilization.

This novel transgenic boar model can be utilized to study the roles of the UPS in other areas than reproduction. The fusion of GFP to the PSMA1 subunit of the 20S proteasomal core allows for easier localization in various tissues and cells through epifluorescence or immunofluorescence methods. Similar GFP affinity purification methods can be optimized to isolate enzymatically active tissue specific proteasomes and can be used for studies of sperm-oocyte interactions or where ever the UPS may play a role. Furthermore, immunoprecipitation experiments targeting the GFP tag can reveal tissue specific proteasome interacting proteins. Ultimately, this novel transgenic boar model can accelerate UPS research in many biological processes, pathologies, and genetic diseases.

Bibliography

Abeydeera, L. R., W. H. Wang, et al. (1998). "Maturation in vitro of pig oocytes in protein-free culture media: fertilization and subsequent embryo development in vitro." Biol Reprod 58(5):1316-1320.

Adenot, P. G., Y. Mercier, et al. (1997). "Differential H4 acetylation of paternal and maternal chromatin precedes DNA replication and differential transcriptional activity in pronuclei of 1-cell mouse embryos." Development 124(22):4615-4625.

Andersen, M. H., H. Graversen, et al. (2000). "Functional analyses of two cellular binding domains of bovine lactadherin." Biochemistry 39(20):6200-6206.

Anderson, J. E., R. L. Matteri, et al. (2001). "Degradation of maternal cdc25c during the maternal to zygotic transition is dependent upon embryonic transcription." Mol Reprod Dev 60(2):181-188.

Austin, C. R. and M. W. Bishop (1958). "Role of the rodent acrosome and perforatorium in fertilization." Proc R Soc Lond B Biol Sci 149(935):241-248.

Baba, T., S. Azuma, et al. (1994). "Sperm from mice carrying a targeted mutation of the acrosin gene can penetrate the oocyte zona pellucida and effect fertilization." J Biol Chem 269(50):31845-31849.

Baker, M. A., G. Reeves, et al. (2007). "Identification of gene products present in Triton X-100 soluble and insoluble fractions of human spermatozoa lysates using LC-MS/MS analysis." Proteomics Clin Appl 1(5):524-532.

Balzar, M., I. H. Briaire-de Bruijn, et al. (2001). "Epidermal growth factor-like repeats mediate lateral and reciprocal interactions of Ep-CAM molecules in homophilic adhesions." Mol Cell Biol 21(7):2570-2580.

Bedard, N., Y. Yang, et al. (2011). "Mice lacking the USP2 deubiquitinating enzyme have severe male subfertility associated with defects in fertilization and sperm motility." Biol Reprod 85(3):594-604.

Bedford, J. M. (1998). "Mammalian fertilization misread? Sperm penetration of the eutherian zona pellucida is unlikely to be a lytic event." Biol Reprod 59(6):1275-1287.

Belote, J. M. and L. Zhong (2009). "Duplicated proteasome subunit genes in Drosophila and their roles in spermatogenesis." Heredity (Edinb) 103(1):23-31.

Bleil, J. D. and P. M. Wassarman (1980). "Mammalian sperm-egg interaction: identification of a glycoprotein in mouse egg zonae pellucidae possessing receptor activity for sperm." Cell 20(3):873-882.

Boavida, L. C., A. M. Vieira, et al. (2005). "Gametophyte interaction and sexual reproduction: how plants make a zygote." Int J Dev Biol 49(5-6):615-632.

Bohring, C., E. Krause, et al. (2001). "Isolation and identification of sperm membrane antigens recognized by antisperm antibodies, and their possible role in immunological infertility disease." Mol Hum Reprod 7(2):113-118.

Bohring, C. and W. Krause (2003). "Characterization of spermatozoa surface antigens by antisperm antibodies and its influence on acrosomal exocytosis." Am J Reprod Immunol 50(5):411-419.

Book, A. J., J. Smalle, et al. (2009). "The RPN5 subunit of the 26s proteasome is essential for gametogenesis, sporophyte development, and complex assembly in Arabidopsis." Plant Cell 21(2):460-478.

Bousquet-Dubouch MP, et al. (2008) Purification and proteomic analysis of 20S proteasomes from human cells. Methods Mol Biol 432:301–320.

Brooks, S. A. (2010). "Functional interactions between mRNA turnover and surveillance and the ubiquitin proteasome system." Wiley Interdiscip Rev RNA 1(2):240-252.

Byrne, K., T. Leahy, et al. (2012). "Comprehensive mapping of the bull sperm surface proteome." Proteomics 12(23-24):3559-3579.

Callis, J. and P. Bedinger (1994). "Developmentally regulated loss of ubiquitin and ubiquitinated proteins during pollen maturation in maize." Proc Natl Acad Sci U S A 91(13):6074-6077.

Catimel, B., C. Schieber, et al. (2008). "The PI(3,5)P2 and PI(4,5)P2 interactomes." J Proteome Res 7(12):5295-5313.

Celik, O., S. Hascalik, et al. (2008). "Combating endometriosis by blocking proteasome and nuclear factor-kappaB pathways." Hum Reprod 23(11):2458-2465.

Chakravarty, S., P. Bansal, et al. (2008). "Role of proteasomal activity in the induction of acrosomal exocytosis in human spermatozoa." Reprod Biomed Online 16(3):391-400.

Chakravarty, S., K. Suraj, et al. (2005). "Baculovirus-expressed recombinant human zona pellucida glycoprotein-B induces acrosomal exocytosis in capacitated spermatozoa in addition to zona pellucida glycoprotein-C." Mol Hum Reprod 11(5):365-372.

Chen, C., C. Huang, et al. (2008). "Subunit-subunit interactions in the human 26S proteasome." Proteomics 8(3):508-520.

Copland, S. D., A. A. Murphy, et al. (2009). "The mouse gamete adhesin, SED1, is expressed on the surface of acrosome-intact human sperm." Fertil Steril 92(6):2014-2019.

DeMott, R. P., R. Lefebvre, et al. (1995). "Carbohydrates mediate the adherence of hamster sperm to oviductal epithelium." Biol Reprod 52(6):1395-1403.

Deveraux, Q., S. van Nocker, et al. (1995). "Inhibition of ubiquitin-mediated proteolysis by the Arabidopsis 26 S protease subunit S5a." J Biol Chem 270(50):29660-29663.

Devoto, A., M. Nieto-Rostro, et al. (2002). "COI1 links jasmonate signalling and fertility to the SCF ubiquitin-ligase complex in Arabidopsis." Plant J 32(4):457-466.

Diaz, E. S., M. Kong, et al. (2007). "Effect of fibronectin on proteasome activity, acrosome reaction, tyrosine phosphorylation and intracellular calcium concentrations of human sperm." Hum Reprod 22(5):1420-1430.

Doelling, J. H., A. R. Phillips, et al. (2007). "The ubiquitin-specific protease subfamily UBP3/UBP4 is essential for pollen development and transmission in Arabidopsis." Plant Physiol 145(3):801-813.

Ducoux-Petit M, et al. (2008). Scaled-down purification protocol to access proteomic analysis of 20S proteasome from human tissue samples: Comparison of normal and tumor colorectal cells. J Proteome Res 7(7):2852–2859.

Ekhlasi-Hundrieser, M., F. Sinowatz, et al. (2002). "Expression of spermadhesin genes in porcine male and female reproductive tracts." Mol Reprod Dev 61(1):32-41.

Ensslin, M., T. Vogel, et al. (1998). "Molecular cloning and characterization of P47, a novel boar sperm-associated zona pellucida-binding protein homologous to a family of mammalian secretory proteins." Biol Reprod 58(4):1057-1064.

Ensslin, M. A. and B. D. Shur (2003). "Identification of mouse sperm SED1, a bimotif EGF repeat and discoidin-domain protein involved in sperm-egg binding." Cell 114(4):405-417.

Ensslin, M. A. and B. D. Shur (2007). "The EGF repeat and discoidin domain protein, SED1/MFG-E8, is required for mammary gland branching morphogenesis." Proc Natl Acad Sci U S A 104(8):2715-2720.

Etlinger, J. D. and A. L. Goldberg (1977). "A soluble ATP-dependent proteolytic system responsible for the degradation of abnormal proteins in reticulocytes." Proc Natl Acad Sci U S A 74(1):54-58.

Ficarro, S., O. Chertihin, et al. (2003). "Phosphoproteome analysis of capacitated human sperm. Evidence of tyrosine phosphorylation of a kinase-anchoring protein 3 and valosin-containing protein/p97 during capacitation." J Biol Chem 278(13):11579-11589.

Glickman, M. H. and A. Ciechanover (2002). "The ubiquitin-proteasome proteolytic pathway: destruction for the sake of construction." Physiol Rev 82(2):373-428.

Goldstein, G., M. Scheid, et al. (1975). "Isolation of a polypeptide that has lymphocyte-differentiating properties and is probably represented universally in living cells." Proc Natl Acad Sci U S A 72(1):11-15.

Green, D. P. and R. D. Purves (1984). "Mechanical hypothesis of sperm penetration." Biophys J 45(4):659-662.

Gupta, S. K., P. Bansal, et al. (2009). "Human zona pellucida glycoproteins: functional relevance during fertilization." J Reprod Immunol 83(1-2):50-55.

Hanna, J. and D. Finley (2007). "A proteasome for all occasions." FEBS Lett 581(15):2854-2861.

Haraguchi, C. M., T. Mabuchi, et al. (2007). "Possible function of caudal nuclear pocket: degradation of nucleoproteins by ubiquitin-proteasome system in rat spermatids and human sperm." J Histochem Cytochem 55(6):585-595.

Hershko, A. and A. Ciechanover (1998). "The ubiquitin system." Annu Rev Biochem 67:425-479.

Hershko, A. (2005). "The ubiquitin system for protein degradation and some of its roles in the control of the cell division cycle." Cell Death Differ 12(9):1191-1197.

Honda, A., J. Siruntawineti, et al. (2002). "Role of acrosomal matrix proteases in sperm-zona pellucida interactions." Hum Reprod Update 8(5):405-412.

Hyttel, P., J. Laurincik, et al. (2000). "Nucleolar proteins and ultrastructure in preimplantation porcine embryos developed in vivo." Biol Reprod 63(6):1848-1856.

Ikawa, M., N. Inoue, et al. (2010). "Fertilization: a sperm's journey to and interaction with the oocyte." J Clin Invest 120(4):984-994.

Iwai, K. (2012). "Synthesis and analysis of linear ubiquitin chains." Methods Mol Biol 832:229-238.

Jarrell, V. L., B. N. Day, et al. (1991). "The transition from maternal to zygotic control of development occurs during the 4-cell stage in the domestic pig, Sus scrofa: quantitative and qualitative aspects of protein synthesis." Biol Reprod 44(1):62-68.

Johnson, D. W. (2011). "Free amino acid quantification by LC-MS/MS using derivatization generated isotope-labelled standards." J Chromatogr B Analyt Technol Biomed Life Sci 879(17-18):1345-1352.

Johnston, D. S., J. Wooters, et al. (2005). "Analysis of the human sperm proteome." Ann N Y Acad Sci 1061:190-202.

Kawano, N., W. Kang, et al. (2010). "Mice lacking two sperm serine proteases, ACR and PRSS21, are subfertile, but the mutant sperm are infertile in vitro." Biol Reprod 83(3):359-369.

Kierszenbaum, A. L., E. Rivkin, et al. (2011). "Cytoskeletal track selection during cargo transport in spermatids is relevant to male fertility." Spermatogenesis 1(3):221-230.

Kim, S. T., K. Zhang, et al. (2006). "Exogenous free ubiquitin enhances lily pollen tube adhesion to an in vitro stylar matrix and may facilitate endocytosis of SCA." Plant Physiol 142(4):1397-1411.

Kong, M., E. S. Diaz, et al. (2009). "Participation of the human sperm proteasome in the capacitation process and its regulation by protein kinase A and tyrosine kinase." Biol Reprod 80(5):1026-1035.

Kwon, J., T. Kikuchi, et al. (2003). "Characterization of the testis in congenitally ubiquitin carboxy-terminal hydrolase-1 (Uch-L1) defective (gad) mice." Exp Anim 52(1):1-9.

Lefebvre, R., P. J. Chenoweth, et al. (1995). "Characterization of the oviductal sperm reservoir in cattle." Biol Reprod 53(5):1066-1074.

Lefebvre, R., M. C. Lo, et al. (1997). "Bovine sperm binding to oviductal epithelium involves fucose recognition." Biol Reprod 56(5):1198-1204.

Lefebvre, R. and S. S. Suarez (1996). "Effect of capacitation on bull sperm binding to homologous oviductal epithelium." Biol Reprod 54(3):575-582.

Li, R., C. N. Murphy, et al. (2009). "Production of piglets after cryopreservation of embryos using a centrifugation-based method for delipation without micromanipulation." Biol Reprod 80(3):563-571.

Liberda, J., P. Manaskova, et al. (2006). "Saccharide-mediated interactions of boar sperm surface proteins with components of the porcine oviduct." J Reprod Immunol 71(2):112-125.

Lin, H., A. Keriel, et al. (2000). "Divergent N-terminal sequences target an inducible testis deubiquitinating enzyme to distinct subcellular structures." Mol Cell Biol 20(17): 6568-6578.

Liu, C. W., X. Li, et al. (2006). "ATP binding and ATP hydrolysis play distinct roles in the function of 26S proteasome." Mol Cell 24(1):39-50.

Lorson, M. A., L. D. Spate, et al. (2011). "Disruption of the Survival Motor Neuron (SMN) gene in pigs using ssDNA." Transgenic Res 20(6): 1293-1304.

Luo, J., S. Megee, et al. (2006). "Protein gene product 9.5 is a spermatogonia-specific marker in the pig testis: application to enrichment and culture of porcine spermatogonia." Mol Reprod Dev 73(12):1531-1540.

Manaskova, P., J. Peknicova, et al. (2007). "Origin, localization and binding abilities of boar DQH sperm surface protein tested by specific monoclonal antibodies." J Reprod Immunol 74(1-2):103-113.

Manaskova-Postlerova, P., N. Davidova, et al. "Biochemical and binding characteristics of boar epididymal fluid proteins." J Chromatogr B Analyt Technol Biomed Life Sci 879(1):100-106.

Matsumura, K. and K. Aketa (1991). "Proteasome (multicatalytic proteinase) of sea urchin sperm and its possible participation in the acrosome reaction." Mol Reprod Dev 29(2):189-199.

Memili, E. and N. L. First (2000). "Zygotic and embryonic gene expression in cow: a review of timing and mechanisms of early gene expression as compared with other species." Zygote 8(1):87-96.

Miles, E. L., C. O'Gorman, et al. (2013). "Transgenic pig carrying green fluorescent proteasomes." Proc Natl Acad Sci U S A 110(16): 6334-6339.

Mochida, K., L. L. Tres, et al. (2000). "Structural features of the 26S proteasome complex isolated from rat testis and sperm tail." Mol Reprod Dev 57(2):176-184.

Morales, P., M. Kong, et al. (2003). "Participation of the sperm proteasome in human fertilization." Hum Reprod 18(5): 1010-1017.

Morales, P., E. Pizarro, et al. (2004). "Extracellular localization of proteasomes in human sperm." Mol Reprod Dev 68(1):115-124.

Mtango, N. R., M. Sutovsky, et al. (2012a). "Essential role of maternal UCHL1 and UCHL3 in fertilization and preimplantation embryo development." J Cell Physiol 227(4):1592-1603.

Mtango, N. R., M. Sutovsky, et al. (2012b). "Essential role of ubiquitin C-terminal hydrolases UCHL1 and UCHL3 in mammalian oocyte maturation." J Cell Physiol 227(5):2022-2029.

Nagyova, E., S. Scsukova, et al. (2012). "Inhibition of proteasomal proteolysis affects expression of extracellular matrix components and steroidogenesis in porcine oocyte-cumulus complexes." Domest Anim Endocrinol 42(1):50-62.

Naz, R. K. and L. Dhandapani (2009). "Identification of human sperm proteins that interact with human zona pellucida3 (ZP3) using yeast two-hybrid system." J Reprod Immunol 84(1):24-31.

Pasten, C., P. Morales, et al. (2005). "Role of the sperm proteasome during fertilization and gamete interaction in the mouse." Mol Reprod Dev 71(2):209-219.

Peng, J., D. Schwartz, et al. (2003). "A proteomics approach to understanding protein ubiquitination." Nat Biotechnol 21(8):921-926.

Petrunkina, A. M., A. Lakamp, et al. (2003). "Fate of lactadherin P47 during post-testicular maturation and capacitation of boar spermatozoa." Reproduction 125(3):377-387.

Petrunkina, A. M., R. Petzoldt, et al. (2001). "Sperm-cell volumetric measurements as parameters in bull semen function evaluation: correlation with nonreturn rate." Andrologia 33(6):360-367.

Petrunkina, A. M., K. Simon, et al. (2003). "Regulation of capacitation of canine spermatozoa during co-culture with heterologous oviductal epithelial cells." Reprod Domest Anim 38(6):455-463.

Pines, J. (1994). "Cell cycle. Ubiquitin with everything." Nature 371(6500):742-743.

Qiao, H., H. Wang, et al. (2004). "The F-box protein AhSLF-S2 physically interacts with S-RNases that may be inhibited by the ubiquitin/26S proteasome pathway of protein degradation during compatible pollination in Antirrhinum." Plant Cell 16(3):582-595.

Raymond, A., M. A. Ensslin, et al. (2009). "SED1/MFG-E8: a bi-motif protein that orchestrates diverse cellular interactions." J Cell Biochem 106(6):957-966.

Redgrove, K. A., A. L. Anderson, et al. (2011). "Involvement of multimeric protein complexes in mediating the capacitation-dependent binding of human spermatozoa to homologous zonae pellucidae." Dev Biol 356(2):460-474.

Rivkin, E., A. L. Kierszenbaum, et al. (2009). "Rnf19a, a ubiquitin protein ligase, and Psmc3, a component of the 26S proteasome, tether to the acrosome membranes and the head-tail coupling apparatus during rat spermatid development." Dev Dyn 238(7):1851-1861.

Rogers, C. S., D. A. Stoltz, et al. (2008). "Disruption of the CFTR gene produces a model of cystic fibrosis in newborn pigs." Science 321(5897):1837-1841.

Rosenzweig, R., P. A. Osmulski, et al. (2008). "The central unit within the 19S regulatory particle of the proteasome." Nat Struct Mol Biol 15(6):573-580.

Ross, J. W., J. J. Whyte, et al. (2010). "Optimization of square-wave electroporation for transfection of porcine fetal fibroblasts." Transgenic Res 19(4):611-620.

Sakai, N., H. Sawada, et al. (2003). "Extracellular ubiquitin system implicated in fertilization of the ascidian, Halocynthia roretzi: isolation and characterization." Dev Biol 264(1):299-307.

Sakai, N., M. T. Sawada, et al. (2004). "Non-traditional roles of ubiquitin-proteasome system in fertilization and gametogenesis." Int J Biochem Cell Biol 36(5):776-784.

Sasanami, T., K. Sugiura, et al. (2012). "Sperm proteasome degrades egg envelope glycoprotein ZP1 during fertilization of Japanese quail (Coturnix japonica)." Reproduction 144(4):423-431.

Sawada, H., N. Sakai, et al. (2002a). "Extracellular ubiquitination and proteasome-mediated degradation of the ascidian sperm receptor." Proc Natl Acad Sci U S A 99(3):1223-1228.

Sawada, H., Y. Takahashi, et al. (2002b). "Localization and roles in fertilization of sperm proteasomes in the ascidian Halocynthia roretzi." Mol Reprod Dev 62(2):271-276.

Schwartz, A. L. and A. Ciechanover (1999). "The ubiquitin-proteasome pathway and pathogenesis of human diseases." Annu Rev Med 50:57-74.

Shi, J., S. W. Pipe, et al. (2008). "Lactadherin blocks thrombosis and hemostasis in vivo: correlation with platelet phosphatidylserine exposure." J Thromb Haemost 6(7):1167-1174.

Shur, B. D., M. A. Ensslin, et al. (2004). "SED1 function during mammalian sperm-egg adhesion." Curr Opin Cell Biol 16(5):477-485.

Shur, B. D., C. Rodeheffer, et al. (2006). "Identification of novel gamete receptors that mediate sperm adhesion to the egg coat." Mol Cell Endocrinol 250(1-2):137-148.

Signorelli, J., E. S. Diaz, et al. (2012). "Kinases, phosphatases and proteases during sperm capacitation." Cell Tissue Res 349(3):765-782.

Speranza, A., V. Scoccianti, et al. (2001). "Inhibition of proteasome activity strongly affects kiwifruit pollen germination. Involvement of the ubiquitin/proteasome pathway as a major regulator." Plant Physiol 126(3):1150-1161.

Su, Y. H., S. H. Chen, et al. (2005). "Tandem mass spectrometry identifies proteins phosphorylated by cyclic AMP-dependent protein kinase when sea urchin sperm undergo the acrosome reaction." Dev Biol 285(1):116-125.

Suarez, S. S., I. Revah, et al. (1998). "Bull sperm binding to oviductal epithelium is mediated by a Ca2+-dependent lectin on sperm that recognizes Lewis-a trisaccharide." Biol Reprod 59(1):39-44.

Susor, A., L. Liskova, et al. (2010). "Role of ubiquitin C-terminal hydrolase-L1 in antipolyspermy defense of mammalian oocytes." Biol Reprod 82(6):1151-1161.

Sutovsky, P. (2011). "Sperm proteasome and fertilization." Reproduction 142(1):1-14.

Sutovsky, P., G. Manandhar, et al. (2004). "Proteasomal interference prevents zona pellucida penetration and fertilization in mammals." Biol Reprod 71(5):1625-1637.

Sutovsky, P., T. C. McCauley, et al. (2003). "Early degradation of paternal mitochondria in domestic pig (Sus scrofa) is prevented by selective proteasomal inhibitors lactacystin and MG132." Biol Reprod 68(5):1793-1800.

Sutovsky, P., R. Moreno, et al. (2001). "A putative, ubiquitin-dependent mechanism for the recognition and elimination of defective spermatozoa in the mammalian epididymis." J Cell Sci 114(Pt 9):1665-1675.

Sutovsky, P., K. Van Leyen, et al. (2004). "Degradation of paternal mitochondria after fertilization: implications for heteroplasmy, assisted reproductive technologies and mtDNA inheritance." Reprod Biomed Online 8(1):24-33.

Tanaka, K. (2009). "The proteasome: overview of structure and functions." Proc Jpn Acad Ser B Phys Biol Sci 85(1):12-36.

Verma, R., L. Aravind, et al. (2002). "Role of Rpn11 metalloprotease in deubiquitination and degradation by the 26S proteasome." Science 298(5593):611-615.

Voges, D., P. Zwickl, et al. (1999). "The 26S proteasome: a molecular machine designed for controlled proteolysis." Annu Rev Biochem 68:1015-1068.

Walczak, H., K. Iwai, et al. (2012). "Generation and physiological roles of linear ubiquitin chains." BMC Biol 10:23.

Wells, K. D., J. A. Foster, et al. (1999). "Codon optimization, genetic insulation, and an rtTA reporter improve performance of the tetracycline switch." Transgenic Res 8(5):371-381.

Yamashita, M., A. Honda, et al. (2008). "Reduced fertility of mouse epididymal sperm lacking Prss21/Tesp5 is rescued by sperm exposure to uterine microenvironment." Genes Cells 13(10):1001-1013.

Yanagimachi, R. (1994). "Fertility of mammalian spermatozoa: its development and relativity." Zygote 2(4):371-372.

Yi, Y. J., G. Manandhar, et al. (2007a). "Mechanism of sperm-zona pellucida penetration during mammalian fertilization: 26S proteasome as a candidate egg coat lysin." Soc Reprod Fertil Suppl 63:385-408.

Yi, Y.-J., G. Manandhar, et al. (2007b). "Ubiquitin C-terminal hydrolase-activity is involved in sperm acrosomal function and anti-polyspermy defense during porcine fertilization." Biol Reprod 77(5):780-793.

Yi, Y. J., C. S. Park, et al. (2009). "Sperm-surface ATP in boar spermatozoa is required for fertilization: relevance to sperm proteasomal function." Syst Biol Reprod Med 55(2):85-96.

Yi, Y.-J., G. Manandhar, et al. (2010a). "Inhibition of 19S proteasomal regulatory complex subunit PSMD8 increases polyspermy during porcine fertilization in vitro." J Reprod Immunol 84(2):154-163.

Yi, Y.-J., G. Manandhar, et al. (2010b). "Interference with the 19S proteasomal regulatory complex subunit PSMD4 on the sperm surface inhibits sperm-zona pellucida penetration during porcine fertilization." Cell Tissue Res 341(2):325-340.

Yi, Y. J., S. W. Zimmerman, et al. (2012). "Ubiquitin-activating enzyme (UBA1) is required for sperm capacitation, acrosomal exocytosis and sperm-egg coat penetration during porcine fertilization." Int J Androl 35(2):196-210.

Yokota, N., Y. Kataoka, et al. (2011). "Sperm-specific C-terminal processing of the proteasome PSMA1/alpha6 subunit." Biochem Biophys Res Commun 410(4):809-815.

Yokota, N. and H. Sawada (2007). "Sperm proteasomes are responsible for the acrosome reaction and sperm penetration of the vitelline envelope during fertilization of the sea urchin Pseudocentrotus depressus." Dev Biol 308(1):222-231.

Yoshioka, K., C. Suzuki, et al. (2002). "Birth of piglets derived from porcine zygotes cultured in a chemically defined medium." Biol Reprod 66(1):112-119.

Yurewicz, E. C., A. G. Sacco, et al. (1998). "Hetero-oligomerization-dependent binding of pig oocyte zona pellucida glycoproteins ZPB and ZPC to boar sperm membrane vesicles." J Biol Chem 273(13):7488-7494.

Zeng, F. and R. M. Schultz (2005). "RNA transcript profiling during zygotic gene activation in the preimplantation mouse embryo." Dev Biol 283(1):40-57.

Zhang, F., Y. Hu, et al. (2007). "Proteasome function is regulated by cyclic AMP-dependent protein kinase through phosphorylation of Rpt6." J Biol Chem 282(31):22460-22471.

Zhao, J., J. W. Ross, et al. (2009). "Significant improvement in cloning efficiency of an inbred miniature pig by histone deacetylase inhibitor treatment after somatic cell nuclear transfer." Biol Reprod 81(3):525-530.

Zhao, M.-T., K. M. Whitworth, et al. (2010). "Deciphering the mesodermal potency of porcine skin-derived progenitors (SKP) by microarray analysis." Cell Reprogram 12(2):161-173.

Zhong, L. and J. M. Belote (2007). "The testis-specific proteasome subunit Prosalpha6T of D. melanogaster is required for individualization and nuclear maturation during spermatogenesis." Development 134(19):3517-3525.

Zimmerman, S. and P. Sutovsky (2009). "The sperm proteasome during sperm capacitation and fertilization." J Reprod Immunol 83(1-2):19-25.

Zimmerman, S. W., G. Manandhar, et al. (2011). "Sperm proteasomes degrade sperm receptor on the egg zona pellucida during mammalian fertilization." PLoS One 6(2): e17256.

Appendix

Transgenic Offspring Semen Analysis and IVF

The sperm concentration of GFP offspring was significantly lower than wild type boar (0.4 *vs*. 1.5×10^9 spermatozoa/ml, $p < 0.05$). Also the semen of GFP offspring showed high agglutination (head to head binding; Appendix Table 2). Collected semen was diluted with X-Cell extender and sperm motility was measured during storage. The semen of GFP offspring showed 60 to 75% motility during storage, and the motility was significantly reduced on day 3 compared to the control wild type boar (87.5%, $p < 0.05$; Appendix Table 3).

There was no significant difference in monospermic fertilization between GFP offspring and wild type boar, however, the percentage of polyspermy was dramatically different (0.0% in GFP offspring vs. 63.9% in wild type boar, $p < 0.05$; Appendix Table 4). The percentage of cleaving embryos was significantly higher in wild type boar (68.8%) than in the GFP offspring (33.5%, $p<0.05$), but there was no significant difference in blastocyst formation rate (3.9% in GFP offspring *vs*. 3.4% in wild type boar). Additionally, mean cell number per blastocyst was higher in GFP offspring than in that of wild type boar (31.5 vs. 18.5; $p < 0.05$; Appendix Table 5). The expression of GFP was first detected in late 2 cell embryos and increased from 4-cell to blastocyst (56.0%; see Figure 2.3 B). We concluded that the male of GFP offspring was fertile *in vitro*.

Appendix Table 1: Embryo Transfer Outcomes. Six embryo transfers were performed, transferring 881 embryos. Eight piglets were recovered at C-Section (six breathed). Five of the eight did not express and one healthy expressing male founder was identified.

Surrogate #	# Transferred	Day of Surrogate	Status
O727	214	1	Cycled day 20
O709	142	1	Cycled day 28
O731	140	0	Delivered 5 (4 live) pigs 6/7/10 - none expressed
O762*	140	1	Delivered 2 piglets 6/14/10 - one never breathed
O753	120	0	Cycled day 25
O754	125	0	2 piglets delivered 6/29/10 - one never breathed and the other died on day 3

*Surviving piglet expressed the transgene.

Appendix Table 2: Comparison of semen characteristics between GFP offspring and wild type boars

Boar	*Breed*	*Boar No.*	*Collected semen volume (ml)*	*Sperm concentration (x10^9/ml)*	*% motile spermatozoa*	*Notes*
GFP offspring	Minnesota mini	G137	117.5±7.5[a]	0.4±0.1[b]	75±5.0	High agglutinations
Wild type	Duroc	89-10	50±0.0[b]	1.5±0.1[a]	90±5.0	None

FOOTNOTES:

- Semen was collected twice from each boar.
- Mean±SEM for 2 ejaculates from each boar are shown.
- [a,b] Means in the same column with different superscripts differ significantly ($p < 0.05$).

Appendix Table 3: Comparison of sperm motility (%) during storage

Boar	*Storage Period (day)*			
	1	2	3	4
GFP offspring	75 ± 5.0	75 ± 5.0	65± 5.0[b]	60 ± 5.0
Wild type	92.5 ± 2.5	92.5 ± 2.5	87.5 ± 2.5[a]	87.5 ± 2.5

FOOTNOTES:

- Boar semen was collected twice from each boar, diluted with X-Cell extender and stored at room temperature; sperm motility was assessed under stereomicroscope at 37.5°C.
- Mean±SEM for 2 ejaculates from each boar.
- [a,b] Means in the same column with different superscripts differ significantly ($p < 0.05$).

Appendix Table 4: Comparison of fertilization parameters on porcine IVF

Boar	*No. oocyte inseminated*	*% monospermic oocyte*	*% polyspermic oocyte*	*% total fertilization*
GFP offspring	49	22.3 ± 6.5	0.0 ± 0.0[b]	22.3 ± 6.5[b]
Wild type	51	32.6 ± 7.5	63.9 ± 9.7[a]	96.5 ± 3.6[a]

FOOTNOTES:

- Experiment was repeated four times, and data indicate Mean±SEM.
- [a,b] Means in the same column with different superscripts differ significantly ($p < 0.05$).

Appendix Table 5: Proteasomal Subunits and Putative Proteasome-Interacting Proteins Co-immunoprecipitated with Anti-GFP-Antibody

Protein annotation	***NCBI gi #***	***Score***	***% Coverage***	***MW (kDa)***
A- PROTEASOMAL SUBUNITS				
Proteasome subunit alpha type-1 like	311248177	440	41	29.5
Proteasome subunit alpha type-3 isoform 1	194034201	985	39	28.4
Proteasome subunit alpha type-3 isoform 2	194034199	985	40	27.6
Proteasome subunit alpha type-4	347300165	1171	59	29.5
Proteasome subunit alpha type-4 isoform 1	347300165	669	64	29.5
Proteasome subunit alpha type-5	222136590	654	55	26.4
Proteasome subunit alpha type-6	8394076	1092	41	27.4
Proteasome subunit alpha type-7-like isoform 1	311259068	601	65	27.9
Proteasome (prosome, macropain) subunit, alpha type (alpha 7)	343887360	467	58	27.8
Proteasome subunit beta type-2 isoform 1	4506195	638	61	22.8
Proteasome subunit beta type-2 isoform 2	315139006	638	69	20.2
Proteasome subunit beta type-5	335292522	2006	59	30.1
Proteasome subunit beta type-6	344259274	566	61	25.4
Full-proteasome subunit beta type-7	194034199	275	39	30
Chain H, Crystal Structure of the Mammalian 20s Proteasome at 2.75 A Resolution (Proteasome subunit beta type-6)	21465649	607	65	21.9
B-OTHER SPERM PROTEINS				
Spermadhesins & Acrosome Associated Proteins				
Spermadhesin AWN	66990208	761	74	16.9
Major Seminal Plasma Glycoprotein PSP-I precursor	47523176	275	46	14.5
Seminal Plasma Sperm Motility Inhibitor	72535165	419	69	15
Seminal Plasma Protein pB1 precursor	47523184	178	43	15.4
Acrosin-binding protein (degradation product)	75052483	940	26	60.5
Seminal Plasma Acrosin Inhibitor A1	123986	177	67	7.6
Disintegrin/ADAM-Family Proteins				
Disintegrin and metalloproteinase domain-containing protein 5	323276507	443	23	45.1
Disintegrin and metalloproteinase domain-containing protein 20-like	311261282	322	26	82.5
Other Sperm Proteins & GFP				
Lactadherin	172072653	1264	49	47.8
Enhanced Green Fluorescent Protein	13194618	713	42	27
Ropporin-1-like	301783203	404	33	23.9

Appendix Table 6: Immunoprecipitation & MS/MS Identification of Proteasome Interacting Sperm Proteins. Identified peptides are shown in red.

Proteasomal Subunits:

Protein	NCBI gi #	Score	% Coverage	MW (kDa)
Proteasome subunit alpha type-1 like	311248177	440	41	29.5

```
  1 mfrnqydndv tvwspqgrih qieyameavk qgsatvglks kthavlvalk raqselaahq
 61 kkilhvdnhi gisiagltad arllcnfmrq ecldsrfvfd rplpvsrlvs ligsktqipt
121 qrygrrpygv glliagyddm gphifqtcps anyfdcrams igarsqsart ylerhmsefm
181 ecnlnelvkh glralretlp aeqdlttknv sigivgkdle ftiyddddvs pflegleerp
241 qrkaqpaqpa depaekadep meh
```

Proteasome subunit alpha type-3 isoform 1	194034201	985	39	28.4

```
  1 mssigtgydl sastfspdgr vfqveyamka vensstaigi rckdgvvfgv eklvlsklye
 61 egsnkrlfnv drhvgmavag lladarslad iareeasnfr snfgyniplk hladrvamyv
121 haytlysavr pfgcsfmlgs ysvndgaqly midpsgvsyg ywgcaigkar qaakteiekl
181 qmkemtcrdv vkevakiiyi vhdevkdkaf elelswvgei tkgrheivpk direeaekya
241 keslkeedes dddnm
```

Proteasome subunit alpha type-3 isoform 2	194034199	985	40	27.6

```
  1 mssigtgydl sastfspdgr vfqveyamka vensstaigi rckdgvvfgv eklvlsklye
 61 egsnkrlfnv drhvgmavag lladarslad iareeasnfr snfgyniplk hladrvamyv
121 haytlysavr pfgcsvndga qlymidpsgv sygywgcaig karqaaktei eklqmkemtc
181 rdvvkevaki iyivhdevkd kafelelswv geitkgrhei vpkdireeae kyakeslkee
241 desdddnm
```

Proteasome subunit alpha type-4	347300165	1171	59	29.5

```
  1 msrrydsrtt ifspegrlyq veyameaigh agtclgilan dgvllaaerr nihklldevf
 61 fsekiyklne dmacsvagit sdanvltnel rliaqryllq yqepipceql vtalcdikqa
121 ytqfggkrpf gvsllyigwd khygfqlyqs dpsgnyggwk atcignnsaa avsmlkqdyk
181 egemtlksal alaikvlnkt mdvsklsaek veiatltren gktvirvlkq keveqlikkh
241 eeeeakaere kkekeqkekd k
```

Proteasome subunit alpha type-4 isoform 1	347300165	669	64	29.5

```
  1 msrrydsrtt ifspegrlyq veyameaigh agtclgilan dgvllaaerr nihklldevf
 61 fsekiyklne dmacsvagit sdanvltnel rliaqryllq yqepipceql vtalcdikqa
121 ytqfggkrpf gvsllyigwd khygfqlyqs dpsgnyggwk atcignnsaa avsmlkqdyk
181 egemtlksal alaikvlnkt mdvsklsaek veiatltren gktvirvlkq keveqlikkh
241 eeeeakaere kkekeqkekd k
```

Proteasome subunit alpha type-	222136590	654	55	26.4

5				

```
  1 mfltrseydr gvntfspegr lfqveyaiea iklgstaigi qtsegvclav ekritsplme
 61 pssiekivei dahigcamsg liadaktlid karvetqnhw ftynetmtve svtqavsnla
121 lqfgeedadp gamsrpfgva llfggvdekg pqlfhmdpsg tfvqcdarai gsasegaqss
181 lqevyhksmt lkeaikssli ilkqvmeekl natnielatv qpgqnfhmft keeleevikd
241 i
```

Proteasome subunit alpha type-6	8394076	1092	41	27.4

```
  1 msrgssagfd rhitifspeg rlyqveyafk ainqggltsv avrgkdcavi vtqkkvpdkl
 61 ldsstvthlf kitenigcvm tgmtadsrsq vqraryeaan wkykygyeip vdmlckriad
121 isqvytqnae mrplgccmil igideeqgpq vykcdpagyy cgfkataagv kqtestsfle
181 kkvkkkfdwt feqtvetait clstvlsidf kpseievgvv tvenpkfril teaeidahlv
241 alaerd
```

Proteasome subunit alpha type-7-like isoform 1	311259068	601	65	27.9

```
  1 masrydrait vfspdghlfq veyaqeavkk gstavairgt divvlgvekk svaklqdert
 61 vrkicalddh vcmafaglta darvvinrar vecqshkltv edpvtveyit rfiatlkqky
121 tqsngrrpfg isalivgfdd dgiprlyqtd psgtyhawka naigrsaktv refleknyte
181 daiandneai klairallev vqsggkniel aiirrnqplk mfsakeielq vneiekekee
241 aekkkskkta
```

Proteasome (prosome, macropain) subunit, alpha type	343887360	467	58	27.8

```
  1 msydraitvf spdghlfqve yaqeavkkgs tavgvrgrdi vvlgvekksv arlqdertvr
 61 kicalddnvc mafagltada rivinrarve cqshrltved pvtveyitry iaslkqrytq
121 sngrrpfgis alivgfdfdg tprlyqtdps gtyhawkana igrgaksvre fleknytdea
181 ietdgltikl vikallevvq sggknielav mrrdqplkil npeeiekyva eiekekeene
241 kkkqkkas
```

Proteasome subunit beta type-2 isoform 1	4506195	638	61	22.8

```
  1 meyligiqgp dyvlvasdrv aasnivqmkd dhdkmfkmse killlcvgea gdtvqfaeyi
 61 qknvqlykmr ngyelsptaa anftrrnlad clrsrtpyhv nlllagydeh egpalyymdy
121 laalakapfa ahgygafltl sildryytpt isreravell rkcleelqkr filnlptfsv
181 riidkngihd ldnisfpkqg s
```

Proteasome subunit beta type-2 isoform 2	315139006	638	69	20.2

```
  1 meylidhdkm fkmsekilll cvgeagdtvq faeyiqknvq lykmrngyel sptaaanftr
 61 rnladclrsr tpyhvnllla gydehegpal yymdylaala kapfaahgyg afltlsildr
121 yytptisrer avellrkcle elqkrfilnl ptfsvriidk ngihdldnis fpkqgs
```

Proteasome subunit beta type-5	335292522	2006	59	30.1

```
  1 mfwrvvpfpl ldmalasvle rplavnrrgf fgfggradll dlgpgspgdg lslvapswgv
 61 peepriemlh gtttlafkfl hgvivaadsr atagayiasq tvkkvieinp yllgtmagga
121 adcsfwerll arqcriyelr nkerisvaaa skllanmvyq ykgmglsmgt micgwdkrgp
```

181 **glyyvdsegn risgatfsvg sgsvyaygvm drgysydlev eqaydlar**ra iyqatyr**day**
241 **sggsvnlyhv redgwirvss dnvadlhdky sestp**

Proteasome subunit beta type-6	344259274	553	61	25.4

1 maatlvaarg aglapawghe aitpdwenre vstgttimav qfdggvvlga dsrtttgsyi
61 anrvtdkltp ihdrifccr**s gsaadtqava davtyqlgfh sielnepplv htaaslfk**em
121 cyr**yredlma giivagwdpq eggqvysvpm ggmmvrqafa iggsgssyiy gyvdatyreg**
181 **mtkeeclqft analalamer** dgssggvir**l aaiaesgver qvllgdqipk ftiatlppp**

Full-proteasome subunit beta type-7	160419232	275	39	30

1 maavsvyerp vggfsfdncr rnaileadfa kkgyklptar ktgttiagvv yk**dgivlgad**
61 **tr**ategmvva dkncskihfi spniyccgag taadtdmttq lissnlelhs lstgrlprvv
121 tanrmlk**qml fryqgyigaa lvlggvdvtg phlysiyphg stdklpyvtm gsgslaamav**
181 **fedkfrpeme eeeak**qlvse aiaagifndl gsgsnidlcv isksk**ldflr pysvpnkk**gt
241 rfgryrcekg ttavltek**vt aldievleet vqtmdts**

Chain H, Crystal Structure of the Mammalian 20s Proteasome at 2.75 A Resolution	21465649	607	65	21.9

1 **ttimavqfdg gvvlgadsr**t ttgsyianrv tdkltpihdr ifccr**sgsaa dtqavadavt**
61 **yqlgfhsiel nepplvhtaa slfk**emcyr**y redlmagiii agwdpqeggq vysvpmggmm**
121 **vr**qsfaiggs gssyiygyvd atyr**egmtke eclqftanal alamer**dgss ggvir**laaia**
181 **esgverqvll gdqipk**fava tlppa

Spermadhesins & Other Acrosome-Associated Proteins:

Spermadhesin AWN	66990208	761	74	16.9

1 mklgsailwa lllstatlvs gawnrrsrsc ggvlr**dppgk ifnsdgpqkd cvwtikvkph**
61 **fhvvlaippl nlscgkeyve lldgppgsei igkicggisl vfrsssniat ikylr**tsgqr
121 **aspfhiyyya dpegplpfpy ferqtiiate knip**

Major Seminal Plasma Glycoprotein PSP-I precursor	47523176	275	46	14.5

1 mklgsaipwa llfstatlis tgwgldyhac ggr**ltddygt iftyk**gpk**te cvwtlqvdpk**
61 ykllvsiptl nltcgk**eyve ilegapgsk**s lgk**fceglsi lnr**gssgmtv kykr**dsghpa**
121 **spyeiiflr**d sqg

Seminal Plasma Sperm Motility Inhibitor	72535165	419	69	15

1 mklgsaipwa lllstatlvs taqnkgsddc ggflk**nysgw isyykalttn cvwtiemkpg**
61 **hk**iilqilpl nltcgkeyle vrdqr**agpdn flkvcggttf vyqsssnvat vk**ysr**dshhp**
121 **assfnvyfyg ipqgak**a

Sp32 Acrosin-binding protein (degradation	75052483	940	26	60.5

product)				

```
  1 qlaagsllsl lkvlllplap apaqdansas tpgsplspte yerffalltp twkaettcrl
 61 rathgcrnpt lvqldqyenh glvpdgavcs dlpyaswfes fcqftqyrcs nhvyyakrvr
121 csqpvsilsp nslkevdtss evpittmtsp vsshitatgr qvfqpwperl nnnveellqs
181 slslggqeqg qehkqehkqe qgqehkqdeg qeqeeqeeeq eeegkqeegq gteesleams
241 glqadsepkf qsefvssnpf sftprvreve stpmmmeniq elirsaqemd emgdvyeeen
301 iwraqspgsl lqlphvdall vlcysivent cvitptakaw qyledetlgf gksvcdslgr
361 rhlaacslcd fcslkleqch setnlqrqqc dnshktpfis pllasqsmsi gtqigtlksg
421 rfygldlygg lrmdfwcarl atkgcednrv aswlqtefls fqdgdfptki cdteyvqypn
481 ycafksqqcm mrnrdrkvsr mrclqnetyt vltqaksedl vlrwsqefst ltlgqag
```

Seminal Plasma Acrosin Inhibitor A1	123986	177	67	7.6

```
  1 trkqpncnvy rshlffctrq mdpicgtngk syanpcifcs ekglrnqkfd fghwghcrey
 61 tsars
```

Seminal Plasma Protein pB1 precursor	47523184	178	43	15.4

```
  1 maprlgifll wagvsvflpl dpvngdqhlp grfltpaits ddkcvfpfiy kgnlyfdctl
 61 hdstyywcsv ttyymkrwry crstdyarca lpfifrgkey dscikegsvf skywcpvtpn
121 ydqdrawryc
```

Disintergins (ADAM Family) Proteins:

Disintegrin and metalloproteinase domain-containing protein 5	323276507	443	23	45.1

```
  1 mhsggvkdfs tcslddfkyf aahsgltclh silldepvyk qrrricgngi leqgeqcdcg
 61 tlencthkhc cdprtcrrkr nkqcgsgecc tqdckirpan vicrksadec dfieycngty
121 shcvadtfar ngqscesgsa ycyggrcrsf tkqcrnligg estgasfscf deinsrkdrf
181 gncgreycny phllcgklvc nwphkylisr anlsviyshv reqmcvstfl naekiprdti
241 ttvqfpgdrd rtfvqdgtvc gpemfclnfs cveikyrvny gecnssrhcn angvcnnfnh
301 chckkgfvpp dcnvgngfgs iddghqskvg prrlwegkvl pskhrfqlif yislpvliia
361 ttaiiikqnk irelcyrget esegsvsees sssksklsptv snsl
```

Disintegrin and metalloproteinase domain-containing protein 20-like	311261282	322	26	82.5

```
  1 mgpasaqaql rgdpclpllw lflgpiccsy appgwrftas eiviprkvsh rvstaeiqgq
 61 lsykirfggq rhvvhmrvkk sllprhfpvi tdndqgamqe dypfvprdcy yygylegvpg
121 smgtldtchg glrgmlqvdd ftyeikplea sskfehvisl lvtqktpged ekckiggedt
181 nqadeealla empragpvym wwphrkyikl lytvahsyfl lnpnqtsvie nvvimnnilh
241 siyfqaglev cirvlciwna gdgmrldiwr dggslvtrfg lwkmqrwqgm iphdtavllt
301 grrfgndryy ahrggicnpn wgasfvcvgn nhiflastla ahtlghmigc rhdgpgcrcf
361 rrdkcvmape tglldmlsnc syvtlhevvh rwdpclstsn vpynnfpyva nrcgdkklda
421 reecdcgtmk dcaedpccen sciltlgstc segsccvgcn yaqpgrmcrd vlgicdlpey
481 ctglthtcpd dsyiqdgtpc splavcvkgn csdrdmqcqa lfgfnvkeaa picyrtlnmr
541 gdrfgncgvr virgggkpvk ceeddimcgm lhcanvqkip gggehttfrh ivvhdvtpkt
601 cfgfdahfgt ltpqlglvvd gascgpgqfc kdqnctfypd lnfscdvstc nfrgvcnnrr
661 hchcqqgwkp pncdvegggg svdsgpppdk rketrakirm svnievalll arfallcisg
721 iigslfhlre vvdqryeeta sekl
```

Other Sperm Proteins & eGFP:

Lactadherin	172072653	1264	49	47.8

```
  1 mpgprlltai cgallcasgl fafsgdfcds sqclnggtcl ldqdpqnpfh clcpegftgl
 61 icnetekgpc fpnpchndae ceviddahrg dvftqyickc phgytgihce iicnaplgme
121 tgaiadfqis assmhlgfmg lqrwapelar lhragivnaw tasnydrnpw iqvnllrrmr
181 vtgvvtqgas ragsaeyikt fkvayssdgr kfqfiqgaee sgdkifmgnl dnsglkvnlf
241 evplevqyvr lvpiichrgc tlrfellgce lsgcaeplgl kdntipnkqi tassfyrtwg
301 lsafswypfy arldnqgkfn awtaqsnsas ewlqidlgsq rrvtgiitqg ardfghiqyv
361 aaykvaysdd gvswteyrdq galegkifpg nldnnshkkn mfetpfltrf vrilpvawhn
421 ritlrvellg c
```

Enhanced Green Fluorescent Protein	13194618 GenBank: AAK15492.1	713	42	27

```
  1 mvskgeelft gvvpilveld gdvnghkfsv sgegegdaty gkltlkfict tgklpvpwpt
 61 lvttltygvq cfsrypdhmk qhdffksamp egyvqertif fkddgnyktr aevkfegdtl
121 vnrielkgid fkedgnilgh kleynynshn vyimadkqkn gikvnfkirh niedgsvqla
181 dhyqqntpig dgpvllpdnh ylstqsalsk dpnekrdhmv llefvtaagi tlgmdelyk
```

Ropporin-1-like	301783203	404	33	23.9

```
  1 mpqtdkqici ppelpellkq ftkaairtqp qdliqwaady fgamshgeip pvrerservа
 61 lsnwaeltpe llkilhsrva grliihadel aqmwkvlslp tdlfnsvmnv grfteeiewl
121 kflalacssl gvtiaktlki vcevlssdhd ggppripfst fqflytyiae vdgeisashv
181 srmlnyieqe vigpdglikv ndftqnprvr le
```

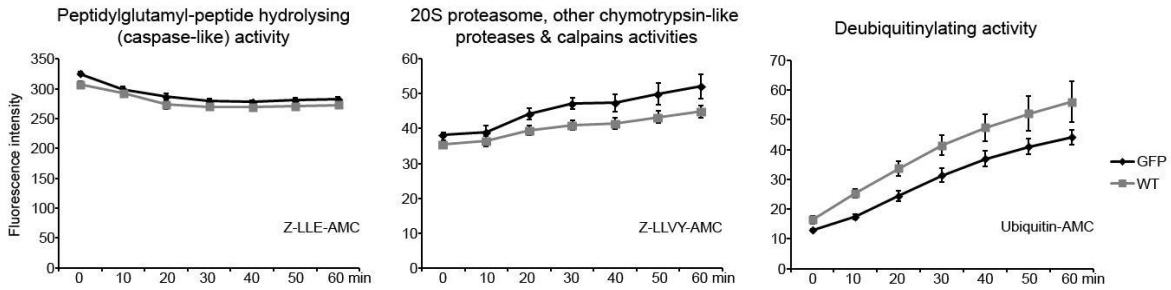

Appendix Figure 1. Comparisons of proteasomal-proteolytic activities in spermatozoa of PSMA1-GFP offspring (GFP) and wild type boars (WT). Proteasomal proteolytic and deubiquitinating activities were measured using specific fluorometric substrates Z-LLE-AMC, Z-LLVY-AMC, and ubiquitin-AMC, respectively. The relative emitted fluorescence (no units) was measured at multiple time points to follow the kinetics of the reaction (ex: 380 nm, em: 460 nm). Experiments were repeated six times (with two different WT boars as a control). Values are expressed as the mean of fluorescence intensity ± SEM.

Methodology: Proteasomal-proteolytic activity of boar spermatozoa was measured by a standard fluorometric proteasomal substrate assay as described (Yi et al., 2009). Spermatozoa preserved in X-cell Extender were loaded onto a 96-well black plate (final sperm con. 1 x 10^6 spermatozoa/ml), and incubated at 37.5°C with Z-LLE-AMC (a specific substrate for 20S chymotrypsin-like peptidyl-glutamylpeptide hydrolyzing [PGPH] activity, final conc. 100 µM; Enzo Life Sciences, Plymouth, PA), Z-LLVY-AMC (a specific substrate for 20S proteasome other chymotrypsin-like proteases and calpains; final con. 100 µM; Enzo), or ubiquitin-AMC (a specific substrate for deubiquitinylating activity; final conc. 300 nM; Enzo). The emitted fluorescence (no units) was measured every 10 min for a period of 1 hr, yielding a curve of relative fluorescence (excitation: 355 nm, emission: 460, Thermo Fluoroskan, ThermoFisher Scientific).

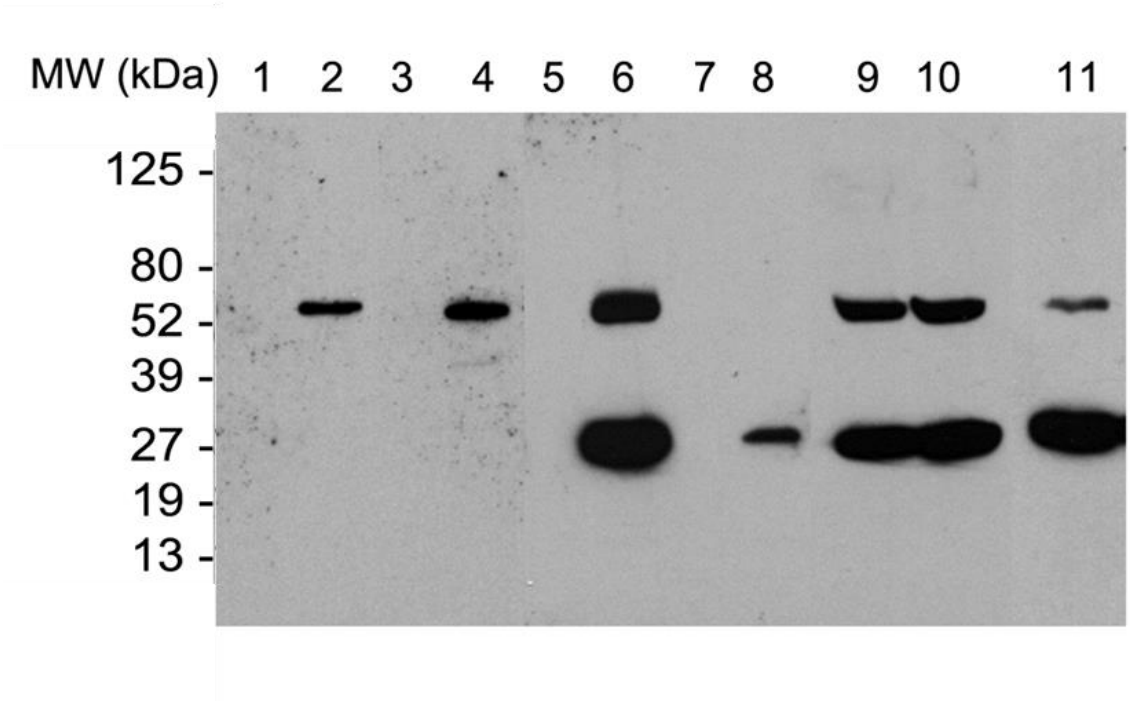

Appendix Figure 2. Western blots of various PSMA1-GFP and wild-type boar tissues. These tissues were probed with mouse monoclonal anti-GFP antibody (1:2000 dilution, cat. #A11120; Invitrogen). Lane 1: WT spermatozoa, lane 2: PSMA1-GFP spermatozoa, lane 3: WT muscle, lane 4: PSMA1-GFP muscle, lane 5: WT lung, lane 6: PSMA1-GFP lung, lane 7: WT brain, lane 8: PSMA1-GFP brain, Lane 9: PSMA1-GFP red blood cells, lane 10: PSMA1-GFP serum (blood), lane 11: PSMA1-GFP uterus. PSMA1-GFP specific 57 kDa bands correspond to the molecular weight of GFP-PSMA1. PSMA1-GFP specific 27 kDa bands correspond to the molecular weight of GFP.

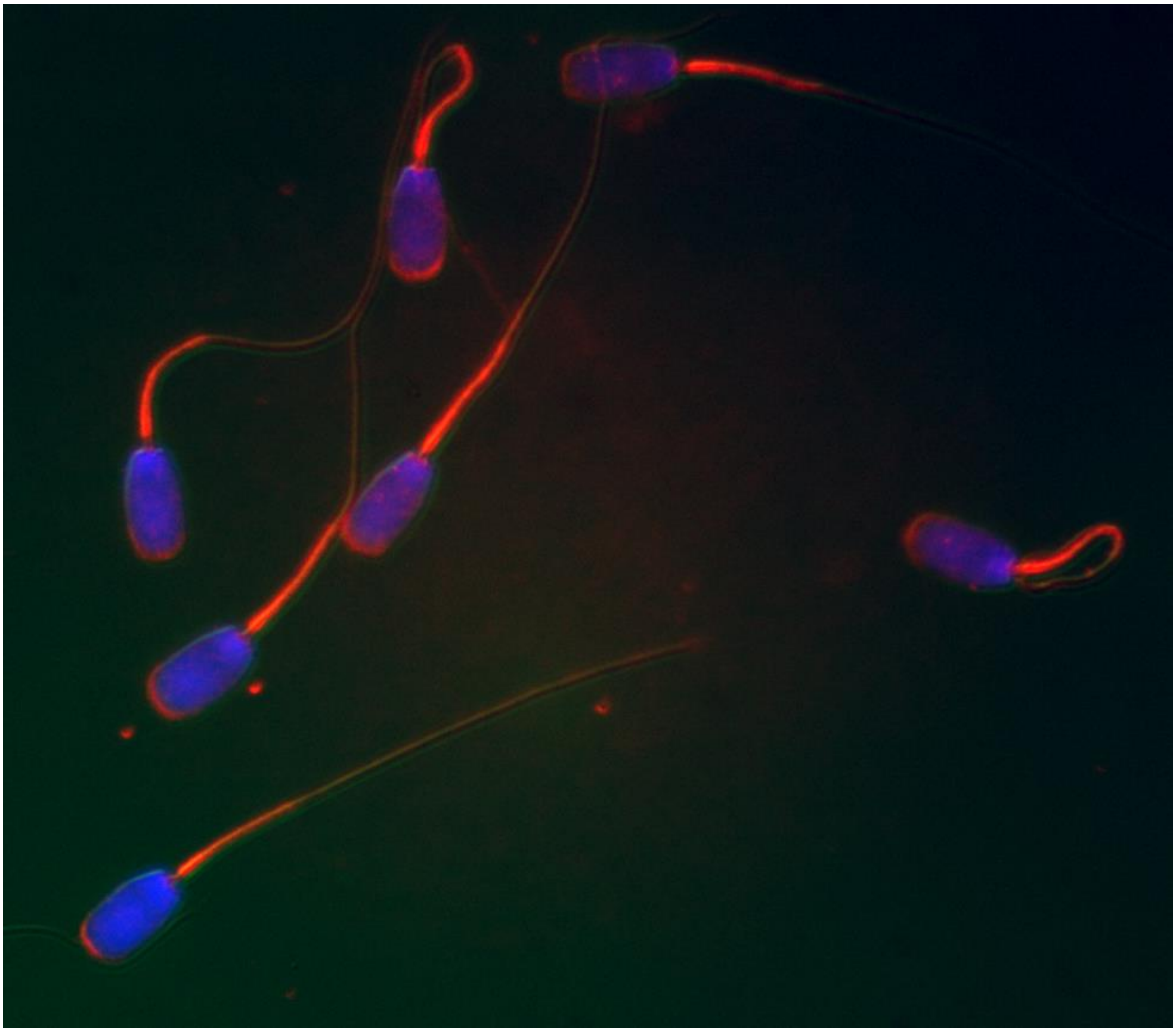

Appendix Figure 3. Immunofluorescence of MFGE8 in wild-type uncapacitated boar spermatozoa. Spermatozoa were affixed to poly-lysine treated microscopy coverslips and fixed in 2% formaldehyde, washed, permeablized in PBS with 0.1% Triton-X-100 (PBS-TX) and blocked in PBS-TX containing 5% normal goat serum. Spermatozoa were incubated with mouse monoclonal antibody raised against Armenian hamster (1:100 dilution, Code No. D199-3; Medical and Biological Laboratories Co., Woburn, MA, USA) overnight. Then they were incubated in PBS-TX containing 1% normal goat serum with goat anti-Armenian hamster IgG-TRITC (1:100 dilution; Cat# sc-2997; Santa Cruz Biotechnology, Inc.) and DAPI (1:100; Molecular Probes - Invitrogen) for 40 min. Image acquisition was performed on a Nikon Eclipse 800 epifluorescence microscope (Nikon Instruments Inc., Melville, NY) with Cool Snap camera (Roper Scientific, Tucson, AZ) and MetaMorph software (Universal Imaging Corp., Downington, PA). MFGE8 fluorescence (red) is localized on the acrosome and midpiece.

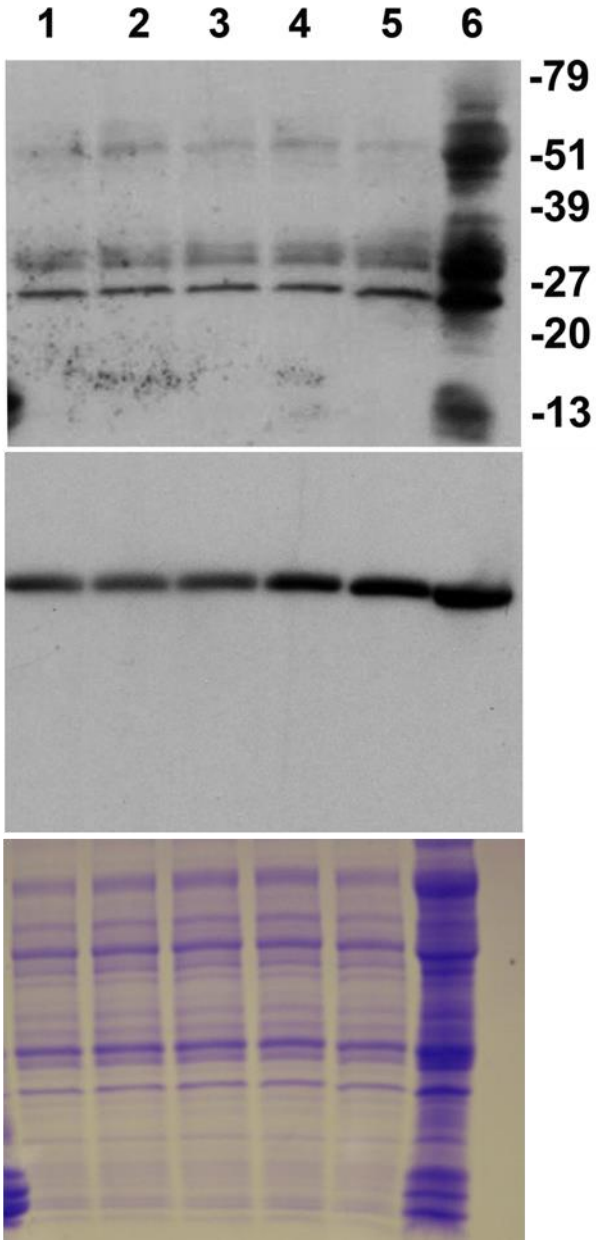

Appendix Figure 4. Wild type boar sperm endogenous MFGE8 Western blot. (A) Resulting film with the ~53 kDa endogenous MFGE8 band which was measured with densitometry. Lane 1: Capacitated boar spermatozoa treated with EtOH vehicle control. Lane 2: Capacitated boar spermatozoa treated with 100 µM MG132. Lane 3: Capacitated boar spermatozoa treated with 50 µM MG132. Lane 4: Capacitated boar spermatozoa treated with 10 µM MG132. Lane 5: Capacitated boar spermatozoa with no MG132 treatment. Lane 6: Uncapacitated boar spermatozoa with no treatment. (B) Reprobing of the membrane with alpha-Tubulin E7 to normalize protein load. (C) Residual Western blot gel.

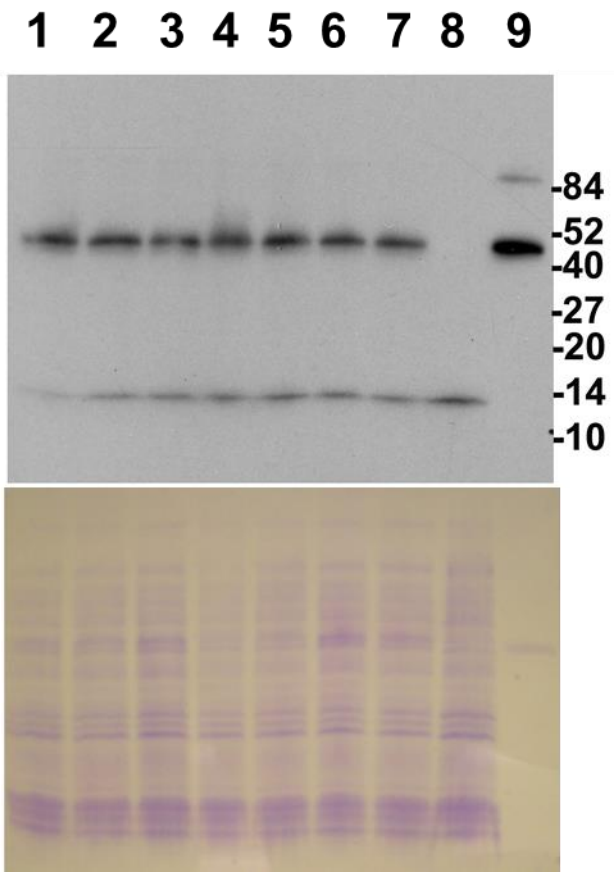

Appendix Figure 5. Western blot of human rMFGE8 incubated with boar sperm acrosomal extracts. (A) Resulting film with the ~49 kDa rMFGE8 band which was measured with densitometry. Lanes 1-3: rMFGE8 and acrosomal extracts treated with EtOH vehicle control. Lane 4: rMFGE8 and acrosomal extracts treated with 100 µM MG132. Lane 5: rMFGE8 and acrosomal extracts treated with 50 µM MG132. Lane 6: rMFGE8 and acrosomal extracts treated with 10 µM MG132. Lane 7: rMFGE8 and acrosomal extracts without MG132. Lane 8: Acrosomal extract alone. Lane 9: rMFGE8 in PBS. (C) Residual Western blot gel.

Vita

Edward (TJ) Miles was born and raised in Ballwin, MO, a suburb of Saint Louis City. Edward is the son of Tess and Tom Miles and brother of Tessa Miles, Noah Miles, and Devin Snodgrass. Edward graduated from Parkway South High School in May 2007 and upon graduation, Edward attended the University of Missouri – Columbia's Biochemistry program. After completing his undergraduate Biochemistry degree in May 2011, he stayed at the University of Missouri – Columbia to pursue a Master's of Science degree in the Animal Science program under the mentoring of Dr. Peter Sutovsky, in whose laboratory he volunteered as an undergraduate. Edward continued his research under Dr. Sutovsky and will complete his MS degree in Animal Science with an emphasis in Reproductive Physiology in May 2013.